University of Alberta

TREF and SEC Characterization of Ethylene/1-Butene Copolymers Produced at Various 1-Butene and Hydrogen Pressures

By

Yves Lacombe ©

A thesis
submitted to the Faculty of Graduate Studies and Research in
partial fulfillment of the requirements for the degree of
Master of Science

Department of Chemical Engineering

Edmonton, Alberta
Fall, 1995

National Library of Canada
Acquisitions and Bibliographic Services Branch
395 Wellington Street
Ottawa, Ontario
K1A 0N4

Bibliothèque nationale du Canada
Direction des acquisitions et des services bibliographiques
395, rue Wellington
Ottawa (Ontario)
K1A 0N4

Your file *Votre référence*

Our file *Notre référence*

THE AUTHOR HAS GRANTED AN IRREVOCABLE NON-EXCLUSIVE LICENCE ALLOWING THE NATIONAL LIBRARY OF CANADA TO REPRODUCE, LOAN, DISTRIBUTE OR SELL COPIES OF HIS/HER THESIS BY ANY MEANS AND IN ANY FORM OR FORMAT, MAKING THIS THESIS AVAILABLE TO INTERESTED PERSONS.

L'AUTEUR A ACCORDE UNE LICENCE IRREVOCABLE ET NON EXCLUSIVE PERMETTANT A LA BIBLIOTHEQUE NATIONALE DU CANADA DE REPRODUIRE, PRETER, DISTRIBUER OU VENDRE DES COPIES DE SA THESE DE QUELQUE MANIERE ET SOUS QUELQUE FORME QUE CE SOIT POUR METTRE DES EXEMPLAIRES DE CETTE THESE A LA DISPOSITION DES PERSONNE INTERESSEES.

THE AUTHOR RETAINS OWNERSHIP OF THE COPYRIGHT IN HIS/HER THESIS. NEITHER THE THESIS NOR SUBSTANTIAL EXTRACTS FROM IT MAY BE PRINTED OR OTHERWISE REPRODUCED WITHOUT HIS/HER PERMISSION.

L'AUTEUR CONSERVE LA PROPRIETE DU DROIT D'AUTEUR QUI PROTEGE SA THESE. NI LA THESE NI DES EXTRAITS SUBSTANTIELS DE CELLE-CI NE DOIVENT ETRE IMPRIMES OU AUTREMENT REPRODUITS SANS SON AUTORISATION.

ISBN 0-612-06493-X

Canada

University of Alberta

Library Release Form

Name of Author: Yves Lacombe

Title of Thesis: TREF and SEC Characterization of Ethylene/1-Butene Copolymers Produced at Various 1-Butene and Hydrogen Pressures

Degree: Master of Science

Year this Degree Granted: 1995

Permission is hereby granted to the University of Alberta Library to reproduce single copies of this thesis and to lend or sell such copies for private, scholarly, or scientific research purposes only.

The author reserves all other publication and other rights in association with the copyright in the thesis, and except as hereinbefore provided, neither the thesis nor any substantial portion thereof may be printed or otherwise reproduced in any material form whatever without the author's prior written permission.

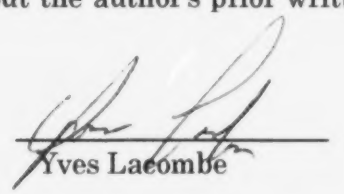

Yves Lacombe

131 Bedridge Place N.E.
Calgary, Alberta
Canada
T3K 1M6

Date: July 26, 1995

University of Alberta

Faculty of Graduate Studies and Research

The undersigned certify that they have read, and recommend to the Faculty of Graduate Studies and Research for acceptance, a thesis entitled **TREF and SEC Characterization of Ethylene/1-Butene Copolymers Produced at Various 1-Butene and Hydrogen Pressures** submitted by **Yves Lacombe** in partial fulfillment of the requirements for the degree of **Master of Science**

S.E. Wanke (co-supervisor)

D.T. Lynch (co-supervisor)

F.D. Otto

R.L. Eadie

Date: July 26, 1995

To

my wife Nancy

Abstract

The effects of H_2 and 1-butene pressures on the properties of LLDPE produced by the copolymerization of ethylene and 1-butene in a gas phase semi-batch reactor over a commercial bisupported Ti catalyst were investigated. The laboratory-produced LLDPEs were characterized by temperature rising elution fractionation (TREF) and size exclusion chromatography (SEC) and TREF-SEC cross fractionation. The TREF profiles were strong functions of the 1-butene pressure; bimodal and trimodal TREF profiles were observed. Cross fractionation showed that the molar mass distributions of the high-temperature TREF fractions were relatively narrow while those of the low-temperature TREF fractions were broader, and at times bimodal. It appears that three or more different types of catalytic sites are involved in producing LLDPE. Hydrogen pressures of 10 to 200 psi had a relatively small effect on 1-butene incorporation. At higher H_2 pressures, the fraction of ethylene homopolymer was much lower than at the lower H_2 pressures, i.e. H_2 decreases the rate of polymerization over the sites responsible for the homopolymerization more than the rate over the sites responsible for copolymerization. Cross fractionation showed that H_2 was a more effective chain-transfer agent for the copolymer fraction of the LLDPE than the homopolymer fraction.

Acknowledgments

Many persons have contributed directly or indirectly to this work; I would like to mention them:

Thanks to Dr. Sieghard Wanke and Dr. David Lynch who guided and supported me during my research.

Thanks are also due to Ms. Bu for her help in the laboratory, especially for performing the molar mass distribution measurements.

I would also like to thank Jim Huang for providing the polyethylene samples and for his cooperation during this project.

Thanks to the staff of Chemical Engineering machine and instrument shops for all the nice parts they built for me, and specially Walter, who spent a lot of time fixing the TREF and GPC apparatus.

I would also like to thank other staff of the department of Chemical Engineering who helped me in various situations: Andrée, Bob, Henry, Cindy, Diane, Beverly and Bonnie.

The support of this research by Novacor Chemicals Ltd. and the Natural Sciences and Engineering Research Council of Canada is gratefully acknowledged.

I am grateful to Dr. Michael Williams for the letter of recruitment he sent me; this letter was the starting point of this challenging experience.

I would like to thank the following people for making my life at the university enjoyable: Kevin, Randy, Welly, Birgitte, Dave, Andy, Sam, Susan, Allan and many others.

I would like to thank my wife Nancy for her love and support. She encouraged me from the beginning to pursue this project and followed me courageously in this venture.

I would like to thank my mother, other members of the family for their support. Thanks to my brother Michel for spending two wonderful weeks with me in the Rockies.

Finally I am grateful to my father and mother in law, Mr. and Ms. Provost for their support and assistance. The believed in me and without their assistance, this enterprise would not have been possible.

Contents

1. Introduction 1

1.1 History of polyolefins 3

1.2 Processes for polymerization of olefins 4

1.2.1 High pressure processes 4

1.2.2 Low pressure processes 6

1.2.2.1 Liquid slurry polymerization 6

1.2.2.2 Solution polymerization 7

1.2.2.3 Gas phase polymerization 8

1.3 Advantages and disadvantages of gas phase polymerization 11

1.4 Structure and properties of LLDPE 14

2. Literature Survey 17

2.1 Ziegler-Natta catalyst and ethylene polymerization 17

2.1.1 Ziegler-Natta catalysts 17

2.1.2 Formation of active center of supported Ziegler-Natta catalyst 22

2.1.3 Multiplicity of active sites in supported Ziegler-Natta catalysts 23

2.1.4 Kinetics of supported Ziegler-Natta catalysts 25

2.2 Characterization of Polyolefins 27

2.2.1 Melt index 28

2.2.2 Differential Scanning Calorimetry 28

2.2.3 Infrared Spectrometry 29

2.2.4 Nuclear magnetic resonance 30

2.2.5 Size exclusion chromatography 31

2.2.6 Temperature rising elution fractionation 35

2.3 TREF: literature survey 36

3. Materials, Equipment and Experimental Procedure 55

3.1 TREF apparatus 55

3.2 Modifications of the TREF system 60

3.3 Operating conditions for the TREF system 63

3.3.1 Determination of IR wavelength 63

3.3.2 Linearity of the IR detector response 66

3.3.3 Pump Calibration 68

3.3.4 Characterization of the TREF columns 69

3.4 TREF experimental procedure 77

3.4.1 Sample preparation 77

3.4.2 TREF procedure 80

3.4.3 TREF-SEC cross fractionation 84

3.5 Data collection and processing for TREF 85

3.6 Calibration curve for TREF 88

4. Results and Discussion 98

4.1 1-Butene series 98

4.1.1 ATREF of 1-butene series 99

4.1.2 TREF-SEC cross fractionation of the 1-butene series 108

4.2 Hydrogen series 116

4.2.1 ATREF of hydrogen series 116

4.2.2 TREF-SEC cross fractionation of H_2 series 120

4.3 Validity of the TREF-SEC results 132

4.4 ATREF of ethylene/vinyl acetate copolymers 141

4.5 ATREF of ethylene/vinyltrimethoxysilane (VTMOS) copolymers 147

5. Conclusions and Recommendations 149

References 151

Appendix A : Descriptions of Polymers
Characterized by TREF 158

Appendix B : Description of ATREF
and PTREF Analyses 166

Appendix C : Data processing for ATREF and PTREF 183

Appendix D : List of Material Needed for TREF 189

Appendix E : Description of the IR cell 191

List of Tables

Table 1.1: Density and chain structure of polyethylenes 1

Table 1.2: Low pressure ethylene polymerization processes 12

Table 2.1: Typical aluminum alkyls for Ziegler-Natta catalysts 18

Table 2.2: Typical transition salts in Z-N catalysts 18

Table 2.3: Industrial catalysts requirements 20

Table 2.4: Main features of high-performance ATREF system 49

Table 2.5: Preparative TREF 53

Table 2.6: Analytical TREF 54

Table 3.1: Solutions for testing IR response linearity 67

Table 3.2: PTREF columns 70

Table 3.3: Outputs from TREF in ASCII file 86

Table 3.4: Standards for TREF calibration curve 90

Table 3.5: Properties of TREF fractions from HDPE GC93048 90

Table 4.1: Branching concentrations and 1-butene consumptions in the 1-butene series. 106

Table 4.2: Percentages of H_2 consumed during the polymerization 131

Table 4.3: Average area and standard deviation of the ATREF profiles for the 1-butene series 134

Table 4.4: Average Area and standard deviation of the ATREF profiles for the H_2 series 135

Table 4.5: Description of the EVA copolymers 141

Table 4.6: Average branching concentration and estimated VA content of the EVA copolymers 142

Table A.1: Description of polymers and reaction conditions for the H_2 series. 159

Table A.2: Description of polymers and reaction conditions for the 1-butene series. 163
Table A.3: Description of the EVA copolymers . 164
Table A.4: Description of the VTMOS copolymers. 165
Table B.1: Operating conditions of the ATREF runs 167
Table B.2: Operating conditions of the PTREF runs 176
Table B.3: Temperature intervals of the TREF fractions from PTREF runs 180

List of Figures

Figure 1.1: Global polyethylene demand 2

Figure 1.2: Flowsheet for high pressure polymerization of ethylene using tubular reactors 5

Figure 1.3: Low pressure slurry loop reactor system 6

Figure 1.4: Medium pressure solution process 8

Figure 1.5: Simplified flowsheet of Union Carbide UNIPOL process 9

Figure 1.6: Chemical structure of linear polyethylene. 14

Figure 1.7: Insertion of short-chain branches by copolymerization of ethylene with 1-butene. 15

Figure 2.1: General scheme of $MgCl_2$ supported catalyst synthesis 21

Figure 2.2: Process of size exclusion chromatography 32

Figure 2.3: Basic parts of SEC apparatus 33

Figure 2.4: Diagram of ATREF system (Wild and Ryle 1977) 41

Figure 2.5: Schematic of an LC oven-based ATREF system (Kelusky 1987) 45

Figure 3.1: TREF apparatus 56

Figure 3.2: Inside of the temperature chamber 57

Figure 3.3: IR scan of o-DCB and hexacontane 65

Figure 3.4: IR signal versus concentration 68

Figure 3.5: Pump calibration 69

Figure 3.6: Residence time distribution of ATREF columns I to IV 71

Figure 3.7: Residence time distribution of the new ATREF columns 73

Figure 3.8: Comparison of the residence time distributions of ATREF column with various packing. 74

Figure 3.9: Residence time distribution of PTREF columns 76

Figure 3.10: Temperature and elution profiles of a typical PTREF procedure 82
Figure 3.11: SEC calibration curve 85
Figure 3.12: MSL versus elution temperature standards 91
Figure 3.13: Comparison of calibration curve generated from the MSL-elution temperature relationship with data obtained from different authors using various solvents and analytical techniques: 94
Figure 4.1: ATREF profiles of 1-butene series 100
Figure 4.2: ATREF profile of PE homopolymer (0 ml 1-butene precharged) 101
Figure 4.3: ATREF profile of ethylene/1-butene LLDPE (30 ml butene precharged) 103
Figure 4.4: Branching distribution for the 30 ml 1-butene LLDPE 105
Figure 4.5: Branching concentration as function of the amount of 1-butene precharged 107
Figure 4.6: 3-D profiles 5 ml 1-butene 109
Figure 4.7: 3-D profiles 20 ml 1-butene 110
Figure 4.8: MMD of two TREF fractions of the 5 ml 1-butene LLDPE 112
Figure 4.9: MMD of two TREF fractions of the 20 ml 1-butene LLDPE 113
Figure 4.10: Fitted MMD of a low temperature fraction (70-80°C) of the 5 ml 1-butene LLDPE. 114
Figure 4.11: Fitted MMD of a high temperature fraction (95-100°C) of the 5 ml 1-butene LLDPE. 114
Figure 4.12: Fitted MMD of a low temperature fraction (70-80°C) of the 20 ml 1-butene LLDPE. 115
Figure 4.13: Fitted MMD of a low temperature fraction (95-100°C) of the 20 ml 1-butene LLDPE. 115

Figure 4.14: ATREF profiles of the H_2 series 117

Figure 4.15: Effect of H_2 partial pressure on the average branching concentration of the LLDPE 119

Figure 4.16: 3-D profiles of the 40 psi H_2 LLDPE 121

Figure 4.17: 3-D profiles of the 150 psi H_2 LLDPE 122

Figure 4.18: 3-D profiles of the 300 psi H_2 LLDPE 123

Figure 4.19: MMD of two TREF fractions of the 40 psi H_2 LLDPE 125

Figure 4.20: MMD of two TREF fractions the 150 psi H_2 LLDPE 126

Figure 4.21: MMD of two TREF fractions of the 300 psi H_2 LLDPE 127

Figure 4.22: Fitted MMD of a low temperature fraction (70-80°C) of the 150 psi H_2 LLDPE 128

Figure 4.23: Fitted MMD of a high temperature fraction (95-100°C) of the 150 psi H_2 LLDPE 128

Figure 4.24: Effect of H_2 on M_w for different TREF fractions 130

Figure 4.25: Areas of ATREF and PTREF runs versus the branching concentration of the corresponding LLDPEs 133

Figure 4.26: Reconstructed MMD of the 5 ml 1-butene LLDPE 136

Figure 4.27: Reconstructed MMD of the 30 ml 1-butene LLDPE 137

Figure 4.28: MMD of TREF fraction from a linear polyethylene (GC93048) 139

Figure 4.29: TREF profiles of EVA copolymers 142

Figure 4.30: VA content estimated by TREF versus actual VA content of the EVA copolymers 145

Figure 4.31: TREF profiles of EVA 1641 with two different IR wavelengths. 146

Figure 4.32: TREF profiles of ethylene/VTMOS copolymers 148

Figure E.1: Diagram of the IR cell heater 191

Figure E.2: Diagram of the IR cell and heater arrangement 192

Figure E.3: Demountable SL-2 cell with all its components 193

Nomenclature

α-CN	α-chloronaphthalene
ASTM	American Society of Testing and Materials
ATREF	Analytical temperature rising elution fractionation
DSC	Differential scanning calorimetry
DTA	Differential thermal analysis
EVA	Ethylene/vinyl acetate copolymer
FTIR	Fourier transform infrared (spectroscopy)
GC	Gas chromatography
GPC	Gel permeation chromatography
HDPE	High density polyethylene
HP-LDPE	High pressure low density polyethylene
HPLC	High performance liquid chromatography
IR	Infrared
LCB	Long chain branching
LCST	Lower critical solution temperature
LLDPE	Linear low density polyethylene
MI	Melt Index

MM	Molar mass
MMD	Molar mass distribution
M_n	Number average molar mass
MSL	Methylene sequence length
M_w	Weight average molar mass
NMR	Nuclear magnetic resonance (spectroscopy)
o-DCB	Ortho-dichlorobenzene
P_d	Polydispersity
PE	Polyethylene
PP	Polypropylene
PTREF	Preparative temperature rising elution fractionation
SCB	Short-chain branching
SEC	Size exclusion chromatography
TCB	1, 2, 4-trichlorobenzene
T_g	Glass-transition temperature (K)
T_m	Melting temperature
T_d^{tcb}	Elution temperature (K)
T_o^{tcb}	Equilibrium dissolution temperature (K)

TNHAL	Tri-n-hexylaluminum
TREF	Temperature rising elution fractionation
ULDPE	Ultra low density polyethylene
UV	Ultraviolet (spectroscopy)
VA	Vinyl acetate
VLDPE	Very low density polyethylene
VTMOS	Vinyltrimethoxysilane
XRD	X-ray diffraction (spectroscopy)

1. Introduction

Polyolefins are widely-used materials and it is difficult to imagine life without them. A few examples of their use are as film, for sheeting and coating of paper, cellophane, metal foil, cloth, glass fiber, wire and cables, for construction of toys, pipe fittings, garbage cans, bags, cups, cans and bottles. Polyethylene (PE) is not only the most widely used polyolefin, it is also the most widely used polymer in the world. Polyethylenes are classified according to their densities and chain structures. PE is usually classified as high density polyethylene (HDPE), high pressure low density polyethylene (HP-LDPE) and linear low density polyethylene (LLDPE). The difference between HP-LDPE and LLDPE is the chain structure. The density range and chain structures of PEs are summarized in Table 1.1.

Table 1.1: Density and chain structure of polyethylenes

Type of PE	Density (g/cm^3)	Chain structure
HDPE	0.940-0.965	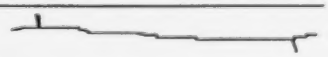
LLDPE	0.910-0.940	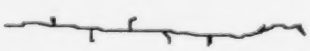
HP-LDPE	0.910-0.925	

Polyethylene has been produced commercially since 1939 just before World War II. Since that time, its production worldwide has grown enormously. Presently, the global demand for polyethylene of all types is about 37 million metric tons per year (Layman, 1994). Of that amount, 15

million metric tons (m.t.) per year is HP-LDPE and HDPE. The remaining 7 million m.t. is LLDPE. The global demand for polyethylene is expected to reach 46 millions m.t. by 1998, and the demand for LLDPEs in 1998 is predicted to be about 12 millions m.t. (Coeyan, 1994). Figure 1.1 shows the global polyethylene demand from 1988 to the predicted values in 1998.

Canada is an important producer of polyethylene. In 1992, the total Canadian production of polyethylene of all kind was 1.67 million m.t. which represents 5% of the world production. Of this amount, 0.75 million m.t. (45% of the Canadian production) was LLDPE. The Canadian capacity for LLDPE is 13% of the world capacity (Schumacher, 1994). Canada's 58% LLDPE share of total LDPE consumption (LLDPE+HP-LDPE) is the highest in the world. LLDPE consumption in Canada was estimated at 0.289 million m.t. in 1991 (Schumacher, 1991).

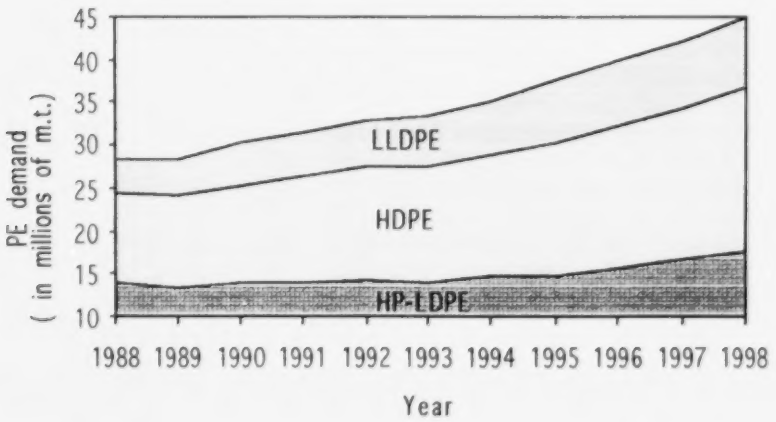

Figure 1.1: Global polyethylene demand (Coeyan, 1994)

Catalysts play a major role in the production of polyolefin. The development of polyethylene is intimately related to the development of catalysts. The polyolefin industry consumes about $1.15 billion per year of

catalyst. This accounts for 39% of the worldwide chemical catalyst market (Rotman, 1994). The reason for that enormous amount of money spent for catalysts is that polyolefins catalysts are consumed in the production process.

1.1 History of polyolefins

The starting point of polyolefins history is the discovery of polyethylene by E. Fawcett and R. Gibson working for ICI in 1933 (Seymour, 1986). At that time, only a few grams of polyethylene were produced and they were not able to get reproducible results. By 1935, ICI researchers advanced polyethylene technology and obtained reproducible results. The first commercial plant for the production of HP-LDPE was built in 1939. During World War II, HP-LDPE was used as an insulator in coaxial cable, essential for Britain's radar system for spotting approaching enemy aircraft. It was also used for telephone cable. To produce HP-LDPE, ICI used a reactor operating at 1500 atm and the mechanism of reaction was radical polymerization. After World War II, ICI licensed polyethylene technology to Union Carbide and DuPont.

In 1953, Karl Ziegler discovered the "Aufbau reaction" (Seymour, 1986). This discovery opened the way to all Ziegler types catalysts. Ziegler-Natta catalysts polymerize ethylene at low pressure and temperature. The initial result of these catalysts was the production of polymer under extremely mild conditions compared to the earlier high pressure and high temperature systems. The Ziegler-Natta catalysts paved the way to the commercial production of polypropylene in 1954. Since 1955 a lot of research has been done to develop new low pressure systems. In the 1960's, DuPont Canada operated a solution plant using the "SCLAIRTECH" process. Also during these years Union Carbide indicated that gas phase polymerization has the greatest potential for versatility. In 1968 Union Carbide started a fluidized-

bed gas phase process. During the 1970s, they improved this system and produced LLDPE in 1975. In 1977 Union Carbide announced their new "UNIPOL" process.

Union Carbide's UNIPOL process is a major technological achievement. This system involves an innovative reactor design and special catalysts. The key to the success of UNIPOL was the development of catalysts that can operate at low pressure and temperature. The UNIPOL process was cited as a good example of the contributions of engineering research to polymer processing in the Amundson report "Frontiers in Chemical Engineering" (1988).

1.2 Processes for polymerization of olefins

In this sub-section, the major processes for the production of polyethylene and other polyolefins are reviewed. There are two major groups of processes: high pressure and low pressure polymerization. In the case of low pressure systems, there are again different types of processes: slurry, solution and gas phase polymerization.

1.2.1 High pressure processes

High pressure processes were the first developed to produce polyethylene. They are still in use today. In 1985, they accounted for 60% of US production of LDPE; today it is also possible to produce LLDPE using this system (Albright, 1985). Typical operating conditions are 1300 to 3400 atm, and temperature between 150-340°C. At these conditions, ethylene is in a fluid phase above its critical temperature and pressure. A typical flowsheet for this process is displayed in Figure 1.2.

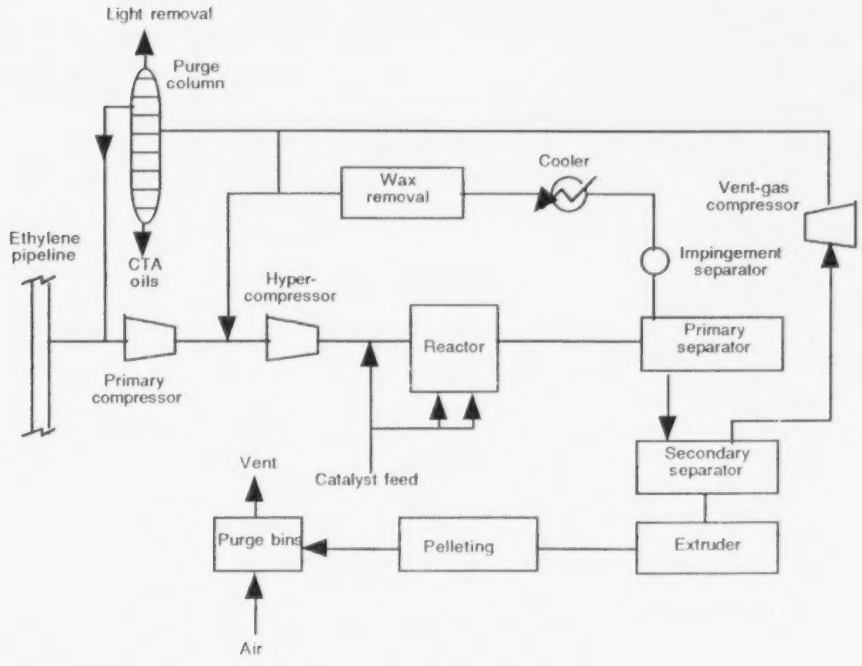

Figure 1.2: Flowsheet for high pressure polymerization of ethylene using tubular reactors (Encyclopedia of Polymer Science and Engineering, 1964-).

In this system, the feed consists of 99.9% pure ethylene and a small amount of initiator. Usual initiators for commercial processes are peroxides, azo compounds and oxygen. Compression of ethylene is a major step and cost in the high pressure processes. For the reaction step, two types of reactors can be used: tubular and autoclave reactors. Tubular reactors are the most important for production of HP-LDPE. The mechanism of reaction for this system is free radical polymerization.

1.2.2 Low pressure processes

1.2.2.1 Liquid slurry polymerization

Liquid slurry processes are the largest group of HDPE technologies. Many industrial producers use this type of system (Phillips, Solvay, Hoechst, Montedison, Dow and Mistsubichi). Loop reactors and continuous stirred tank reactors (CSTR) can be used for liquid slurry polymerization. Usually these processes operate at 80-110°C. Pressures are in the range of 30-35 atm and can be as low as 7.8 atm for a CSTR. A schematic of a loop reactor is shown in Figure 1.3.

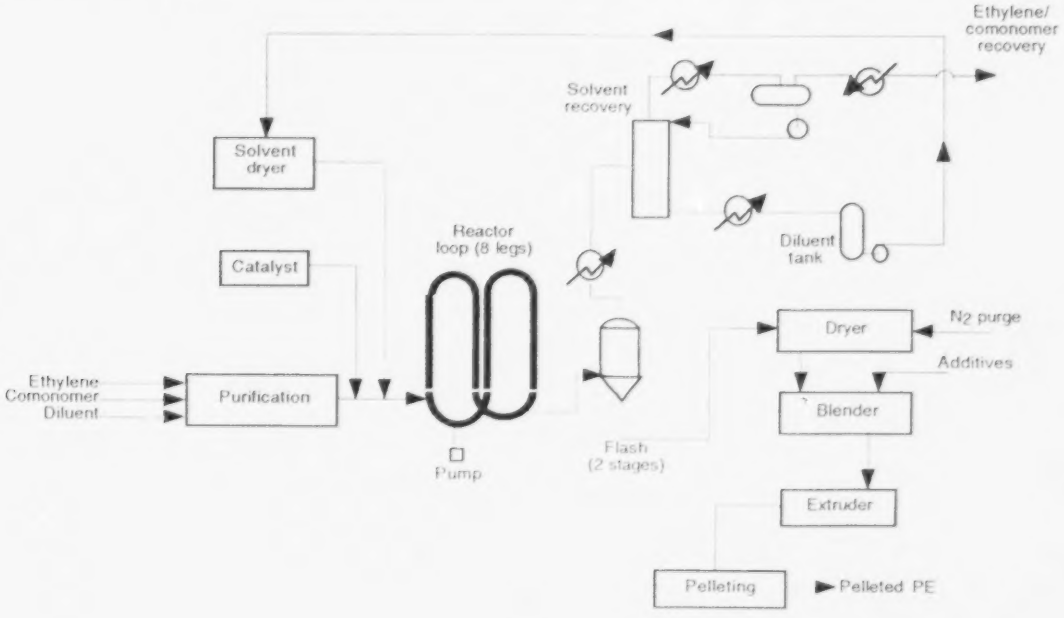

Figure 1.3: Low pressure slurry loop reactor system
(Encyclopedia of Polymer Science and Engineering, 1964-).

The main characteristic of these systems is that a solution of ethylene and comonomer is fed to the reactor in which polymer products form a suspension of solid particles in the reactor. The solvent must be selected carefully to avoid swelling of the polymer. Typical solvents in these processes

are light hydrocarbons in which the polymer must be insoluble at the operating temperatures. Catalysts used in slurry phase polymerization are supported Cr and supported Mg Ziegler-Natta catalysts. Residence times for these processes are between 1.5-2.7 hours (depending on the type of reactor). Typical conversions of ethylene in the reactor are in the range of 97 to 98%. The major attraction of this process is easy temperature control.

1.2.2.2 Solution polymerization

Solution processes were the first commercial low pressure systems and the first to produce HDPE. Now they have been supplanted by slurry processes because of their high operating cost. However, the arrival of the new metallocene catalysts has increased the interest of PE producers in solution polymerization. These processes are currently used by Dow, Mitsui, Phillips and Stamicarbon to produce LLDPE. Recently, Novacor Chemicals Ltd. purchased the DuPont Canada Sclair business to pursue the use of different solvents and catalysts, including metallocenes (Coeyan, 1994). A typical flowsheet of a solution process in shown in figure 1.4.

This process involves polymerization in a solvent at a temperature above the melting point of the polymer. Typical solvents for this system are n-hexane and cyclohexane. Reactants and products are in solution. The polymer is recovered by evaporation of the solvent. Because of the low solid content, this system requires extensive solvent recovery.

Continuous stirred reactors are used for solution polymerization. Operating temperatures for this type of reaction are above 130°C. High temperatures are needed to keep the polymer in solution. Pressures vary

significantly among companies. For example, the DuPont solution process operates at 80 atm and Stamicarbon operates at 30 atm. High pressures are needed to dissolve ethylene in the solvent. The residence times in the reactor are in the range of 5 to 10 min.

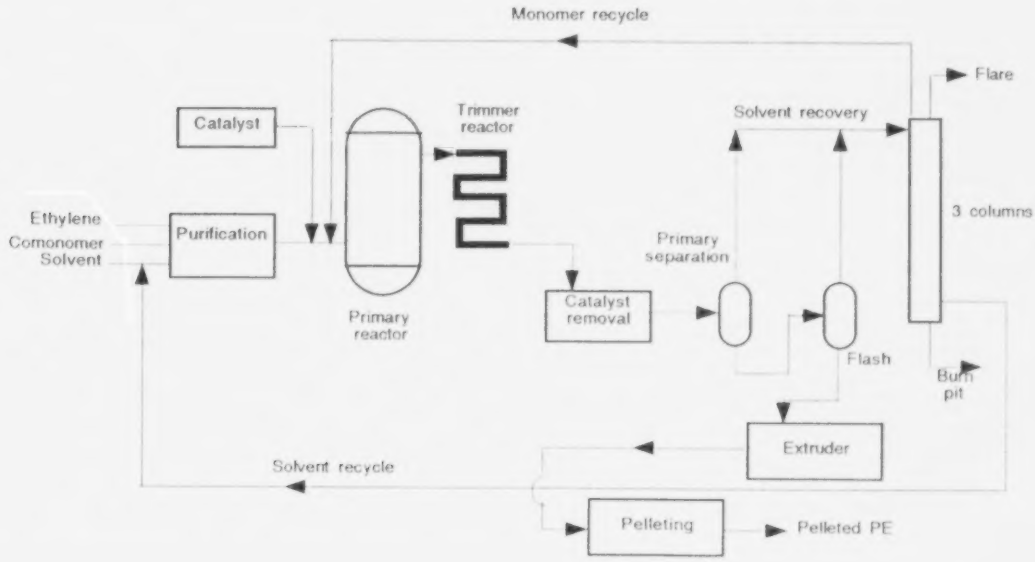

Figure 1.4: **Medium pressure solution process**

(Encyclopedia of Polymer Science and Engineering, 1964-)

Catalysts involved in solution polymerization are different among companies. Some catalysts used in solution are $TiCl_4$, $VOCl_3$, $Al(i\text{-}bu)_3$, chromic oxides and solution forms of Ti-Mg-Al compounds.

1.2.2.3 Gas phase polymerization

Gas phase polymerization is the latest technology for the production of polyolefins. In 1992, gas phase processes accounted for 22% of the world polyethylene capacity (Schumacher, 1994). There are several different gas phase processes in use. Union Carbide, BASF, Amoco and BP Chimie all

have developed their technologies. The most important process is UNIPOL developed by Union Carbide. This process was developed initially for HDPE and was commercialized in 1968 at the Seadrift, Texas plant. The process was later extended to produce LLDPE. At the end of 1992, the technology had more than 31 licensees operating in 17 countries (Burdett, 1992). Novacor Chemicals Ltd. has one such plant operating at Joffre, Alberta. UNIPOL can produce both HDPE and LLDPE at low pressure and temperature. These units can also be used to produce polypropylene and there are many possibilities for future developments for other types of polyolefins and copolymers. Figure 1.5 displays a simple flow diagram of the UNIPOL process.

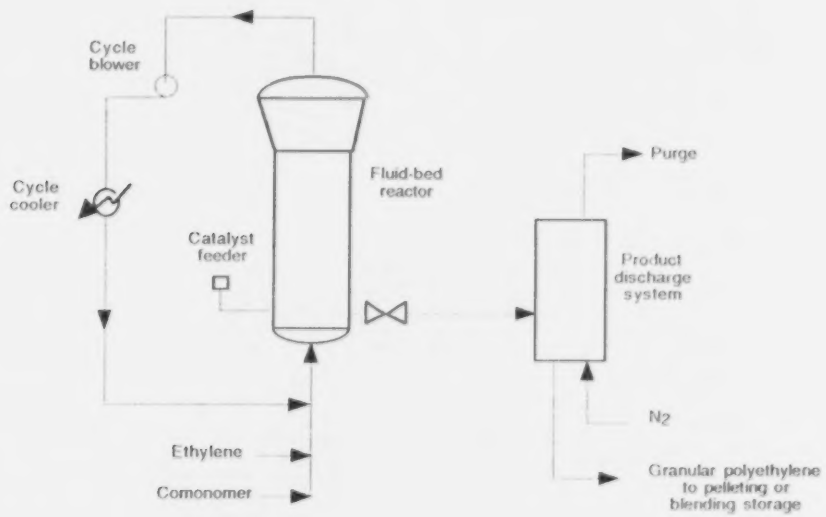

Figure 1.5: Simplified flowsheet of Union Carbide UNIPOL process (Staub, 1983)

The UNIPOL process is relatively simple. Ethylene and comonomer, if any, are fed to the bottom of the reactor and mixed with a recycled stream of unreacted monomers. The solid catalyst is added continuously in a separate

stream to the reactor. The reactor is a fluidized bed where particles of polymer produced by the reaction are fluidized by the flow of the reactants. Products are retrieved at the bottom of the reactor intermittently by a discharge system to keep a constant bed volume. Residual hydrocarbons in the products are purged with nitrogen. Then the granular product is ready for packaging if no additives are needed. Since a very active catalyst is used, only a small amount is needed and it is not necessary to separate catalyst residues from the products. The fluidized bed is usually operated at a temperature between 85 and 100°C. The operating pressure is in the range of 20 to 30 atm. Only 2% of ethylene is converted per pass so large recycle flows are needed. The overall combined conversion rate of ethylene and comonomer is about 97% to 99%. The average residence time of polymer particles in the reactor is about 2 to 3 hours. Common dimensions for the reactor are 12 m in height and a diameter of 3.5 m in the largest section of the column.

Catalyst development was the most important part for the achievement of this process. Catalyst used in the UNIPOL process must fulfill many requirements. The catalyst should have a high level of productivity (>10^5 kg product/kg transition metal). This is necessary because only a small amount of catalyst can be present in the product to avoid the need of separation of catalyst from the polymer. Catalyst types affect the molar mass distribution. Hence, it is important to have a catalyst that allows good control of MMD and that gives the required range of molar masses. It is also important that the catalyst allows a suitable comonomer incorporation. It must have also an attractive morphology since it is the template for the growth of polymer particles. Finally, the catalyst preparation must be reproducible. Final specifications for a good catalyst in UNIPOL process are based on favorable experimental results. It takes

several years of precommercial development before a catalyst can be used in full-scale industrial use. Typical catalyst used for the UNIPOL process are supported Ti, Cr and V.

Table 1.2 summarizes the low pressure polymerization processes discussed in this section.

1.3 Advantages and disadvantages of gas phase polymerization

The UNIPOL process has many economical and environmental advantages compared with the older high pressure process and low pressure liquid phase process. The Union Carbide UNIPOL process is simpler, more versatile and more economical than the other low pressure processes for the production of LLDPE and HDPE.

High pressure systems are expensive, requiring huge compressor units. Low pressure systems like the UNIPOL process require smaller and fewer pieces of equipment. Typically, high pressure systems have one 11000 hp compressor fed with several smaller compressors. In the case of the UNIPOL process, there is only one 2000 hp recirculating compressor. Hence, UNIPOL requires less energy. In fact the energy consumption of the gas phase process is 75% less than the older high pressure processes. Therefore, operating costs are much lower for a gas phase system. Because of these differences the capital investment is 50% lower for the UNIPOL process (Staub, 1983). Gas phase polymerization has advantages over the low pressure liquid phase polymerization as well. No diluent is required in the UNIPOL process. Hence, there is no need for costly diluent storage, recovery and purification.

Table 1.2: Low pressure ethylene polymerization processes (Choi, 1989)

Process								
	Liquid slurry			Solution		Gas phase		
Company:	Phillips	Solvay	Hoechst, Montedison, Dow, Mitsubichi	Stamicarbon	DuPont	Union Carbide	BASF	Amoco
Reactor	Loop reactor	Loop reactor	CSTR	CSTR	CSTR	Fluidized bed	Stirred bed	Compartmented stirred bed
Diluent (or solvent)	i-Butane	n-Hexane	n-Hexane	n-Hexane	Cyclohexane			
Catalyst	Supported Cr-catalyst	Mg-supported Z-N catalyst	Mg-supported Z-N catalyst	Solution form Ti-Mg-Al component	$TiCl_4$/ $VOCl_3$/ $Al(i\text{-}Bu)_3$	Supported Cr-catalyst/Ti-Mg catalyst	Supported Cr- catalyst	Supported Z-N catalyst
Catalyst productivity (g/g cat)	3, 000-10, 000	11, 000	3, 000			9, 000	8, 500	2, 000-40, 000
Temperature (°C)	85-110	80	80-90	130	140-150	85-100	110	70-95
Pressure (atm)	30-35	30	7.8-35	30	80	20-30	35	20-30
Residence time (hr)	1.5	2.5	2.0-2.7	0.17	0.08-0.17	3-5	4	
Conversion (%)	97-98	97	95-98	95		99		
Comonomer	1-Hexene				1-Octene	1-Butene	1-Butene	1-Butene or propylene
MM control	Temperature	H_2	H_2		H_2	H_2	H_2	H_2
MMD		Narrow-broad		Narrow P_d=3.5-5.0			Narrow-Broad	

Besides the economic advantages of the UNIPOL process, there are environmental benefits as well. The simplicity of the process and low operating pressure minimize the risk of explosion and disaster. Because there is no solvent involved in the process, hazards implied with handling large quantities of flammable liquid and the risks of major pool fires are eliminated. Levels of hydrocarbon emissions are also considerably reduced by the absence of solvent. In the case of the solution process, there are many emissions caused by residual solvent in the products.

Gas phase polymerization has other advantages. Because there is no solvent involved in the system, the process is more versatile. For slurry processes, the hydrocarbon diluent limits the polymer density for LLDPE because particles swell at practical operating temperatures. In addition, only low molar mass polymer can be produced with the slurry process because high molar mass polymer will cause a drastic increase in viscosity. In general, the UNIPOL process can achieve superior properties for LLDPE.

Besides all the advantages of the UNIPOL process, there are also some disadvantages. The gas phase is a poor heat transfer agent so it is difficult to control the reactor temperature. If the heat of reaction is not efficiently removed, local hot spots may result. This makes gas phase processes vulnerable to thermal runaway. The UNIPOL process has also some limitations on the use of comonomer. The comonomer must remain in the gas phase at the operating pressure. Consequently the choice of comonomer is confined to volatile α-olefins; 1-hexene is the largest comonomer in use with the UNIPOL process.

1.4 Structure and properties of LLDPE

The physical properties of LLDPEs depend on four structural parameters: molar mass (MM), molar mass distribution (MMD), branching and branching distribution. These properties will determine the end use of the resins. The molar mass is a measure of the chain length, or the number of monomer units that added together to form the polymer. The molar mass of LLDPE is controlled using H_2 as a chain transfer agent. Figure 1.6 shows the chemical structure of linear PE. High molar mass will give higher abrasion and impact resistance, however these polymers are more difficult to process. In a polymer resin, the molecules are not all the same size; they have a distribution of sizes. Polymers produced using different processes or operating conditions will all have distinct molar mass distributions; some will have broader distributions than others. The MMD will also affect the physical properties of polymers. Resins with a broad or bimodal MMD are easier to process than those with a narrow MMD.

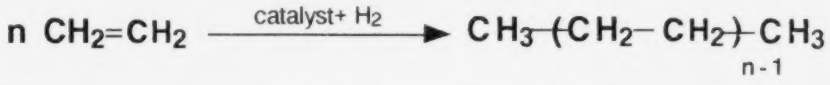

Figure 1.6: Chemical structure of linear polyethylene.

The amount of branching and the branching distribution will also affect the physical properties of polyethylene. Branching decreases the density of PE. There is two types of branching: long-chain branching (LCB) and short-chain branching (SCB). The type of branching depends upon the polymerization process. LCB occurs in high pressure LDPE (HP-LDPE) and SCB happens in both HP-LDPE and LLDPE. Long-chain branches have a marked effect on solution viscosity and melt rheology because of molecular size reduction and entanglements (Usami, 1989).

Short-chain branches have a profound effect on the morphology and solid state properties of polyethylene because they prevent an ordered arrangement of the chains. In HP-LDPE, SCB are produced by a free-radical, backbiting mechanism, while in LLDPE short-chain branches are introduced by copolymerization with α-olefin. Typical comonomers used for LLDPE are 1-butene, 1-hexene and 1-octene. The amount of SCB in LLDPE is controlled by the concentration of the comonomer in the reactor. The molecular structure of LLDPE is characterized by a linear polymer backbone with short-chain branches. Figure 1.7 shows the insertion of 1-butene in a polyethylene chain. The density of LLDPE will decrease with an increase on the number of side groups. The length of the side group will also influence the density; density decreases as the length of side groups increases. The length of the SCB is (n-2) carbon atoms, where n is the number of carbon atoms in the straight chain portion of the α-olefin molecule.

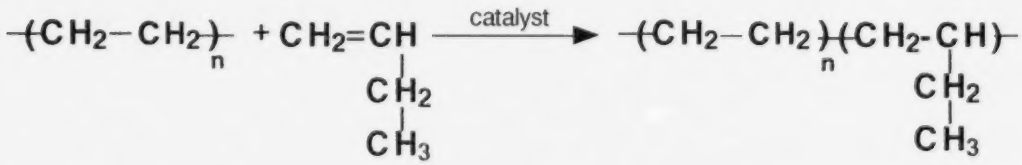

Figure 1.7: Insertion of short-chain branches by copolymerization of ethylene with 1-butene.

Gas phase polymerization using Ziegler-Natta catalysts has been investigated by many people over the last two decades. Much work has been done up to now but there are still many things that remain unexplained. Also, relatively little experimental work in gas phase polymerization has

been conducted in academic laboratories. For the production of LLDPE, the major concerns are the control of the molar mass, molar mass distribution and the incorporation of the comonomer species. Both properties will greatly affect the performance of the products. LLDPEs are more difficult to process than HP-LDPE. However, broad or bimodal MMD makes LLDPEs easier to process. The amount of comonomer incorporated and branching homogeneity will affect the impact strength, tear strength and clarity of films. The type of process and catalyst used to produce LLDPE will influence the MMD and the distribution of branches of LLDPE. It is typically found that polymers produced by gas phase polymerization with a supported catalyst have a broad MMD and a multimodal branching distribution. When a LLDPE is fractionated using temperature rising elution fractionation (TREF), two distinct peaks are usually observed: one peak with a low comonomer content and the other one with a higher comonomer level. It is believed that those observations are the result of multiple active sites in Ziegler-Natta catalysts. The purpose of this work was to examine these phenomena in detail by performing TREF and cross fractionation using size exclusion chromatography (SEC) on PE samples produced in our laboratory. The effect of H_2 and 1-butene partial pressure on properties of LLDPE produced by the copolymerization of ethylene and 1-butene in a gas phase reactor was investigated in this study.

2. Literature Survey

The discovery of Ziegler-Natta type catalysts is an important achievement in the area of catalysis and polymer chemistry. It has given new prospects for the polymerization of olefins. The production of materials like HDPE and LLDPE and other polyolefins was linked to the developments in the Ziegler-Natta catalysts area. The properties of LLDPE have been the subject of many investigations. TREF-SEC cross fractionation is a powerful tool to obtain information about molar mass and branching distributions of such polymers. The subject of this chapter is a survey of Ziegler-Natta catalyst, mechanisms of polymerization over supported Z-N catalysts and characterization of polyethylene, specifically by TREF and SEC. This section is mostly devoted to TREF literature.

2.1 Ziegler-Natta catalyst and ethylene polymerization

2.1.1 Ziegler-Natta catalysts

According to the broad patent definition, the Ziegler Natta catalyst is a mixture of a metal alkyl from group I to III and a transition metal salt from groups IV to VIII. Not all the possible combinations are effective, and many of these combinations are active only for certain monomers or under certain conditions (Boor, 1979). Aluminum alkyls have been the most extensively used metal alkyls for scientific and economic reasons. Table 2.1 shows a list of typical aluminum alkyl compounds used in Z-N polymerization.

Table 2.1: Typical aluminum alkyls for Ziegler-Natta catalysts (Kissin, 1989)

Name	Formula	Abbreviation
Triethylaluminum	$Al(C_2H_5)_3$	TEAL
Triisobutylaluminum	$Al(i\text{-}C_4H_9)_3$	TIBAL
Tri-n-hexylaluminum	$Al(n\text{-}C_6H_{13})_3$	TNHAL
Diethylaluminum chloride	$Al(C_2H_5)_2Cl$	DEAC
Diisobutylaluminum chloride	$Al(i\text{-}C_4H_9)_2Cl$	DIBAC

Transition metal salts that are used with the metal alkyl must be selected on the basis of the monomer polymerized as well as constraints like yield, stereoregularity, copolymer composition, morphology or a combination of these. The most common transition salts are $TiCl_3$ or a derivative. Other transition metals such as vanadium and zirconium are also frequently used.

Table 2.2: Typical transition metal salts in Z-N catalysts (Kissin, 1989)

Ti	V	Zr
$TiCl_4$	VCl_4	$ZrCl_4$
$TiCl_3$	$VOCl_3$	Zr tetrabenzyl
$TiCl_2$	VCl_3	$(C_5H_2)_2ZrCl_2$
$Ti(OR)_4$	V acetyl compounds	
TiI_4		

A crystalline modification of the transition metal salt can influence the activity and stereochemical control of a catalyst. Because in many catalysts, the transition metal salt and metal alkyl undergo exchange of ligand, the activity of the catalyst is sensitive to the molecular ratio of the two components.

Since the discovery of Z-N type catalysts, many improvements have been made to enhance the performance of catalysts. The first generation of Ziegler-Natta catalysts were a solid solution of δ-$TiCl_3$ with 33% of $AlCl_3$. This catalyst was ball milled and heat treated. Surface areas were typically in the range of 10 to 40 m^2/g (Tait, 1986). The co-catalyst used was an aluminum alkyl. The second generation of Z-N catalyst was an effort to improve the activity and the stereospecificity (for polypropylene polymerization) of the catalyst. This amelioration involves the addition of a third component called an electron donor. Electron donors are usually Lewis bases added together with the activator before ball milling.

Solvay & Cie had developed a catalyst preparation to enhance the performance of a $TiCl_3$ catalyst (Seymour and Cheng, 1986). $TiCl_4$ was reduced by $AlEt_2Cl$ in an inert solvent to generate a solid product. This solid was then treated with diisoamyl ether to dissolve out of the solid matrix much of the $AlCl_3$ and $AlEt_2$ that had been previously formed. Then the solid was isolated and reacted with $TiCl_4$. The resulting catalyst had a higher porosity with a surface area greater than 150 m^2/g. When used in conjunction with AlEt2Cl, this catalyst polymerized polypropylene and other α-olefins. This type of catalyst had a five-fold increase in activity over the first generation δ-$TiCl_3$ catalysts (Tait, 1986).

The next step in the evolution of Z-N catalysts has been the development of highly active supported catalysts. The characteristics that the industry was aiming for were a high level of activity and an improvement of polymer quality. Table 2.3 shows a summary of the optimal characteristics of a good industrial catalyst. In addition to the two main components, modern Z-N catalysts also contain supports, inert carrier and electron donors. The support is inactive by itself but it increases catalyst activity or changes the properties of produced polymer. Typical supports are $MgCl_2$, silica and alumina. The most widely used support is $MgCl_2$ (Kissin, 1989). For gas phase polymerization, a typical catalyst consists of an active metal such as Ti, V or Cr and a porous silica and magnesium chloride support.

Table 2.3: Industrial catalysts requirements (Tait, 1986).

High catalyst productivity
Range of molar mass
Range of molar mass distribution
Good comonomer incorporation
Attractive particle morphology (spheres)
Simple, reproducible catalyst preparation

The synthesis of supported catalyst involves two steps: preparation of the support and preparation of the catalyst. For $MgCl_2$ to be a suitable support, the $MgCl_2$ must contain less than 1 mass% of water. Several methods have been developed for the preparation of the $MgCl_2$ support: 1) the support is pretreated thorough prolonged grinding in a pure state, in the

presence of an electron-donor or in the presence of $TiCl_4$; 2) chemical pretreatment of $MgCl_2$ by electron-donor compounds; 3) a highly dispersed $MgCl_2$ can be synthesized via reactions of Grignard reagents with halogen-containing compounds. In the second step of the catalyst preparation, a tetravalent titanium derivative is put in contact with the pretreated solid to generate the supported catalyst (Kissin, 1985). Figure 2.1 summarizes the preparation of a $MgCl_2$ supported catalyst.

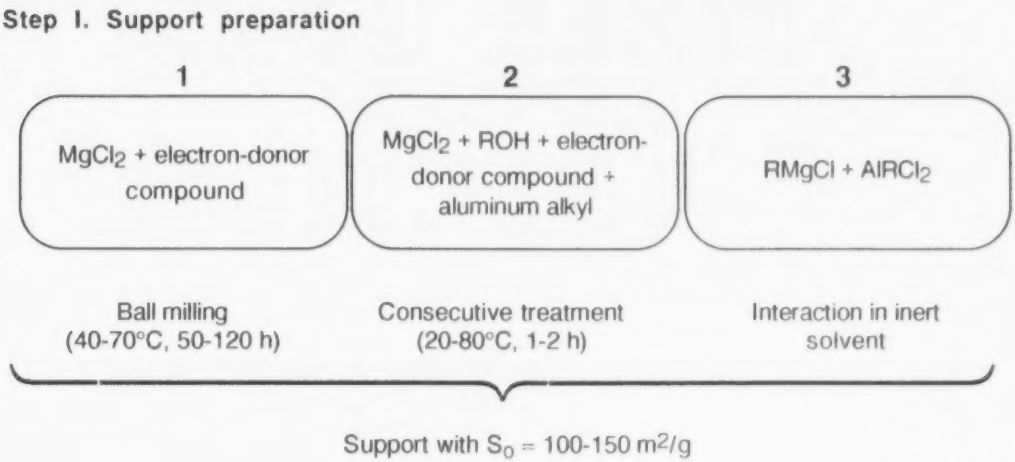
Step I. Support preparation
1
2
3
MgCl2 + electron-donor compound
MgCl2 + ROH + electron-donor compound + aluminum alkyl
RMgCl + AlRCl2
Ball milling (40-70°C, 50-120 h)
Consecutive treatment (20-80°C, 1-2 h)
Interaction in inert solvent
Support with S0 = 100-150 m2/g
Step II. Catalyst preparation
Support + TiCl4 3,3' (80-135°C, 2 h)
Active solid component. [Ti] = 1.3-2.2 wt%, S0 = 150-200 m2/g

Figure 2.1: General scheme of $MgCl_2$ supported catalyst synthesis (Kissin, 1985)

The latest advances in the development of catalysts for olefin polymerization involve supported Z-N catalysts with a better morphological control and the family of metallocenes catalysts. Metallocenes catalysts will

take an important place in the catalyst market in the future years. Metallocenes catalysts have some interesting features: they can polymerize different types of monomers, polymers with narrow MMD can be produced because of their single site characteristic, polymers with unsaturated vinyl end groups can be generated which means that this double bond could be use for functionalisation and finally, metallocene catalysts can produce polymer with very high stereoregularity (Sinclair and Wilson, 1994). It is expected that the sales of metallocene-based polymers will reach $21.6 billion/year by the year 2000 (Rotman, 1994).

2.1.2 Formation of active center of supported Ziegler-Natta catalyst

The mechanisms of formation of active sites, chain propagation and chain transfer for supported Ziegler-Natta catalyst system were discussed by Karol (1978). The formation of the active site for polymerization using a support such as Mg(OH)Cl involves three stages. The first step is the formation of an active surface complex of $TiCl_4$/Mg(OH)Cl by chemisorption of $TiCl_4$ on the support. This is accomplished by the reaction of a halogen atom from $TiCl_4$ with the hydroxyl groups at the surface of Mg(OH)Cl resulting in a Ti-O bond.

(2.1)

In the second step, the supported titanium compound is activated by addition of an aluminum alkyl. This stage involves the exchange of halogen atoms in the transition metal compounds and alkyl groups.

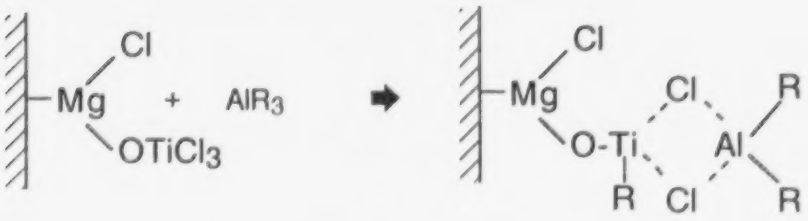

(2.2)

The initiation of the propagation is achieved by the insertion of a coordinated monomer into the Ti-C bond. The repetition of this step constitutes the propagation reaction. An illustration of this step is shown below.

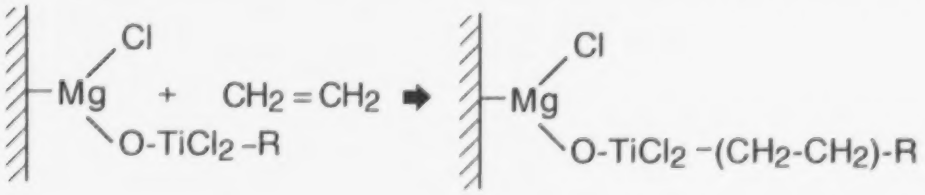

(2.3)

2.1.3 Multiplicity of active sites in supported Ziegler-Natta catalysts

Active center inhomogeneity is a well-known attribute of heterogeneous catalysts. The very first experiments on polyolefin synthesis with polypropylene using heterogeneous Z-N catalyst revealed inhomogeneity of active sites. The products were a mixture of molecules with different molar mass and stereoregularity. The data obtained on the chemical structure of the polymer suggested that the polymers produced were the results of chemically similar, but different types of catalytic centers (Kissin, 1986). It also has generally been observed that polyolefins produced with this type of catalyst have broad MMD with polydispersities ranging from 4 to 11 and even

higher. Two theories have been developed to explain the broad MMD of polyolefins produced with supported catalysts: diffusion theory and multiple active centers theory. The diffusion theory emphasizes the effect of monomer concentration on the molar mass development; the multiple active centers theory highlights the influences of active centers and kinetic parameters. A brief description of the experimental results that support each of these theories was compiled by Xie et al., 1994.

Diffusion limitations:

- Polymerization rate depends on stirring speed when agitation speed is below a critical level.
- Molar mass of PE formed in the initial period of polymerization is much higher than that of polymer formed in the later stages.
- The polymerization rate of ethylene increases significantly in the presence of small amounts of comonomers. This was explained by the reduction of the diffusion resistances caused by a decrease of the crystallinity of polymer. Comonomer incorporation in a polymer chain results in a decrease of both crystallinity and density.

Multiple active centers:

- Different transition metal catalysts can provide large changes in polymer MMD
- Heterogeneous catalyst can produce broad MMD, even when the polymer is in solution.
- Homogeneous soluble catalysts provide narrow MMD, even when the polymer is insoluble in the reaction medium.
- High-activity catalyst does not necessarily provide broad MMD.

- Copolymer produced using supported catalyst generally show a bimodal composition distribution and even trimodal distributions have been observed. The reactivity ratios measured by ^{13}C NMR were different for each of these peaks.

The last evidence strongly suggests that polymer chains are formed at different active sites. However, these phenomena cannot provide conclusive proof of multiple active sites formation mechanisms, but they suggest that the molar mass development of PE is a function of the nature of the catalyst and polymerization mechanisms.

2.1.4 Kinetics of supported Ziegler-Natta catalysts

Despite the tremendous amount of research that has been conducted in the area of Ziegler-Natta catalysis, no definitive chemical reaction mechanism has been developed to describe fully the kinetic behavior of ethylene homo/copolymerization due to the complexity of the systems employed (Xie et al., 1994). However, the key elementary reactions have been established as follow:

- Formation of active centers
- Insertion of monomer into growing polymer chains
- Chain transfer reaction
- Catalyst deactivation

The mechanism mentioned above has been developed from the Cossee mechanism (Cossee, 1964) and adapted for the case of multiple sites. The most important steps in polymerization reactions are chain propagation and chain transfer. In the case of ethylene/1-butene copolymerization, the chain

propagation and chain transfer reactions for a single site, according to Caracotsios (1992), can be represented as follows:

Chain propagation

$$[E] + [C_2^=] \xrightarrow{k_{11}} [E] \quad (2.4) \qquad [B] + [C_2^=] \xrightarrow{k_{21}} [E] \quad (2.5)$$

$$[E] + [C_4^=] \xrightarrow{k_{12}} [B] \quad (2.6) \qquad [B] + [C_4^=] \xrightarrow{k_{22}} [B] \quad (2.7)$$

Chain transfer to hydrogen and aluminum alkyl

$$[E] + [H_2] \xrightarrow{k_{h1}} [D] \quad (2.8) \qquad [E] + [Al] \xrightarrow{k_{a1}} [D] \quad (2.9)$$

$$[P] + [H_2] \xrightarrow{k_{h2}} [D] \quad (2.10) \qquad [P] + [Al] \xrightarrow{k_{a2}} [D] \quad (2.11)$$

The notation for the reaction mechanism is as follows (chemical species concentration are in kmole per unit volume): [E] represents active polymer chains that end with an ethylene monomer, [B] active polymer chains that end with a 1-butene monomer and [D] are inactive polymer chains detached from the active centers. [Al], [H_2], [$C_1^=$] and [$C_2^=$] represent bulk phase concentration of aluminum alkyl, hydrogen, 1-butene and ethylene. The polymer chain self- and cross-propagation constants are k_{11}, k_{22}, k_{21} and k_{22}; k_{h1} and k_{h2} are the hydrogen termination constants and k_{a1} and k_{a2} are the chain transfer to aluminum constants.

In the case of multiple active sites, the development is similar when it is assumed that each type of active site has the same reaction mechanism. The difference is that each site will have its reaction rate. These elementary reactions have been commonly adopted in modeling studies (de Carvalho et al., 1989,1990; McAuley et al. 1990; Caracotsios, 1992).

A standard treatment of the Equation (2.4 to 2.7) consists of the introduction of two reactivity ratios:

$$r_1 = k_{11}/k_{12} \qquad (2.12)$$

$$r_2 = k_{22}/k_{21} \qquad (2.13)$$

The reactivity ratios can be easily obtained if the copolymerization is carried out at constant monomer concentration using the following relationship (Kissin, 1985):

$$f = F\frac{r_1 F + 1}{r_2 + F} \qquad (2.14)$$

where F is the ratio of the monomer and comonomer concentrations in the reactor ($[M_1]/[M_2]$) and f is the ratio of molar concentration of the momomer and comonomer, M_1 and M_2 respectively, in the copolymer produced. The calculation of r_1 and r_2 can be performed by a numerical curve fitting method (Braun et al., 1973). This method is based only on the measurements of copolymer composition corresponding to different compositions of monomer mixtures. The reactivity ratio gives information about monomer reactivities and can also be used to get kinetic parameters.

2.2 Characterization of Polyolefins

Polyethylene properties are strong functions of the polymerization conditions. It is important to have tools that will allow a complete characterization of the polymer produced. The properties of interest can be: elemental composition, branching distribution, molar mass distribution, molar mass, density and rheological properties. In this section, a description of the tools for the characterization of polyethylene will be presented as follows: melt index, differential scanning calorimetry (DSC), infrared

spectroscopy, ^{13}C NMR, size exclusion chromatography (SEC) and temperature rising elution fractionation (TREF).

2.2.1 Melt index

In the industry, polyethylene grade specifications are given in terms of melt index (MI) and density. The melt index is the amount of polymer that will flow trough an orifice under a standard weight. The results are usually reported in g/10 min. Melt indexes are used to provide relative properties of a polymer. It gives no information about the structure. The melt index of a polymer is a function of the branching and molar mass distributions. Polymers with the same molar mass but different branching distributions may have different melt indexes. The melt index is a convenient method to determine relative molecular sizes in an industrial environment. While the melt indexes are correlated with molar mass, there is however, no simple relationship between MM and MI for a broad range of molar mass. Simplified expressions are available for limited MM ranges (Bremner and Rudin, 1990). Usually an increase in molar mass will cause a decrease of the melt index. MI can be used to get a rough estimation of polymer properties and can be used to compare the effects of different operating conditions on average MM.

2.2.2 Differential Scanning Calorimetry

Differential scanning calorimetry (DSC) has many applications in the polymer area. It can be used to estimate properties such as glass transition temperature, heat capacity, crystallinity and heat of fusion. In a typical DSC measurement, the sample is brought to a desired initial temperature and then the temperature is changed to the final temperature according to a

predetermined rate. The device records the power as a function of time needed to reach the final temperature. When a transition such as melting or crystallization occurs, an endothermic or exothermic reaction takes place. These transitions can be observed as a peak on a plot of heat flow versus temperature. The area of the peak indicates the total energy transferred to the sample. The area under the melting peak is a direct measure of the heat of fusion. Since DSC is an instrument that is sensitive to the crystallinity of material, it can also be considered as a possible alternative to analytical TREF characterization. DSC can provide a profile of relative amounts of material with differing crystallinities, in terms of melting temperature (Karbashewski et al. 1992).

2.2.3 Infrared Spectrometry

Infrared spectroscopy (IR) can be used to characterize polymers. The absorption of light by the different bonds in a molecule leaves a distinctive fingerprint for each group present in that molecule. By performing an IR scan on a polymer sample, information can be obtained about chemical structure of the polymer. IR spectroscopy is excellent to detect carbon chains, methyl, OH and NH groups. The frequencies of interest for LLDPE are the ones corresponding to the absorption by the CH_2-CH_2 stretch of the polymer backbone and by the methyl groups corresponding to the branches. Fourier transform infrared spectroscopy (FTIR) can be used to evaluate the branching concentration of a polymer by measuring the absorbance of polyethylene due to methyl groups (ASTM D2238-92). IR spectrometers are frequently used as detectors for other applications. For example, IR detectors are used to measure the polymer concentration in TREF systems. For this application, the wavelength of interest is corresponding to the CH_2-CH_2 stretch (3.41 μm).

2.2.4 Nuclear magnetic resonance

Nuclear magnetic resonance (NMR) is a spectrometric method based upon the measurement of absorption of electromagnetic radiation. In contrast to infrared and UV absorption, nuclei of atoms are involved in the absorption process. In the NMR technique, a compound is positioned in a strong magnetic field and irradiated with a radio-frequency signal. This signal will be absorbed at some discrete frequencies. The exact frequency at which the energy is absorbed is very sensitive to the atomic environment of the nuclei investigated. The most common nuclei examined are ^{1}H and ^{13}C. ^{1}H is more sensitive than ^{13}C on an equal nuclei basis. However, ^{13}C has an interesting feature: it can be used directly to determine the skeleton of an organic molecule. The chemical shift for ^{13}C NMR depends on the structure of the molecule for up to three bonds in all directions from the site of interest. This makes ^{13}C NMR a useful tool to characterize the structures of polymers. It is an effective tool to get branching information of a polymer. However, analysis of short-chain branching by this method gives only average values rather than distributions. It is limited in the case of LLDPE because these polymers typically exhibit multimodal chain branching distributions which cannot be described by an average number of branches (Karbashewski et al., 1992). ^{13}C NMR is also used for many other applications including: compositional analysis, determination of isotactic-atactic ratio and for solid polymers it is possible to measure T_g and T_m (Rodrigez, 1989).

^{13}C NMR analysis is usually carried out using a solution of the polymer to be studied. It can also be performed on a solid but the resolution is lower. NMR can be operated at temperatures ranging from -195.8°C (liquid

nitrogen) to 150°C. It provides the best characterization of the structure of a compound. It may also provide a general characterization by functional groups which cannot be obtained by other methods (Cheremisinoff, 1989). However, ^{13}C NMR is very difficult to use routinely and it is expensive.

2.2.5 Size exclusion chromatography

Molar masses and molar mass distributions are important properties of polymers. They affect the rheology, processability and many other physical properties. There are a few methods that can be used to determine average molar masses: light scattering, osmotic pressure and a method related to the viscosity of melts. These methods give only an average molar mass. They provide no information about the molar mass distribution. The most efficient method to get molar mass distribution is size exclusion chromatography (SEC). It is also frequently referred to as gel permeation chromatography (GPC). SEC is a means of separating molecules by differences in their effective size in solution. This separation is accomplished by injecting the polymer solution into a continuously flowing stream of solvent which passes through rigid gel particles closely packed together in a column (Waters/Millipore SEC operating manual). The principle of the method is illustrated in Figure 2.2.

The process starts with the injection of a mixture of small and large molecules into one end of a column packed with porous beads. Initially there is a concentration gradient causing diffusion of polymer into the beads. However, the large molecules cannot infiltrate into the beads. As the large molecules are carried away by the solvent, the concentration gradient is

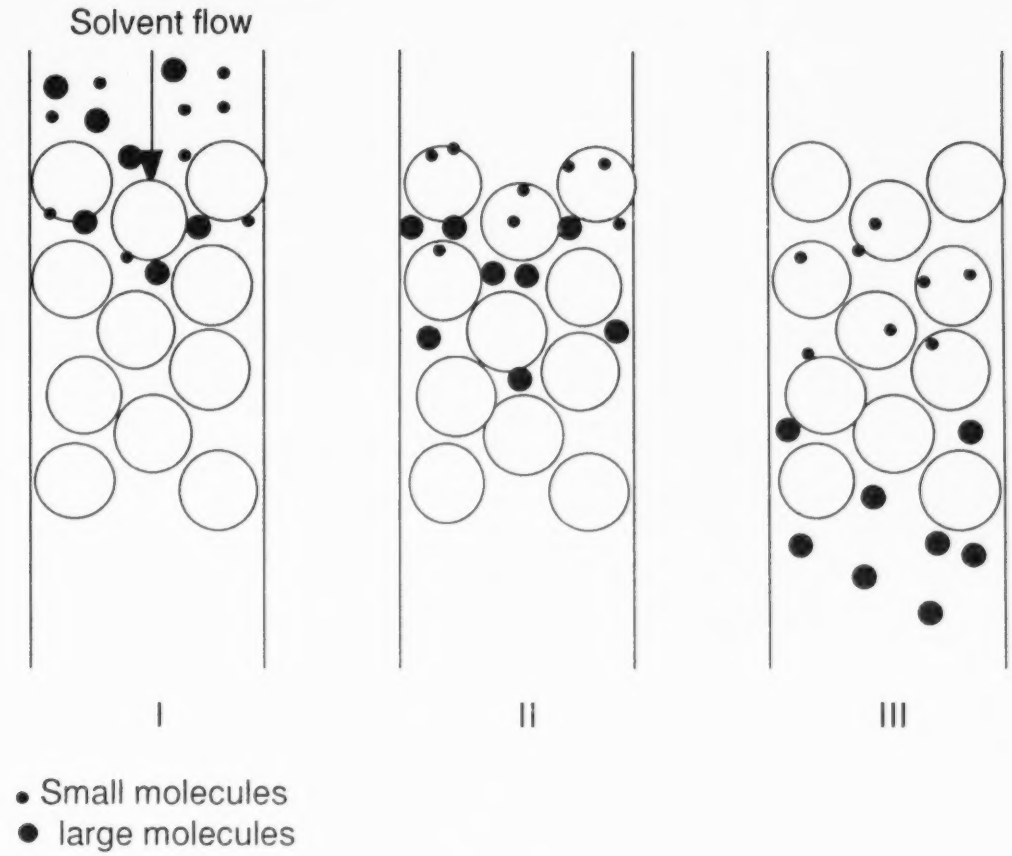

Figure 2.2: Process of size exclusion chromatography: I Sample injection, II elution and III continued elution (Rodrigez, 1989).

reversed, allowing the small molecules to diffuse back out of the beads. This process is repeated as the sample moves through the column. This process results in the large molecules emerging first from the column. The smallest molecules, which have been retarded by the diffusion process, will come out last.

A typical system for gel permeation chromatography is shown in Figure 2.3. The apparatus consists of the following basic components: solvent reservoir, pump, sample injection valve, packed columns, a detector and a data processing system. The most important parts of the system are the

columns responsible for the separation process. The detector monitors the concentration of the molecules eluting from the SEC columns. The most widely used detector in SEC is the differential refractometer (DRI). Other frequently used detectors are functional group detectors such as ultraviolet and infrared (Provder, 1987), low angle laser light scattering detectors and viscosity detectors.

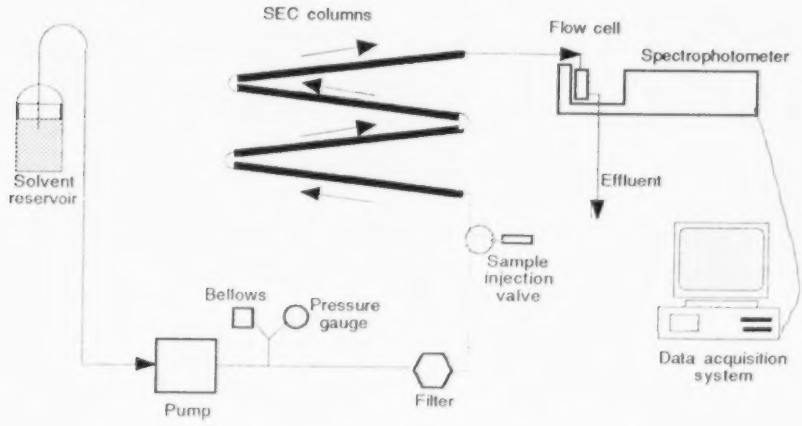

Figure 2.3: Basic parts of SEC apparatus (Rodrigez, 1989)

The molar mass of a sample can be determined by different methods: narrow standard method, broad standard method and universal calibration. In the narrow standard method, narrow molar mass samples with known values are injected and their retention times are recorded. These retention times can be correlated according to their specific molar mass. This correlation becomes the basis of calibration and allows the determination of the molar mass of an unknown by comparing its retention time with the standards retention time. In the case of the broad standard method, the goal is to find an effective calibration curve so that the computed molar mass values are in agreement with the known values of the polymer standards.

Universal calibration is an empirical method used to obtain more precise molar mass values. This method involves the use of the hydrodynamic volume concept. The SEC separation mechanism is based upon molecular size in solution (hydrodynamic volume). Therefore, if a parameter related to this volume is used, a common calibration curve for various polymers can be obtained. Polymers having different chemical structures or polymers having the same chemical structure but different chain configuration will have a unique calibration curve (Provder, 1987). It is primarily used with narrow standards but can also be used with broad standards. The method involves the use of Mark-Houwink constants to generate the calibration curve (de Kok and Oomens, 1982).

The molar mass distribution of a sample is constructed from the retention time and the corresponding polymer concentration obtained from the SEC analysis. The data are processed using the calibration curve and the results are given as molar mass distribution plots. The average molar masses are computed from the distribution using the following relationships:

$$M_n = \frac{\sum N_i M_i}{\sum N_i} = \frac{\sum W_i}{\sum (W_i/M_i)} \tag{2.15}$$

$$M_w = \frac{\sum N_i M_i^2}{\sum N_i M_i} = \frac{\sum W_i M_i}{\sum W_i} \tag{2.16}$$

where M_n is the number average molar mass and M_w is the weight average molar mass. In the industry, the properties of the polymer are often correlated with M_w. The polydispersity (P_d) of a polymer is related to its molar mass distribution. Polymers with broad MMD will have higher polydispersities. The polydispersity of a polymer is defined as the ratio of M_w to M_n

$$P_d = \frac{M_w}{M_n} \qquad (2.17)$$

2.2.6 Temperature rising elution fractionation

The wide range of physical properties observed for polyolefins results from the diversity of composition distributions produced by the various polymerization processes. Temperature rising elution fractionation (TREF) is a recent tool that has been developed to obtain the branching distribution of a polymer. TREF is based upon crystallizability differences in polyolefins. Crystallizability in polyethylene and α-olefin copolymers arises from strong van der Waals' forces between neighboring carbon chains. The absence of side branches in a linear polyethylene will produce a highly crystalline polymer. However, if side branches are introduced through the polymerization process, as with high pressure low density polyethylene (HP-LDPE) or by the copolymerization of an α-olefin, such as 1-butene, the crystallizability and the density of the polymer will be reduced (Wild, 1993). The objective of the TREF technique is to provide a separation based upon differences in crystallizability.

The TREF procedure is divided in two steps: crystallization and elution of the sample. The crystallization is achieved by slow-cooling of a polymer solution. The crystallization step is important because it will affect the quality and reproducibility of the separation. In the elution step, the polymer is stripped from the column by eluting with a solvent at increasing temperature. When the crystallized species dissolve, they are carried away by the solvent. In a typical TREF apparatus, an IR detector is used to measure the concentration of polymer and a computer is used to collect both temperature and IR signal from the TREF apparatus. The output from the

TREF is a profile of concentration versus elution temperature, which can be related to the composition distribution via a calibration curve. TREF can be operated in two ways: analytical TREF (ATREF) and preparative TREF (PTREF). Preparative TREF involves the fractionation of a polymer sample to recover fractions that can be further analyzed by other techniques such as ^{13}C NMR or SEC. In analytical TREF, a sample is eluted and the concentration is recorded as the temperature of the solvent increases. The analytical TREF method is used to obtain branching distributions.

TREF is the main technique used in this research. Hence, a detailed literature survey of this topic is presented below.

2.3 TREF: literature survey

The origin of TREF goes back to the 1950s when Desreux and Spiegels (1950) first described a method for the fractionation of polyethylene samples. At that time, many authors proposed that polymers had a distribution of chain lengths and they assumed the possibility of heterogeneity in branching distribution. However, no tools were available to observe these facts. It is with this idea in mind that Desreux and Spiegels tried to develop a tool that would provide information about molar mass and branching distributions of a polymer. Their method involved the deposition of a polyethylene sample from a solution on a support followed by elution in a column at controlled temperature using toluene as the solvent. They recognized that the separation process was based upon differences in molar mass and crystallinity of polyethylene. In the years that followed their initial efforts, the main objective of polymer separation was to establish molar mass distributions.

It is the work of Shiramaya et al. (1965) that began the development of TREF as we know today. They were the first to introduce the term "temperature rising elution fractionation". They described a method to fractionate HP-LDPE according to the degree of short-chain branching. The development of the current TREF technology is related to the TREF method developed by Shiramaya et al. (1965) to investigate short-chain branching on commercial HP-LDPE. In their system, large amounts of polymer (10 g) were fractionated. About 1400 g of sea sand coated with polymer was introduced into a column (70 mm in diameter and 380 mm in length). The polymer sample was coated onto sea sand by slow-cooling of a hot xylene solution. The temperature was raised in a stepwise fashion from 50°C to 80°C using a temperature controlled oil bath. The temperature was kept constant at each level for 30 minutes to assure temperature equilibrium before starting the next extraction. Then 350 ml of preheated xylene was added dropwise over a 60 min period at each level of temperature. They were able to obtain 10 fractions for each run. The fractions were characterized by infrared to obtain the degree of short-chain branching.

The work by Shiramaya et al. (1965) was a good demonstration of the practical application of TREF and it encouraged further developments of the technique for polyethylene analysis (Wild, 1990). Their work led, many years later, to the development of systems with more robustness and continuity.

In the 1960s, the focus was on the elaboration of a technique that could separate a polymer according to molar mass. Most efforts in polyolefin characterization were put to the development of size exclusion chromatography (SEC). In the mid 1970s SEC was an efficient method to

obtain information about molar mass distributions. However, the broad range of properties of new resins like HDPE and LLDPE could not be explained only by MMD. More information about the structure and composition of the resins was necessary. The TREF technique that had been dormant for a decade was a potential method to obtain such information.

The TREF technique came on the scene again when Wild and Ryle (1977) described a new type of TREF system constructed with metal and using a temperature controlled oil bath. They also described the first analytical TREF system. The preparative TREF system consisted of a stainless steel column (50.8cm x 12.7cm) packed with Chromosorb-P support onto which a polymer sample (4 g) was crystallized by slow cooling from a programmable oil bath. The fractionation was achieved by eluting the column with xylene with a flow rate of 20 ml/min while increasing the temperature at a rate of 8°C/min. The short-chain branching (SCB) distribution of the polyethylene was obtained by collecting the fractions, weighting and analyzing by IR spectroscopy (ASTM D2238-64T Method B).

Wild and Ryle (1977) were the first to recognize the importance of the crystallization step. Using their PTREF system, they conducted a series of experiments with different cooling rates to obtain optimum separation in the elution step. Using a series of constant cooling rates ranging from 20°C/h to 0.5°C/h it was concluded that the separation improved down to a rate of 2°C/h and no improvement was noted for lower cooling rates. This series of experiments was conducted using different polyethylenes samples. A single linear relationship was observed between elution temperature and methyl group content when the cooling rate was less than or equal to 2°C/hour. This relationship was a potential calibration curve for TREF.

Bergström and Avela (1979) developed a similar PTREF apparatus to study HDPE and HP-LDPE. They used a 5 liter column filled with Chromosorb and loaded with a 4 g polymer sample in a 1% xylene solution. The column was loaded at 120°C, cooled down quickly to 90°C and then a cooling rate of 1°C/h was used until the temperature reached 40°C. The elution was performed using 20 ml/min of xylene with a temperature increasing rate of 4°C/h from 50 to 90°C. The temperature was controlled using a programmable oil bath. Four fractions were collected per hour. The fractions were precipitated with ethanol, filtered, dried and weighed. The methyl content of HP-LDPE was measured by IR spectroscopy according to ASTM D 2238-64T method B from pressed plaques. Differential thermal analyses (DTA) were also performed on the fractions to obtain melt temperatures. Contrary to Wild and Ryle (1977), their results showed that the methyl content of the fractions did not correlate well with the elution temperature of TREF.

A very sophisticated TREF system has been introduced by Nakano et al. (1981). This system performed automatic cross fractionation. This TREF procedure involved the fractionation of samples by differences in crystallinity, followed by a molar mass fractionation using SEC. This was the first attempt to combine both TREF and SEC to produce a detailed characterization of a polymer. With this system they studied four LDPEs and one HDPE. For the analysis, 3.5 g of polymer were dissolved in ortho-dichlorobenzene (o-DCB) and deposited by slow cooling of the solution in a column (150 x 8 mm) packed with glass beads. The sample concentration was 10 mg/ml. The elution was performed using stepwise temperature increases from 40 to 140°C with a solvent flow rate of 1 ml/min. Typical temperature

steps used were: 40, 50, 60, 65, 70, 73, 76, 80, 84, 88, 90, 92, 95, 98, 101, 105, 110 and 140°C. The fractions were injected directly from the TREF apparatus to a SEC. Each cross fractionation took about 10 hours to complete. Some fractions were collected by bypassing the SEC. These fractions were collected in sufficient amount to be analyzed by IR spectrometry to generate a relationship between methyl group concentration and elution temperature. Contrary to the results of Wild and Ryle (1977), they concluded that there is no universal linear relationship between methyl group concentration and elution temperature. A universal linear relationship was not obtained because crystallinity depends on the type of short-chain branching. However, the TREF-SEC cross fractionation revealed itself to be a powerful tool to obtain quantitative, combined information about branching and MMD.

From their conclusions with the use of PTREF, Wild and Ryle (1977) developed an analytical TREF system. The basic idea of the ATREF was to obtain branching information from elution temperature using a relationship between methyl group content and elution temperature. The system that came from this idea had many new features compared to the older PTREF system. A high temperature differential refractometer, a temperature-programmable recirculating oil system, easily removable column with reduced size (38 cm x 2.4 cm) and a two pen-recorder was incorporated in the system. The crystallization was now carried out in a separate oil bath to optimize the time spent on the TREF. This way, up to 6 columns loaded with hot solutions of 0.2 g polymer in 50 ml 1,2,4-trichlorobenzene (TCB) could be crystallized simultaneously at a rate of 1.5°C/h. The samples were eluted with a heating rate of 8°C/h using 6 ml/min TCB. The concentration of polymer in the eluent

and the elution temperature were displayed on a two-pen recorder. A diagram of this system is shown on Figure 2.4. ATREF was performed on commercial HDPE and HP-LDPE using this system. From their results, they concluded that ATREF is an effective tool to obtain branching information. They suggest that polyethylene and all semicrystalline polymers could be characterized by analytical TREF using a single calibration curve.

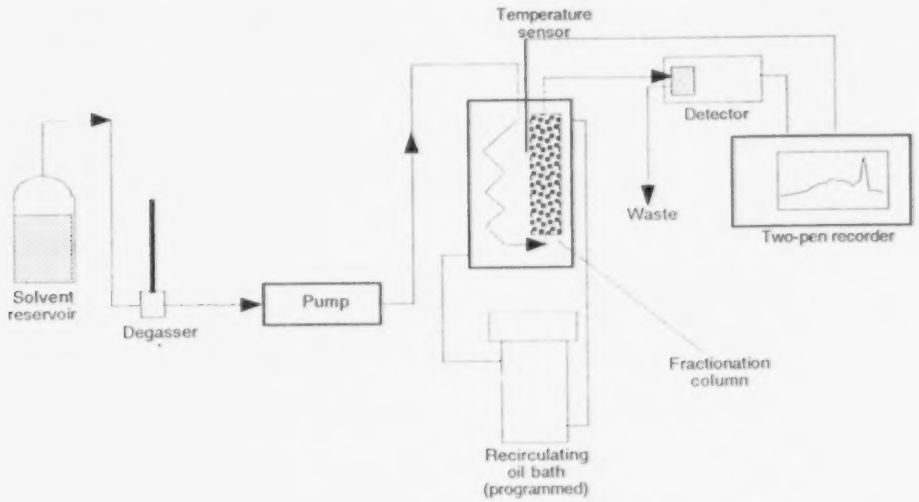

Figure 2.4: Diagram of ATREF system
(Wild and Ryle, 1977)

The first to who investigate LLDPEs using the analytical TREF technique were Wild and Ryle (1982a). The system they used has been improved considerably since the original unit. It is more effective and it is a more efficient means of determining SCB distribution. They decreased the time required to do ATREF analysis and improved the resolution. Two fractionations could easily be done per day, which was a huge improvement compared to the earlier two or three runs per week. The column and the sample size were reduced considerably to 12.7 mm x 2.5 mm and 0.05 g, respectively. The use of a smaller column reduced the channeling, dead spots

and temperature gradients in the column. In that publication, they looked at the dependence of molar mass in the mechanisms of fractionation in TREF. They concluded that if the molar mass of a sample is lower than 10000, separation by molar mass can take place. However the strongest effects were for MM lower than 1000. Wild and Ryle (1982a) also studied cocrystallization effects and observed that they were negligible. They used ATREF to characterize HDPE, HP-LDPE, ethylene/1-butene copolymer, ethylene/vinyl acetate (EVA) copolymer and ethylene/ethyl acrylate copolymer. Bimodal branching distributions were observed for ethylene/1-butene LLDPE.

To generate the distribution of methyl group concentrations, a calibration curve relating methyl group concentration and elution temperature is needed. However, no commercial standards are available to produce such calibration. Wild and Ryle (1982a) produced a calibration curve using fractions from narrow MM polyethylene samples and fractions from ethylene/1-butene copolymer. The degree of branching for the fraction was determined using FTIR on pressed films. An excellent linear relationship was observed by Wild and Ryle.

In a short publication released shortly after the aforementioned paper, Wild and Ryle (1982b) described the cross fractionation of a series of LLDPE and a HP-LDPE. The PTREF method used has been described previously. The fractions collected were analyzed by SEC to obtain the MMD of each fraction. The results from the cross fractionation were used to generate 3-D profiles describing the frequency distribution of the polymer as a function of both molar mass and SCB. It was observed that there is a significant trend toward the lower molar mass species to be more branched. However, this

trend was stronger in the case of HP-LDPE than LLDPE for which the dependency was very slight. Bimodal branching distributions were observed for LLDPE. The MMD obtained from HP-LDPE fractions were narrower than the ones from LLDPEs.

The heterogeneity of the branching distribution of LLDPE was a phenomena of great interest. Usami et al. (1986) performed a complete characterization of LLDPEs produced on $MgCl_2$ supported, $TiCl_4$ or $TiCl_3$ based Z-N catalysts. The LLDPEs were fractionated by an automatic TREF-SEC apparatus. Analytical TREF profiles were obtained and fractions were recovered by TREF-SEC cross fractionation. The fractions recovered were further analyzed using ^{13}C NMR, DSC and FTIR. Comparison of the analytical TREF curves indicated that LLDPEs produced using different conditions of temperature, pressure and solvent had in common a characteristic bimodal distribution of SCB. Using ^{13}C NMR, they estimated values of reactivity ratio $r_1 \cdot r_2$ from the different TREF fractions. They came to the conclusion that the bimodal SCB distribution was caused by two kinds of active sites in heterogeneous Z-N catalysts: one site having an alternating character of copolymerization and the other having a random character. The site with an alternating character of copolymerization ($r_1 \cdot r_2$=0.5-0.6) gave a higher SCB concentration and lower molar mass while the other site having a random character ($r_1 \cdot r_2$=1.0) produces species with lower SCB concentration and higher MM.

Mirabella and Ford (1987) also performed cross fractionation on LLDPE, HDPE and HP-LDPE. The technique and system used was similar to Wild and Ryle (1982a and 1982b) except that the differential refractometer was replaced by an IR detector set at a detection wavelength of 3.41 μm (C-H

stretch) to detect the species eluting from the column. The fractions recovered from the TREF were characterized by SEC, ^{13}C NMR and X-ray diffraction (XRD). They did not observe long-chain branching in the LLDPEs. The SCB distributions of the LLDPEs were extremely broad and multimodal. Bimodal and even trimodal distributions were observed in one case and had never been reported previously. Their observations from the cross fractionation suggested a decrease of SCB with an increase in MM in typical commercial LLDPEs.

While most publications were focused on the complete characterization of LLDPE using PTREF followed by SEC or ^{13}C NMR, Kelusky et al. (1987) explored new areas for analytical TREF. They made use of ATREF to characterize polyethylene blends (50/50 or 10/90) of HD-LDPE/LLDPE, LLDPE/EVA, PE/EPDM and PE/polyisobutylene. The TREF apparatus used for that study was similar to the systems of Mirabella and Ford (1987) and Wild and Ryle (1982a). The solvent used for the crystallization and elution steps was α-chloronaphthalene. The concentration of eluting polymer was measured by an IR detector set at 3.42 μm. A liquid chromatography air oven was also incorporated in the system to control the temperature program. The TREF system could also be operated in PTREF mode. The advantage over an oil bath is the convenience and ease of changing the columns as well as the decreased turn-around time (Wild, 1990). A diagram of their system is shown in Figure 2.5. The fractions were collected by stop-flow experiments to obtain samples over narrow temperature intervals. The fractions were precipitated with methanol and then analyzed by DSC, IR, SEC and ^{13}C NMR. The results showed that ATREF is an excellent way to characterize blends based on PE. It was possible to quantitatively characterize a HP-LDPE/LLDPE blend if the ATREF profiles of the individual components were known. A calibration curve

relating branching frequency to elution temperature was constructed using an ethylene/1-butene LLDPE. A linear relationship between branching frequency and elution temperature was observed. However, it was suggested that a calibration curve constructed from a polyethylene sample will not necessarily apply to other polymers.

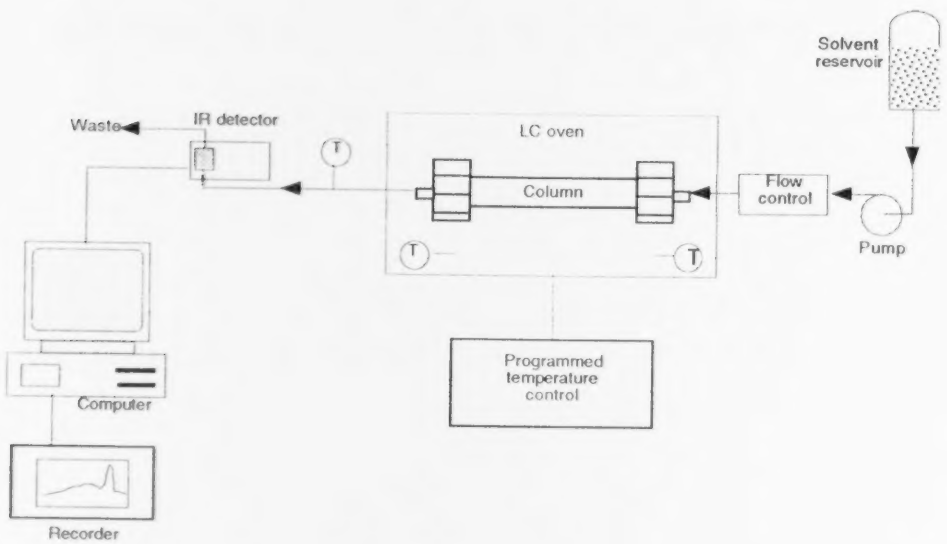

Figure 2.5: Schematic of an LC oven-based ATREF system (Kelusky, 1987).

Since TREF is a time consuming method and it is not readily available, some studies focused on DSC as a possible alternative to analytical TREF. Such attempts have been reported by Wild et al. (1990) and Karbashewski et al. (1992). Wild et al. (1990) characterized blends of LLDPE and blends of four components including VLDPE, HP-LDPE, HDPE and polypropylene. In that paper, an interesting concept was introduced regarding analytical TREF, namely off-column crystallization. This idea was mentioned for the first time

by Wild (1989) at a TREF workshop. In the off-column method, the crystallization of the dissolved polymer occurs in a vial during the controlled cooling; in the previously used on-column method the crystallization was done in the TREF column. The off-column method has some significant advantages over the on-column method such as the ability to prepare multiple samples, improved resolution, reduced sample zone in the column and larger scale fractionation (Chakravarty, 1993). The results from Wild et al. (1990) showed that the resolution of DSC was not as good as the resolution of ATREF for blends. However, the resolution by DSC can be improved by conducting the crystallization step in solution instead of from melts.

Karbashewski et al. (1992) characterized LLDPE by ATREF and DSC. Samples were also fractionated and analyzed by ^{13}C NMR and SEC. The TREF apparatus used for the experiments is very similar to the one used by Kelusky et al. (1987). The comparison of ATREF and DSC results revealed that both are qualitatively similar but ATREF produces more quantitative information. One advantage of ATREF is the ability to generate mass distributions. However, the full power of TREF resides in preparative TREF mode. From the MMD obtained using SEC on the individual PTREF fractions, Karbashewski et al. (1992) observed an unquestionable trend for increasing molar mass as a function of elution temperature. This is similar to the trends observed by Mirabella and Ford (1987).

Karaghian et al. (1992) compared ATREF to DSC using an ultra low density polyethylene (ULDPE). They reported that TREF and DSC provide similar compositional distributions even though the shapes of the profiles were not identical.

PTREF is often chosen as a preliminary tool to generate fractions for other characterization methods. Many publications report the use of preparative TREF to perform a detailed analysis of polymers. Barbalata et al. (1992) compared PTREF fractions with fractions obtained from lower critical solution temperature (LCST). They analyzed both sets of fractions using IR, DSC and SEC. They concluded that LCST fractionation is sensitive to molar mass wheras TREF largely depends on comonomer content. Neves et al. (1993) undertook to a complete characterization of a commercial LLDPE where PTREF had been adopted to generate fractions to be analyzed by DSC, FTIR and SEC. Zhou et al. (1993) used TREF-SEC cross fractionation to characterize commercial LLDPEs with ethyl, hexyl and iso-butyl branches. They observed a very broad SCB distribution and MMD. Usami et al. (1993) characterized impact-resistant PP/PE copolymers using the PTREF technique combined with SEC to generate samples to be analyzed by ^{13}C NMR and transmission electron microscopy. Mirabella (1993) also characterized impact polypropylene copolymers using PTREF combined with ^{13}C NMR and DSC.

Gilet et al. (1992) characterized mixtures of ethylene- and propylene-based polymer using PTREF and ^{13}C NMR. The material studied was produced using a $MgCl_2/TiCl_4$-supported catalyst. The polymer was formed in three steps: propylene homopolymerization followed by on-line ethylene/propylene copolymerization and addition of linear polyethylene by extrusion. The results indicated that the ethylene/propylene copolymer contains two or three major components and that the polypropylene exhibits high compositional heterogeneity. Defoor et al. (1993) used PTREF to study the thermal and morphological properties of a commercial 1-octene LLDPE produced in a solution process.

The recent advances in analytical TREF involve the design of automated systems, high performance systems and the development of new methods to relate methyl group concentration to elution temperature.

An automated analytical TREF (auto-ATREF) system has been described by Hazlitt (1990). With this system it is possible to perform eight fractionations within a 24 hour period, even allowing 10 hours for the cooling step. A process control gas chromatographic (GC) analyzer was used extensively as the basis of the design. The system involves two large forced-air, isothermal ovens and four smaller, programmable GC ovens. In each of the GC ovens there is a small ATREF column packed with steel shot. Sixteen solutions of polymer are placed into a carousel and then the operation is fully automated for the next 48 hours. Crystallization and elution steps are performed automatically by this system. Ethylene/α-olefin copolymers have been investigated using the auto-ATREF. It is reported that the automation of the ATREF technique has provided a reliable method for evaluation of copolymer SCB distributions. The system can perform 56 fractionations/week. However, the cost of producing and maintaining such a system puts it beyond the reach of most researchers (Wild, 1993).

Wild and Blast (1992) described the development of a high performance analytical TREF in which there was no attempt to automate the sample preparation and loading steps. However, the time spent for ATREF analysis was reduced considerably. Using a heating rate of 4°C/min, it was possible to run up to six samples in an 8 hour working day. The main features of the high-performance ATREF system are described in Table 2.4. This TREF unit has been used to analyze HDPE/EVA and LLDPE/EVA blends.

Table 2.4: Main features of high performance ATREF system (Wild, 1993)

• Multiple crystallizations by conducting slow-cooling of dilute solution off-line.
• Crystallized polymer loaded onto the column by slurrying with column packing.
• Temperature-programmed GC oven for rapid rate of temperature rise, allowing quick turn-around time and sub-ambient operation.
• Elution using a dual column system to allow monitoring of actual separation temperatures.
• IR detector used along with relatively large sample to achieve baseline stability and high detector response.
• Data capture on PC disc but stored and manipulated through a mainframe computer.

In a recent publication by Kuroda et al. (1992) ATREF has been used to characterize LLDPE prepared with a soluble vanadium-based Ziegler-Natta catalyst. The results from the ATREF showed a unimodal SCB distribution which is very distinctive from the multimodal distributions obtained from polymer produced with heterogeneous Ziegler-Natta catalysts.

Analytical TREF involves the use of a calibration curve to correlate the methyl group concentration to the elution temperature. The calibration curve is usually obtained from PTREF combined with ^{13}C NMR or FTIR. However, in ATREF the temperature is raised continuously as opposed to the common stepwise temperature ramp in PTREF. This difference in the methods can introduce some errors in the ATREF procedure. The residence time of the solvent in the column will cause a lag between the real elution temperature and the temperature at which the polymer will reach the IR detector. Pigeon et al. (1993) introduced a mathematical approach to correct analytical TREF data. This method involves the determination of the elution profile of the TREF column. This is done using a 1% wt solution of heptane in TCB which is loaded in the column and then eluted with a flow rate of 1 ml/min. Once the

elution profile of the TREF column is known, an iterative procedure is used to correct the data. The results showed that the correction method works equally well for various LLDPEs and HP-LDPEs and it is useful to obtain accurate branching distributions from ATREF.

In another paper, Pigeon et al. (1994) described a fully quantitative analytical TREF. It is suggested that for each polymer there exists a relationship between branching frequency and crystalline melting point. This is due to differences in branch length, clustering of branches and types of comonomer. They described a technique for generating calibration curves by measuring branching frequencies from ATREF using dual IR detectors. A second on-line IR detector was introduced to detect methyl group concentration at 2960 cm^{-1}. With this system, a calibration curve can be generated for each sample analyzed. This technique also eliminates the need for preparative TREF fractionation followed by IR or ^{13}C NMR to generate calibration curves.

Karbashewski and Rudin (1993) discussed the effect of comonomer sequence distribution on TREF branching distribution. They suggested that the crystallinity distribution measured by TREF is a measure of the effective branch content rather than the average branch content. Hence the concept of universal calibration for ATREF proposed by Wild et al. (1977) and Mirabella and Ford (1987) is not likely to be applicable over the broad class of commercially available resins.

An interesting method for the calibration of ATREF has been introduced by Bonner et al. (1993). Instead of the usual linear relationship between methyl group concentration versus temperature, this method is

based on the length of crystallizable sequences between SCB points, commonly referred to as the methylene sequence length (MSL). The calibration curve gives elution temperature as a function of MSL by fitting values obtained from narrow molar mass distribution standards to a derived form of the Flory melting equation (Equation 2.18) It involves only two parameters: T_o^{tcb} and c, where T_o^{tcb} is the equilibrium dissolution temperature and c is a constant.

$$T_d^{tcb} = \frac{1}{\frac{1}{T_o^{tcb}} + c\frac{\ln MSL}{MSL}} \tag{2.18}$$

Bonner et al. (1993) constructed the calibration curve using five standards which were eluted in ATREF using TCB as solvent. The value of T_d^{tcb} is obtained from the temperature at which the last trace polymer eluted from TREF. Using a curve fit of temperature versus MSL they obtained T_o^{tcb}=382.5 K and c=6.36x10^{-3}. MSL distributions were generated from TREF profiles using the calibration curve. The use of this technique will be discussed in detail in the next chapter.

Excellent reviews of TREF have been published recently by Wild (1990 and 1993) and Glöckner (1990). These publications present a good description of the various systems and methods that have been developed, and give a good summary of the applications of TREF.

Among the publications presented in this survey, there were variations in the TREF apparatus designs and procedures. Table 2.5 and Table 2.6 summarize the different ATREF and PTREF operating conditions. The

crystallization is usually performed in the TREF column with a cooling rate of 1.5 °C/h. Xylene and TCB are the most preferred solvents for PTREF; TCB and o-DCB are commonly used for ATREF. The most common way to perform PTREF is by a stepwise temperature increase. PTREF is frequently used to generate fractions to be analyzed by SEC and ^{13}C NMR. The trend in ATREF is toward a reduction of sample size and sampling time. Heating rates vary from 4 to 120°C/h. An IR detector is the most common device used to monitor the polymer concentration. PTREF and ATREF have mostly been used to characterize commercial LLDPEs and blends. ATREF and TREF-SEC cross fractionation have never been used as a part of a polymerization study to monitor the effect of the operating conditions on branching and molar mass distributions.

Table 2.5: Preparative TREF

Polymer	Sample Size (g)	Solvent	Column Dimensions (cm)	Packing Material	Cooling Rate (°C/h)	Heating Rate (°C/h)	Fraction Analysis	References
HP-LDPE	4	Xylene		Chromosorb-P	1	4	IR, DTA	Bergström and Avela (1979)
HP-LDPE	4	Xylene	38x7	Sand	Slow	Stepwise	IR, IV	Shiramaya et al. (1965)
HP-LDPE	4	Xylene	60x12	Chromosorb-P	1.5	8	IR	Wild and Ryle (1977)
HP-LDPE, HDPE	3.5	o-DCB	15x0.8	Glass beads	100	Stepwise	SEC	Nakano and Goto (1981)
LLDPE	0.27	TCB	10x0.3	Steel shot	2.5	12	SEC, IR	Hazlitt et al. (1989)
LLDPE		TCB	30.5x1.27	Silanized silica	1.5	Stepwise	SEC, NMR	Karbashewski et al. (1992)
LLDPE	0.75	∝-CN		Silanized Silica gel	Slow	Stepwise	DSC, IR, SEC, NMR	Kelusky et al. (1987)
LLDPE		TCB	25x1	Chromosorb-P	1.5	20	DSC, SEC, IR, NMR	Mirabella and Ford (1987)
LLDPE	8	o/p-Xylene		Celite 535		Stepwise	DSC, IR, SEC	Neves et al. (1993)
LLDPE		TCB	25x2.5	Silanized silica	1.5	Stepwise	SEC, NMR	Pigeon and Rudin (1993)
LLDPE	2.5	o-DCB		Glass beads	Slow	Stepwise	DSC, SEC, IR, NMR	Usami et al. (1986)
LLDPE	4	Xylene	60x12	Chromosorb-P	1.5	Stepwise	SEC	Wild et al. (1982b)
PE/PP copolymer		Xylene		Silica	1.2	Stepwise	SEC, NMR	Gilet et al. (1992)

Table 2.6: Analytical TREF

Polymer	Sample size (mg)	Solvent	Column Dimension (cm)	Packing material	Cooling rate (°C/h)	Heating rate (°C/h)	Detector	References
HP-LDPE	200	TCB	3.8x2.5	Chromosorb-P	1.5	8	RI	Wild and Ryle (1977)
HP-LDPE, LLDPE, EVA	100	TCB	12.5x2.5	Chromosorb-P	1.5	20	RI	Wild et al. (1982a)
LLDPE, HP-LDPE	20	o-DCB	7x0.9	Chromosorb-P	1.5		IR	Knobeloch et al. (1984)
LLDPE	2	o-DCB	15x0.8	Glass beads	Slow	Stepwise	IR	Usami et al. (1986)
HP-LDPE, HDPE, LLDPE, EVA	10	∝-CN		Silanized silica gel	0.5	10-40	IR	Kelusky et al. (1987)
LLDPE	15	TCB	7.5x0.9	Steel shot	10	50	RI, IR	Hazlitt and Moldovan (1989)
VLDPE		TCB		Chromosorb-P	1.5	25	IR	Karoglanian and Harrison (1989)
LLDPE		TCB	30.5x1.27	Silanized silica	1.5	10	IR	Karbashewski (1992)
LLDPE	10	o-DCB			5	120	IR	Wild et al. (1990)
LLDPE		TCB	25x2.5	Silanized silica	1.5	10	IR	Pigeon and Rudin (1993)
LLDPE		TCB	30x0.7	Glass beads	1	20	IR	Bonner et al. (1993)
LLDPE, HDPE EVA	5	o-DCB			5	4	IR	Wild and Blast (1992)

3. Materials, Equipment and Experimental Procedure

The main objective of this project was to investigate the effects of H_2 and 1-butene concentrations on the molar mass and branching distributions of laboratory-produced LLDPEs. The analytical techniques chosen to accomplish this task were temperature rising elution fractionation (TREF) and size exclusion chromatography (SEC). When these two tools are combined they generate a fairly detailed characterization of polymers. In this chapter, the materials, equipment and experimental procedures involved in this project are described in detail. A complete description of the TREF apparatus is presented. The method used to generate a calibration curve relating elution temperature to branching concentration is also discussed.

3.1 TREF apparatus

The TREF system used in this project has the same features as other systems described in the literature (see Chapter 2). The main components of the apparatus are shown in figures 3.1 and 3.2. The system includes a solvent reservoir, an HPLC pump, a temperature chamber, a column, an IR detector and a computer for the data acquisition. This system has already been described by Chakravarty (1993). The solvent used is 1,2,4-trichlorobenzene (TCB) or ortho-dichlorobenzene (o-DCB). The pump (❷) is a DuPont Instruments 860 Chromatographic pump which can be operated with a flow rate ranging from 0.2 to 10 ml/min at a pressure up to 400 bars. A pressure transducer is located at the exit of the pump to measure the exit pressure. The temperature chamber (❸) is a Thermotron model S-1.2C-B programmable temperature chamber.

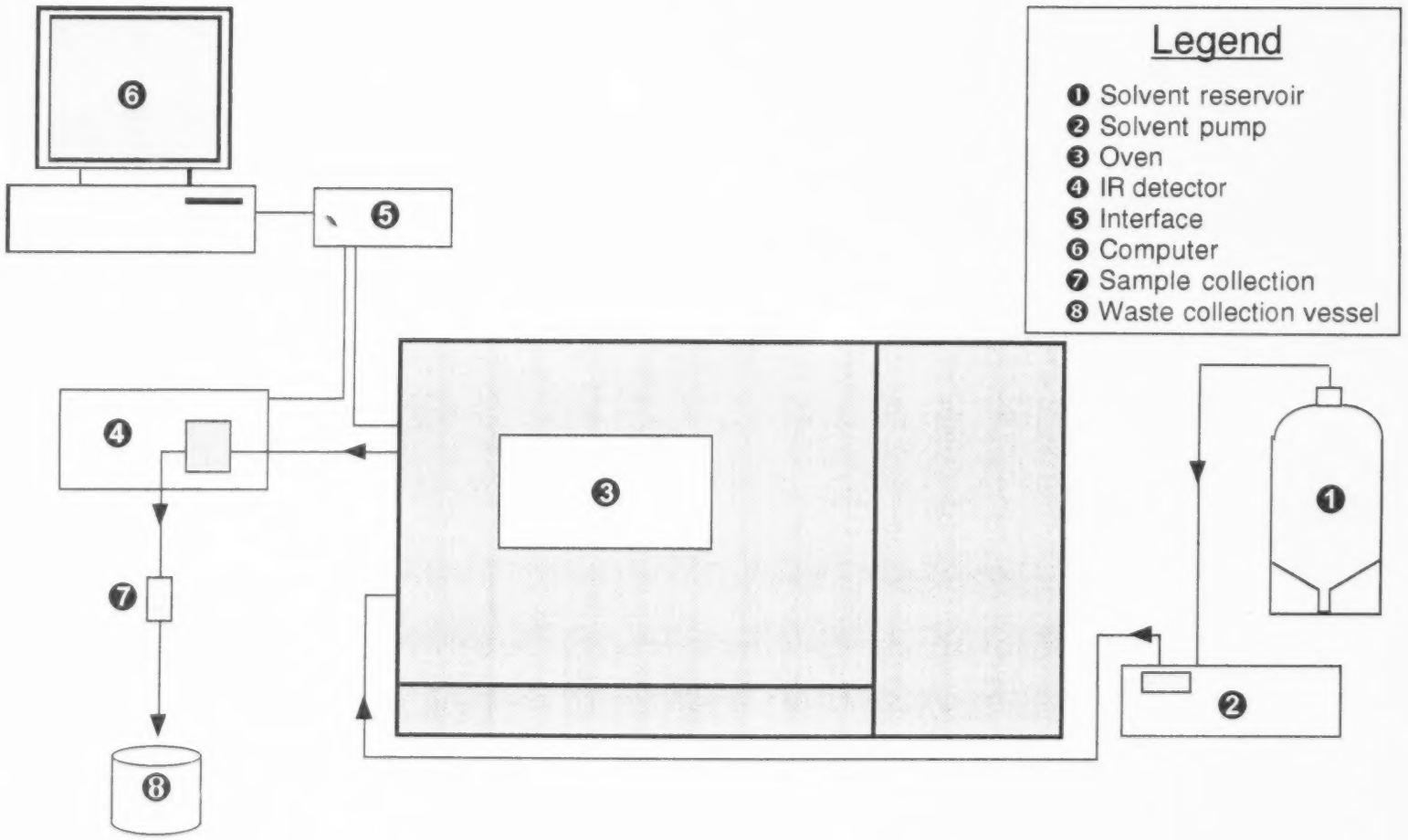

Figure 3.1: TREF apparatus

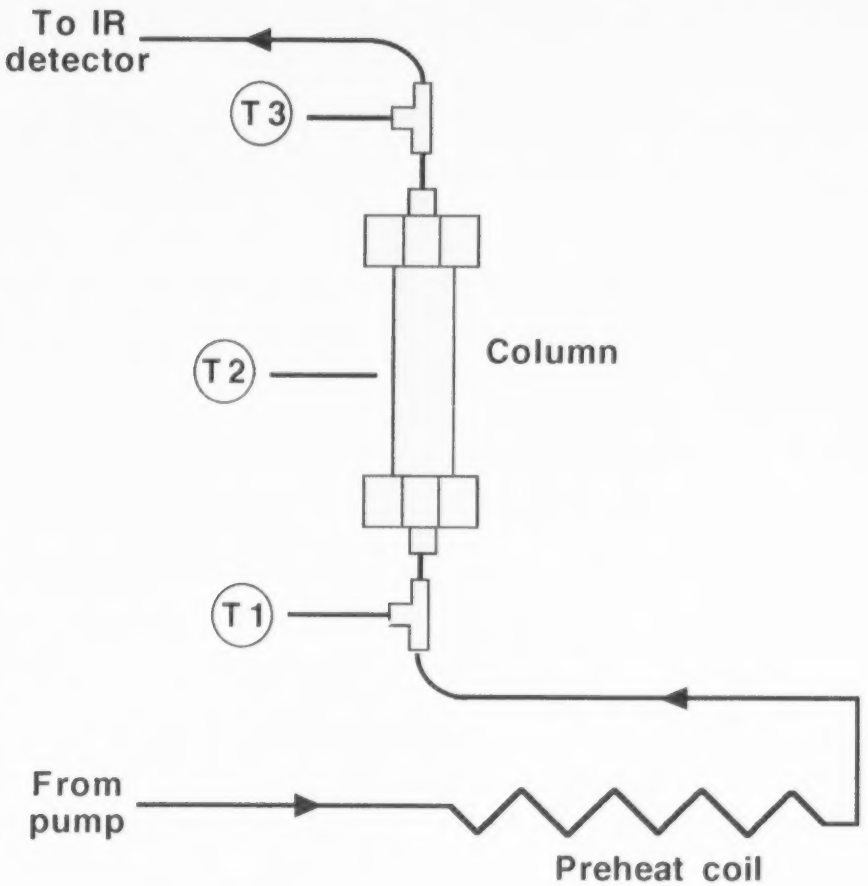

Figure 3.2: Inside of the temperature chamber

This programmable temperature chamber can attain temperatures from -73°C to 177°C with a precision of ±1.1°C. The temperature of the chamber is monitored by a type T thermocouple at the inlet of the TREF column (see T_1, Figure 3.2). The volume of the chamber is 34 L.

The TREF column is located inside the temperature chamber. The solvent comes from the HPLC pump and passes through a preheat coil (total length 1.5 m) and then goes into the column. There are three thermocouples to measure the solvent temperature. T1 measures the temperature at the inlet of the column which is used as the set point for the temperature chamber controller. T2 measures the air temperature in the vicinity of the column. T3 measures the temperature at the outlet of the column. T3 is the temperature used as the elution temperature for the TREF profile. T2 is recorded in the data file but it is not an essential parameter. It can be used as a check point in case of problems. During an ATREF run, T2 has a slightly higher temperature than T3 (≈2°C) because of the temperature gradient between the air and the solvent inside the tube. The difference between the temperatures measured by T1 and T3 is usually within 1°C. Even if the temperature chamber is maintained at constant temperature for a long time, the 1°C difference is still observed. T2 and T3 are type J thermocouples.

After the solvent passes through the column, it goes to the IR detector (❹). The detector measures the concentration of polymer in the solvent. The detector is a DuPont liquid chromatography IR detector equipped with a temperature control unit for the IR cell. The IR detector is set to a wavelength of 3.38 μm (2960 cm^{-1}) which corresponds to the CH_2-CH_2 stretch of the polyethylene backbone. The IR cell is maintained at 130°C to keep the polymer in solution. The IR cell is a modified SL-2 type cell which fit in a

home-made heating device. The IR windows are two CaF_2 disks (32x3 mm) separated by a 0.5 mm Teflon™ spacer. The solvent flows continuously through the cell.

After passing through the IR detector, the solvent goes by the sample collection point used for PTREF. The sample collection point is a flow-through Swagelock Quick connect device that was easily opened to collect the samples. A mini lab lift is used to hold the 4 ml vials in which the sample is collected. The sample collection is done manually. In the ATREF procedure no fractions are collected. The solvent goes directly to the waste collection vessel.

Two sizes of column were used in the TREF system. For ATREF, the column was a 63.5x9.5 mm stainless steel 316 tube with Swagelock end column fittings. Inside the end column fittings, there were 5 μm or 10 μm filters. The frit with the larger pores was used at the outlet of the column. The column was packed with 100 mesh glass beads. The polymer sample formed a slug in the middle of the column. For PTREF, the column had a larger diameter. In the preliminary experiments, some pressure problems were observed with the large PTREF samples. The problems were eliminated by using a larger diameter column (63.5x12.7 mm). The filters used for the PTREF column have 7μm pores. More details about the columns are given later in this chapter.

An OPTO22 system and a 486 PC computer were used for data acquisition of the TREF apparatus. The system records the temperature of the various thermocouples, the concentration of polymer from the IR detector and the line pressure at the exit of the pump. The data are stored in an ASCII

data file which can easily be imported in other applications for data processing.

3.2 Modifications of the TREF system

Several parts of the current TREF system have been modified from the original design described by Chakravarty (1993). The IR detector was installed on a stand to reduce the distance between the IR cell and the TREF column. The length of the inlet and outlet tubes of the IR cell were reduced in length considerably. The inlet tube, connecting the IR cell to the TREF column, was reduced from 60 to 25 cm. This reduced the time decay between the IR measurements and the temperature at which the polymer was eluted. The length of the outlet tube of the IR cell was reduced drastically. The distance from the IR cell to the sample collection point was about 100 cm; this was reduced to 20 cm. Therefore, the residence time of the solution in the tubes was reduced by a factor of about four. The overall length of tube from the TREF column to the sample collection point is now ≈45 cm.

A miniature quick-connect device was installed to facilitate sample collection. The original design was simply a 1/16" tube inserted in a larger 1/8" tube. The connection was open to collect the sample. This connection was not well sealed and was not appropriate for this kind of operation. The miniature quick-connect device provided a good seal, and it was easy to open the line and collect samples. However, the connection could not be heated adequately. The external surface of the quick-connect device must be clear to be able to open it. This created problems because the complex internal design of the quick-connect is vulnerable to polymer crystallization which at times plugged the device. Therefore, it was important to dismantle the connection

regularly to clean the internal parts and to be sure that there was no accumulation of material.

The sample collection point was installed at a fixed position near the outlet of the IR cell. To collect the sample, the miniature quick-connect was opened and the collection vial was held in place on a mini lab lift. This way all the parts were stable and the risk for spills was considerably reduced. The use of a mini lab lift also provided a good contact between the edge of the collection vial and the stem of the miniature quick connect. The vaporization of the hot solvent during PTREF procedure was reduced by using this arrangement.

The heating tape on the tube connecting the TREF column to the IR cell was removed. The tube was too short to properly install such a device. The length of tube exposed to the air is short. The solvent did not cool down enough to cause problems.

The type J thermocouples used to measure the temperature at the outlet of the column and outside the TREF column were replaced for new ones. The original thermocouples were not providing accurate temperatures. The thermocouple used by the controller of the temperature chamber was replaced and relocated. The original thermocouple was located at the upper right corner of the chamber and measured the air temperature. The new thermocouple was located at the inlet of the TREF column to measure the solvent temperature. This way, the controlled temperature was more meaningful and it offered better performance in the PTREF mode.

The TREF columns were replaced by new ones. The original columns were not constructed properly. The junction between the tube and the frits inside the end column fittings were not tight. Once the column was filled with packing and assembled, the packing was free to move to the empty sections of the column caused by the improper junction. This could create channeling of the solvent through the packing. Consequently, the columns could behave differently for each experiment. This is discussed subsequently in Section 3.3

The most important modification to improve the reliability of the TREF system is the design of a new cell for the IR detector. The original cell leaked frequently and the CaF_2 windows often broke after a short time of use. This cell caused months of trouble and expenses. The original cell assembly was a commercial design. A SL-2 type cell was used in the new design instead of the SL-3 type cell. The problems with the SL-3 cell resulted from the way the front plate was fixed to the main body of the heater to hold the IR windows. Two screws were used to hold the front plate. To have a good seal, the front plate must push all the components of the cell very tight and the pressure must be even at the surface of the windows. If there was a slight difference in the way the screws were tightened, the windows cracked at the operating temperature (130°C). The SL-3 design is very vulnerable to these kinds of problems.

The SL-2 type cell is a better design. This cell assembly uses CaF_2 disks and Teflon spacers. The components of the cell are held together by a single screw cap that produces a uniform pressure at the surface of the window. This way the cell can be sealed very tight without risk of breaking the windows. Another advantage of this design is that a good seal is obtained using a Teflon spacer and gaskets. In the SL-3 type cell, a lead spacer was

used with mercury to form an amalgam tnat produced the seal. Four days were needed to produce a good seal. With the SL-2 cell, the whole assembling process only takes a few minutes. The only problem with the SL-2 cell is that no commercial heaters are available. The heater was designed and constructed in our facilities. The heater constructed was similar to the one used for the SL-3 cell. More details about the heater are given in Appendix E.

3.3 Operating conditions for the TREF system

An important step in the use of TREF is the determination of the optimum operating conditions. The optimization of the following parameters was examined: IR wavelength for CH_2-CH_2 stretch, the linearity of the response of the IR detector, calibration of the pump flow rate and the residence time distribution of the TREF columns.

3.3.1 Determination of IR wavelength

The wavelength used to measure the concentration of the polymer in the solution corresponds to the CH_2-CH_2 stretch of the polymer backbone. Typical values used in the literature are 3.41 and 3.42 μm. However, the best way to obtain the optimum value for the system is to run a scan of the solvent and a scan of the polymer in solution. The best value is obtained where the difference between the two scans is a maximum.

The solvent used for this experiment was ortho-dichlorobenzene (o-DCB). A 5 mg sample of hexacontane was used to obtain the wavelength of the CH_2-CH_2 stretch. The IR detector response time was set to 1 s for both

scans. The temperature of the solvent was 80°C. The scan of the solvent was performed as following:

- The solvent was pumped through the system until a stable baseline was achieved.
- The pump was stopped for the duration of the scan
- The scan started at a wavelength of 2.5 μm. During the scan the IR signal (absorbance) and the time were recorded by the data acquisition system. A stop-watch was used to relate the time to the IR wavelength.

The scan for the hexacontane was performed as following:

- The sample was loaded in the TREF column and heated at 80 °C.
- The pump was started with a flow rate of o-DCB at a rate of 1 ml/min. While the content of the column was eluted the IR signal at 3.41 μm was monitored.
- When the signal showed that the polymer was in the IR cell, the pump was stopped.
- The scan was then started at a wavelength of 2.5 μm and performed in the same way as the previous scan.

The results from both scans are displayed in Figure 3.3. The scans show that the optimum wavelength to detect the polymer concentration is 3.38 μm.

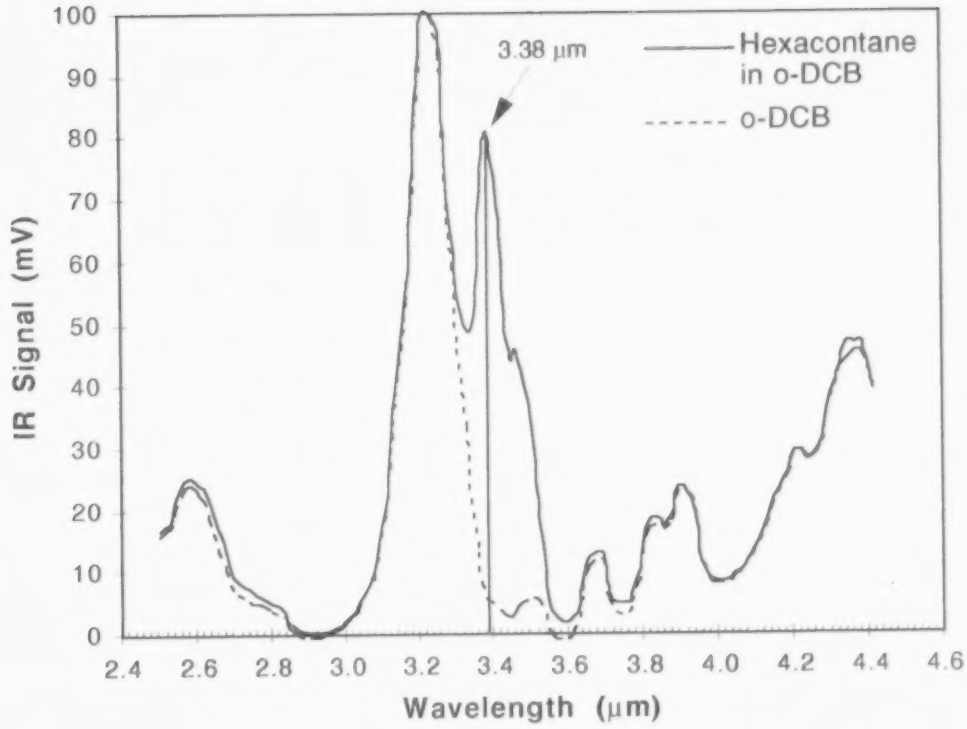

Figure 3.3: IR scan of o-DCB and hexacontane

3.3.2 Linearity of the IR detector response

During the TREF runs, the IR detector measured the absorbance of the solution at a fixed wavelength. The absorbance of the solution is related to the mass concentration of the material in solution. For dilute solution, the relationship between concentration and absorbance follows Beer's law (Skoog and Leary, 1992), i.e. the concentration is a linear function of the absorbance. However, deviation from Beer's law occurs at high concentrations. Consequently, it is important to know if Beer's law is applicable at the TREF operating conditions.

A simple method to verify the linearity of the IR response is to inject samples with different concentrations and measure the absorbance. A series of polymer solutions with concentration ranging from 0.01 to 2 mg/ml was injected in the IR cell. The solutions were produced by dissolving various amounts of a polyethylene standard (SRM 1482 obtained from the National Bureau of Standards) in 20 ml of o-DCB at 120°C. The composition of these calibration solutions are listed in Table 3.1.

The solutions were injected into the TREF system using a syringe. The syringe and the solution were kept at 120°C in the temperature chamber. The IR signal was recorded by the data acquisition system. The contents of the IR cell was purged using o-DCB between each injection.

Table 3.1: Solutions for testing IR response linearity

Solution	mass of polymer (mg)	o-DCB (ml)	Concentration (mg/ml)	IR signal (mV)
1	0.21	20	0.01	0.14
2	0.45	20	0.02	0.26
3	3.15	20	0.04	0.41
4	1.25	30	0.16	1.50
5	7.61	20	0.38	2.70
6	20.1	20	1.01	7.70
7	40.4	20	2.02	16.30

Figure 3.4 shows the relationship between the IR signal and polymer concentration. It can be seen that the IR signal is a linear function of the concentration for all the solutions tested. In ATREF, a concentration of 2.02 mg/ml corresponds to all of the 5 mg sample eluting in a 5°C interval. This situation did not occur even for polymers with very narrow branching distributions such as HDPEs. The maximum concentrations could occur in PTREF runs where 20 mg of polymer were used. The maximum concentration obtained in all the PTREF runs was 1.7 mg/ml when 26% of a 20 mg sample was eluted in 3 ml. Therefore, all the TREF runs performed were within the range of the concentrations tested and IR signal linearity.

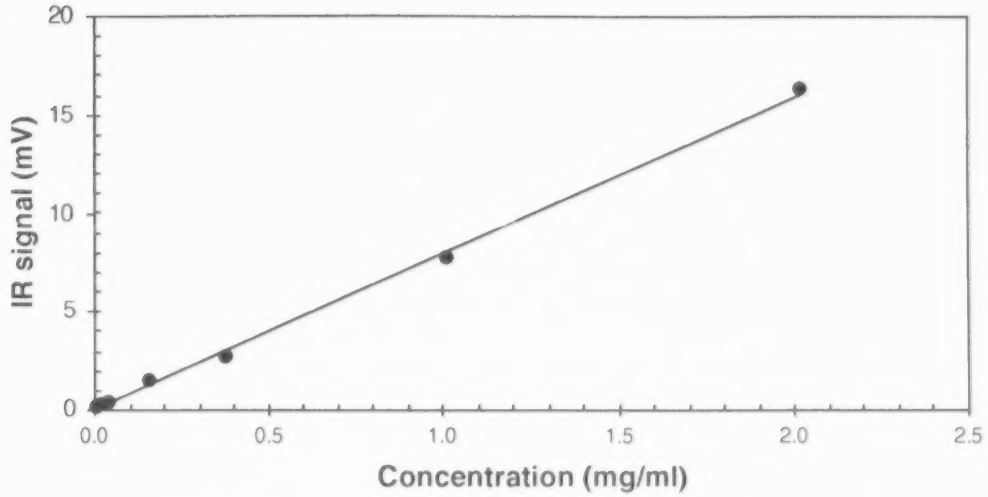

Figure 3.4: IR signal versus concentration

3.3.3 Pump Calibration

A calibration curve for the pump was obtained by measuring the volumetric flow rate as a function of pump set point. The solvent was collected in 4 ml vials and the time required to fill the vials was measured using a stopwatch. The vials were weighed before and after the experiments. The actual flow rate was obtained by dividing the total volume in the vial by the time elapsed. The resulting calibration curve is shown in Figure 3.5. The calibration curve shows an offset between the setpoint and the actual flow rate.

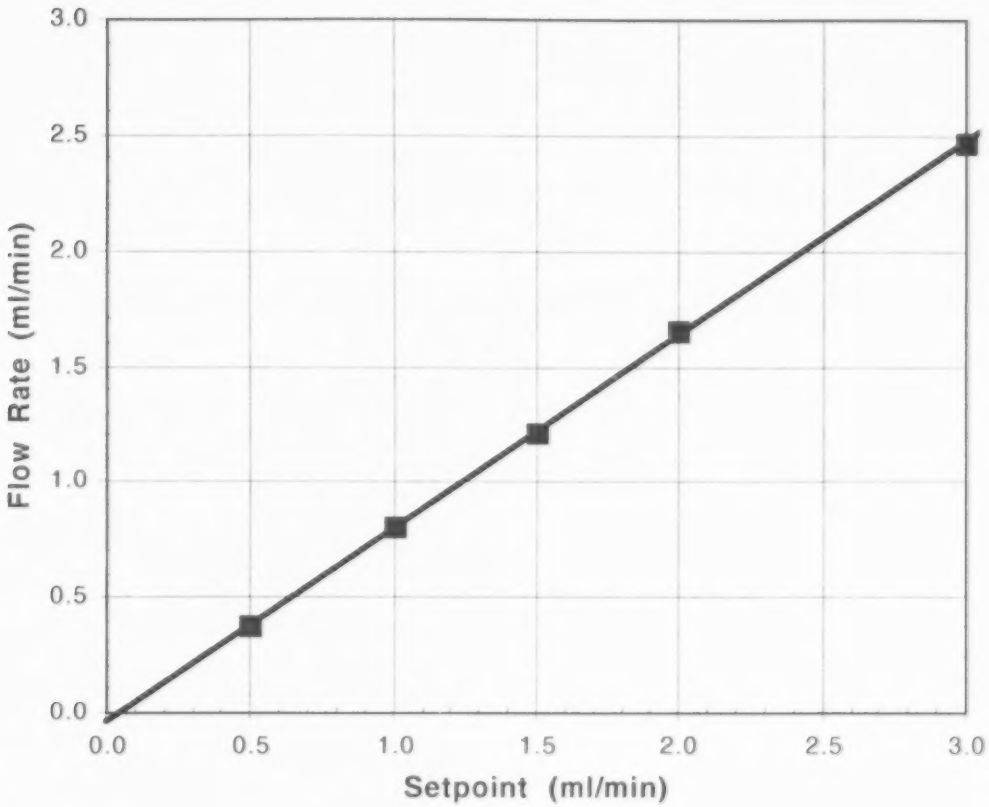

Figure 3.5: Pump calibration

3.3.4 Characterization of the TREF columns

To obtain reproducible TREF profiles, it is important that the flow profiles of all the TREF columns used be similar. If the columns do not have the same residence time distributions, the TREF profiles will not be reproducible. It is also important to know the time needed to elute the contents of the column. The accuracy of the TREF profile can depend upon this factor. If the residence time of the solvent in the TREF column is long compared to the heating rate, the resulting TREF profile can be due to polymer that has eluted at a higher temperature than it should have been.

The residence time distributions of the TREF columns were obtained by loading the columns with 0.1% by weight decane in o-DCB and then eluting the decane with a flow rate of 1 ml/min of o-DCB. The solution was loaded in the column by using a syringe and then the column was sealed with stoppers. After being loaded, the column was installed in the TREF system and ready for elution. The columns must be installed carefully to avoid air bubbles in the system. The experiments were performed with four ATREF columns and two larger PTREF columns. The ATREF columns had a length of 45 mm, O.D. of 10 mm and I.D. of 6 mm. They are referred as column I to IV. The PTREF columns are described in Table 3.2. Column A has a funnel shape on one side going from 10.9 mm to 3.1 mm in about 25 mm of length. Column B has a constant I.D. across the column. The packing used for the column was 100 mesh glass beads and Celite has also been tested in column B.

Table 3.2: PTREF columns

Column	Length (mm)	O.D. (mm)	I.D. (mm)	Shape
A	51	12.7	10.9	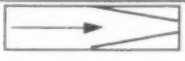
A'	51	12.7	10.9	
B	51	12.7	10.9	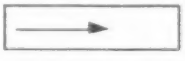

The first set of columns tested consisted of columns I to IV. The elution profiles of the columns are shown in Figure 3.6. The columns were all packed in the same way with glass beads. It can be seen from this figure that the elution profiles of the columns are not the same. After examination of the columns, it was found that they were not properly built. The Swagelock fittings were not installed properly.

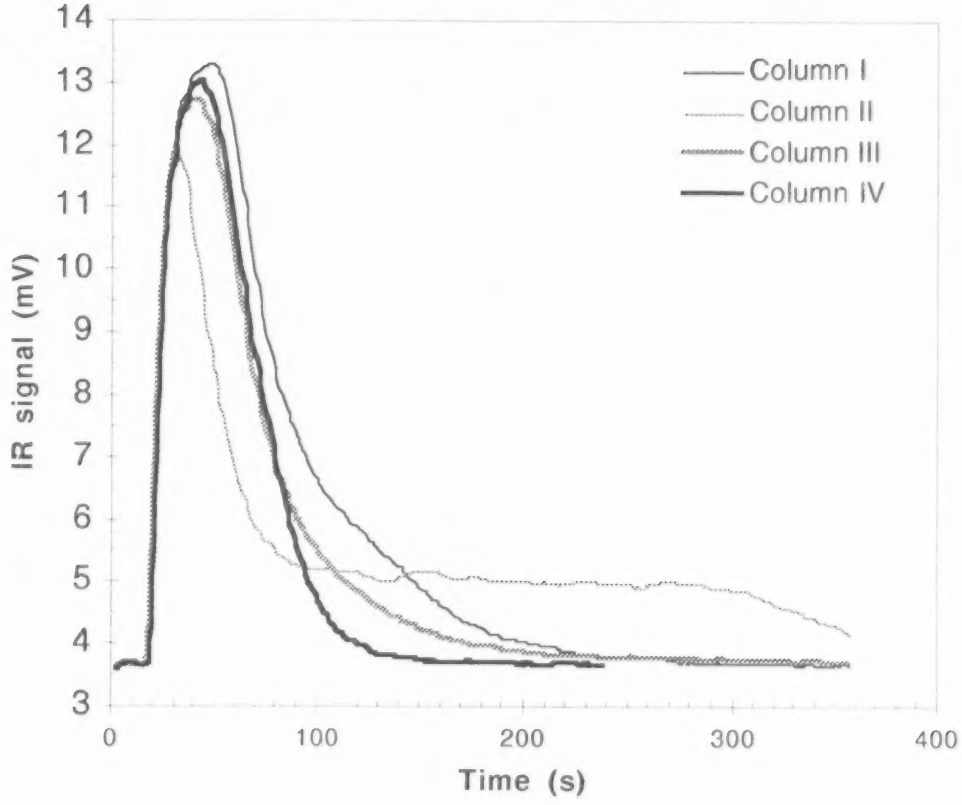

Figure 3.6: Residence time distribution of ATREF columns I to IV

The ends of the columns were not sitting at the bottom of the reducing union to hold the frit tight in place. Once the column was packed and assembled, the packing could move into the empty spaces of the column. These spaces were not the same in all the columns. During the elution, it was possible for the packing to move and to create channels in the column. Consequently, the residence time distribution was affected by the irregularity of the packing in the column which creates dead spots and channeling conditions.

New TREF columns were constructed to replace column I to IV. Two new columns were constructed. The columns had a length of 45 mm and inside and outside diameter of 7.7 and 9.5 mm. The Swagelock fittings were installed properly. The residence time profiles of the new TREF columns are shown in Figure 3.7. Each column was tested twice. The residence time profiles of the new columns are similar and reproducible. Therefore, it can be expected that the TREF profiles obtained with these columns are more reproducible than those with previous columns.

The packing material used for the TREF columns has also an effect on the residence time distribution. Two types of packing were used to investigate the effect of packing material on the elution profile of the TREF columns: Celite and 100 mesh glass beads. The procedure to obtain the profiles was the same as described earlier. The results from these experiments are shown in Figure 3.8.

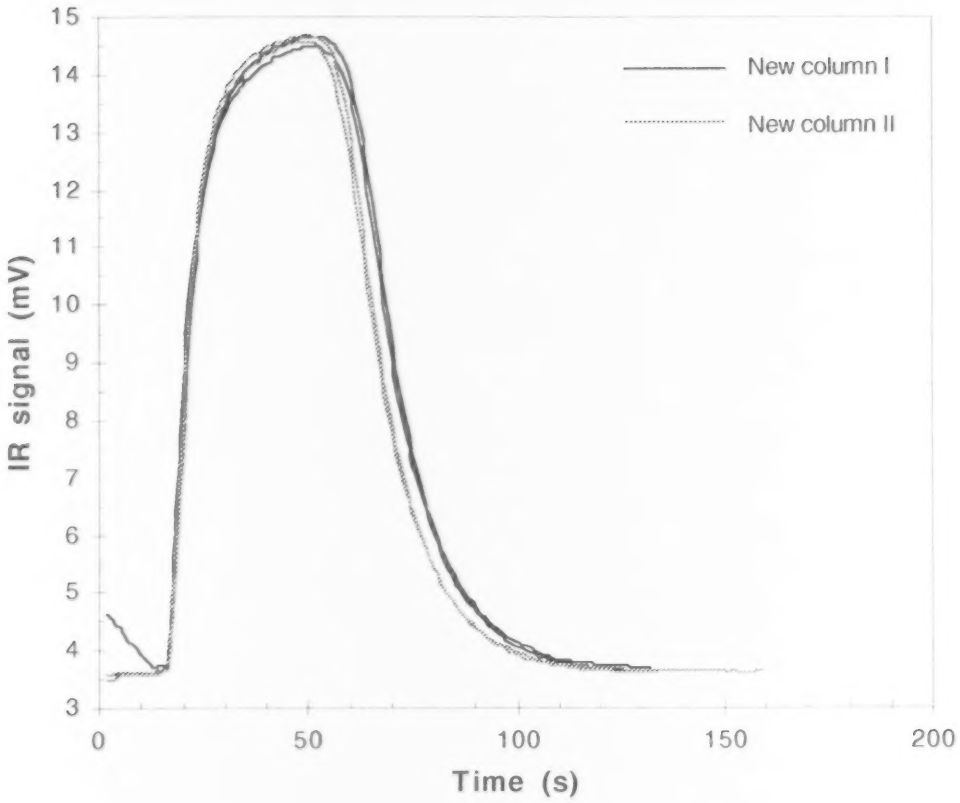

Figure 3.7: Residence time distribution of the new ATREF columns

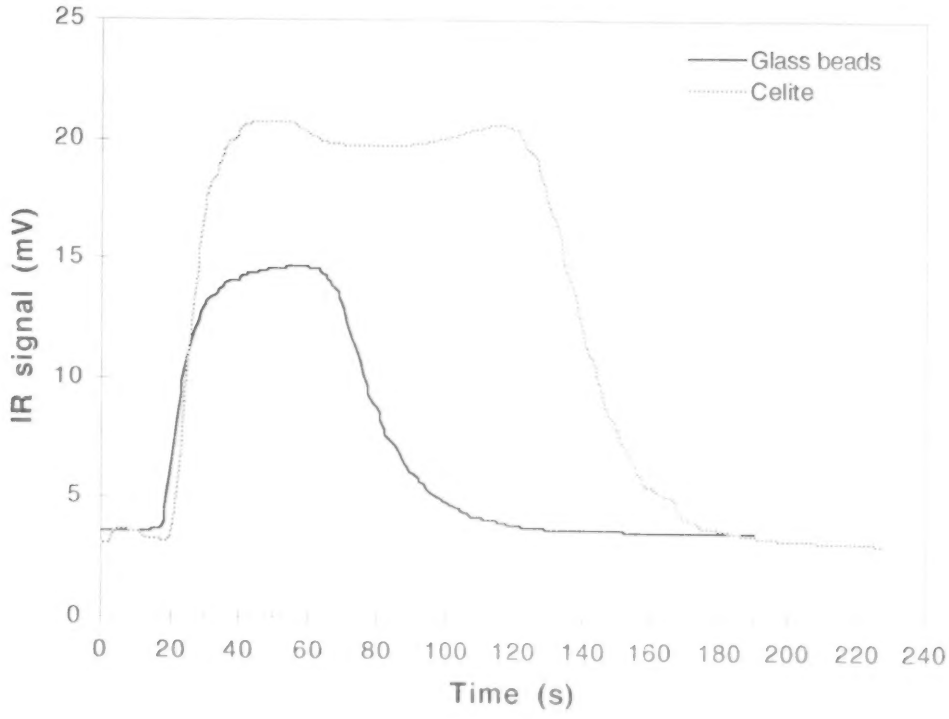

Figure 3.8: Comparison of the residence time distributions of ATREF column with various packing.

It can be seen that the residence time distribution of the columns packed with Celite is much broader. The time needed to elute the contents of the columns is about two times larger. The longer residence time can be caused by entrapment of material within the pores of the Celite packing. It also seems that the volume of liquid hold-up in the TREF column is larger for Celite. For TREF, a packing that offers the shortest residence time is desirable. By minimizing the residence time, the accumulation of dissolved polymer in the TREF column during the elution process is minimized. With a shorter residence time, the concentration measured by the IR detector is closer to the real amount of material that dissolved at the corresponding temperature.

The residence time distributions of the PTREF columns are shown in Figure 3.9. Different feed patterns were tested for column A. The results show that the shape of the TREF column or the feed pattern does not have significant effects on the elution profile of the columns. Therefore, the simplest design (column B) was chosen as the PTREF column (see Table 3.2 for geometry of TREF columns).

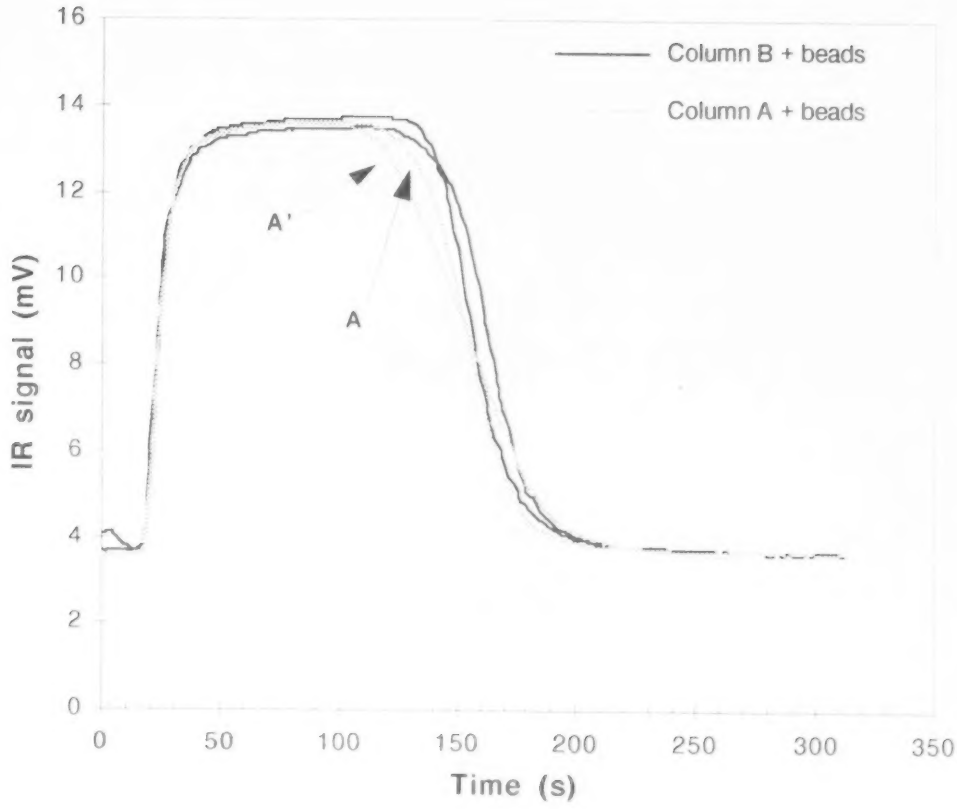

Figure 3.9: Residence time distribution of PTREF columns (see Table 3.2 for geometry of TREF columns).

3.4 TREF experimental procedure

Analytical TREF and preparative TREF procedures are divided in two steps: sample preparation and elution. The crystallization of the polymer is included in the sample preparation step. The experimental procedures used in TREF are described in detail in this section. The experimental procedure has been described by Chakravarty (1993). However, some minor changes in the procedure were introduced.

3.4.1 Sample preparation

The samples analyzed were ethylene/1-butene LLDPE produced in a bench-scale gas phase reactor. The LLDPEs were made by Huang (1995) as part of his M.Sc. project. The LLDPEs were produced by copolymerization of ethylene and 1-butene over a commercial bisupported Ti catalyst with various H_2 and 1-butene partial pressures. The operating conditions are described in Chapter 4 with the corresponding results.

The LLDPEs were received as a fine powder. The samples were weighed using a Mettler HL52 electronic balance having a precision of 10^{-5} grams. The sample sizes used were 5 mg for ATREF and 20 mg for PTREF. The samples were put in 15 or 30 ml vials and the solvent (o-xylene or o-DCB) was added (1 ml of solvent per mg of sample). Disposable stir bars (12x3 mm) were put in the vials for the subsequent stirring operation. The vials were sealed with 90/10 mil Tegrabond silicon septa.

The LLDPE-solvent mixtures were then heated and stirred at 125°C for two hours. This was achieved by placing the vials in a container filled with diethylene glycol on a hot-plate stirrer. The reason for stirring was to ensure

that the dissolved polymer mixes properly with the solvent to produce a homogeneous solution. The stirring should also disentangle the long polymer chains. The disentanglement increased the efficiency of the crystallization that was carried out subsequently (Chakravarty, 1993). Sixteen samples were usually prepared for crystallization. Eight samples could be dissolved simultaneously using two hot-plate stirrers. The samples were prepared in two batches. While the second batch was being heated and stirred, the first batch was kept at 125°C in the TREF temperature chamber.

After the dissolution step was completed, the vials were transferred into a liquid bath for the crystallization stage. The liquid bath was an Endocal RTE 220 bath/circulator equipped with a M-RS-232 interface connected to a PC computer for temperature control. The bath was filled with diethylene glycol. The vials were placed in a tray inside the bath. The samples were kept at 125°C for 2 hours before starting the cooling for the crystallization. This was done to be sure that the polymer that could have crystallized during the transfer procedure was dissolved. The crystallization was achieved by slowly cooling at a rate of 1.5°C/h from 125°C to -8°C. The total time for dissolution and crystallization was about 90 hours. After crystallization, the samples were kept in a freezer at -15°C until used for TREF elution.

The next step for the sample preparation is the transfer of the crystallized polymer/solvent slurry to the TREF columns. This step was performed in two ways. Initially, the suspension of crystallized polymer was filtered using an Anodisc inorganic filter having a pore size of 0.02 μm. The cold polymer suspension was poured in a filtering funnel and the solvent was drawn out by vacuum generated by a water-jet. The walls of the vials were

scrapped using a spatula to remove the polymer coating produced during crystallization. The vials were washed many times with cold acetone to remove the remaining polymer crystals. Once the filtration was completed, the contents of the funnel was transferred to the TREF column.

The column was initially filled to about half of its length with untreated 100 mesh glass beads. Then, the content of the funnel was washed with acetone and poured down in a funnel connected to the TREF column. A modified sleeve stopper was used to provide a good junction between the funnel and the TREF column. Glass beads were mixed with the polymer suspension to produce a slug of polymer and glass beads in the middle of the TREF column. After the polymer was transferred, the column was filled to the top with glass beads. The ends of the column were capped with column end fittings containing frits. The columns were then ready to be inserted in the TREF apparatus.

In the second method used to transfer the polymer to the TREF columns, the filtration using Anodisc filter has been eliminated. Instead, the polymer suspension was deposited directly in the TREF column by filtration through the column packing. The filtration using the Anodisc filter was an unnecessary step that was time consuming. The elimination of this step reduced the chances to lose polymer during the transfer to the TREF columns.

3.4.2 TREF procedure

The TREF apparatus used in this project has already been described in Section 3.1. The TREF procedures for ATREF and PTREF are presented separately in the following sections.

3.4.2.1 Analytical TREF procedure

The analytical TREF method was used to obtain the branching distribution of the polymer sample. The 5 mg samples were loaded into the small TREF columns for ATREF. Then the column was introduced into the temperature chamber and connected to the TREF circuit. The initial temperature of the chamber was -10 or 25°C depending on the type of polymer to be analyzed. The pump was started with a flow rate of 1 ml/min of solvent to remove the air from the column and to achieve a stable baseline. During this operation, which took about 10 min, the temperature was kept constant at its initial value.

Once a stable baseline was achieved, the flow rate was reduced to 0.5 ml/min and the temperature kept at its initial value for about 5 min. Then the elution was started by heating the TREF column at a rate of 1°C/min, the solvent flow rate was maintained at 0.5 ml/min. Initially, the heating rate used for ATREF was 2°C/min with a flow rate of 1 ml/min. However, it was observed during the preliminary runs that a heating rate of 1°C/min with a flow rate of 0.5 ml/min gave better resolution and the TREF profiles were more reproducible.

During the elution process, the temperature of the various thermocouples, the IR signal and the line pressure were recorded into a file by

the data acquisition system. The frequency of data acquisition was 3 s. The elution process was stopped at about 110°C or when all the polymer sample had been eluted. When the elution was completed, the temperature chamber was cooled down to 25°C in about 30 min. The total time required for the ATREF procedure ranged from 130 to 165 min.

3.4.2.2 Preparative TREF procedure

The preparative TREF method was used to generate fractions for analysis by SEC, to obtain MMD as a function of TREF elution temperature. For PTREF, 20 mg samples were used. The sample was loaded in the large TREF column (see column B in Section 3.3.4). A large TREF column was used to avoid pressure excursions which occurred when 20 mg sample were loaded into ATREF columns. The pressure excursions were caused by the blockage of the 7 μm frit at the outlet of the column. The use of a larger diameter column increased the surface of the frit. Therefore, the risk of blockages was reduced considerably.

For PTREF, a stepwise temperature increase was adopted for the elution of the polymer samples. The procedure is illustrated in Figure 3.10. Prior to the elution, the pump was started with a flow rate of 1 ml/min of o-DCB or TCB to remove the air from the column and to achieve a stable baseline. During this operation, the temperature was kept constant at -10 or 25 °C depending on the type of polymer analyzed.

Once a stable baseline was achieved, the temperature was increased to the desired initial value with a solvent flow rate of 1 ml/min. Once the initial temperature was attained, the pump was stopped and the stepwise procedure was initiated. The temperature was increased from the lowest to the highest temperature of the interval in 10 min.

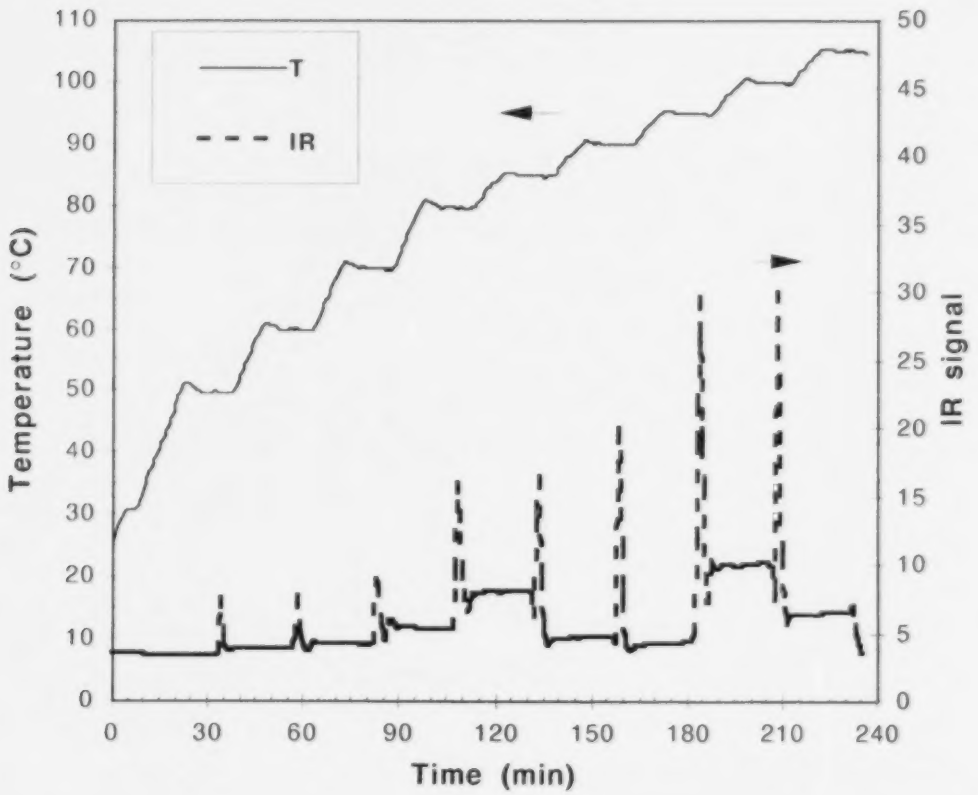

Figure 3.10: Temperature and elution profiles of a typical PTREF procedure

Once the final temperature of the interval was reached, it was kept constant for about 10 min. Then the pump was started with a flow rate of 1 ml/min and the content of the line was purge for about 40 seconds until the IR detector showed the presence of polymer in solution. At this point the pump was stopped, and a 4 ml GPC vial was inserted at the sample collection point to collect the fraction. The pump was started again and the solution was collected for 3 min to obtain 3 ml of the polymer solution. As shown in Figure 3.10, 3 min is enough to elute the content of the column and to return the IR signal to the baseline value. After the 3 min was elapsed, the pump was stopped, the vial was removed and sealed with a cap. The sample collection line was then closed. In some cases, the IR signal increased while the pump was stopped. This was caused by the evaporation of the solvent in the IR cell.

The procedure was repeated for all the chosen temperature intervals. During the elution process, the temperature of the various thermocouples, the IR signal and the line pressure were recorded into a file by the data acquisition system. The frequency of data acquisition was 4 s. Typical temperature intervals for PTREF were 30-50-60-70-80-85-90-95-100-105°C. Once the elution was completed, the temperature of the chamber was brought back to 25°C. The total time required to complete a PTREF run was typically 5 h.

3.4.3 TREF-SEC cross fractionation

The TREF-SEC cross fractionation consists of separating the polymer according to its degree of branching using PTREF followed by SEC to obtain the molar mass distribution of the individual fractions. TREF-SEC cross fractionation yields combined information about the branching and molar mass distributions.

A Waters/Millipore 150-C ALC/GPC was used for determining the molar mass distributions of the TREF fractions. The SEC apparatus is equipped with a differential refractometer. The separation is achieved by four Shodex columns AT 800P. The column and the detector were maintained at 140°C. The carrier solvent was 1,2,4-trichlorobenzene (TCB) and the flow rate was 1.0 ml/min. The samples were heated at 160°C prior to injection into SEC. Two 0.3 ml injections were done for each TREF fraction and the time between injections was one hour. The SEC apparatus was operated by Ms. Naiyu Bu.

In SEC, the retention time of the polymer species is a function of the molar mass. A calibration curve in needed to relate the retention time to the molar mass. The method used to produce this calibration was a universal calibration produced with narrow standards (polystyrenes and polyethylenes). The calibration curve is shown in Figure 3.11. The molar masses are computed from this calibration curve using the software provided with the SEC apparatus.

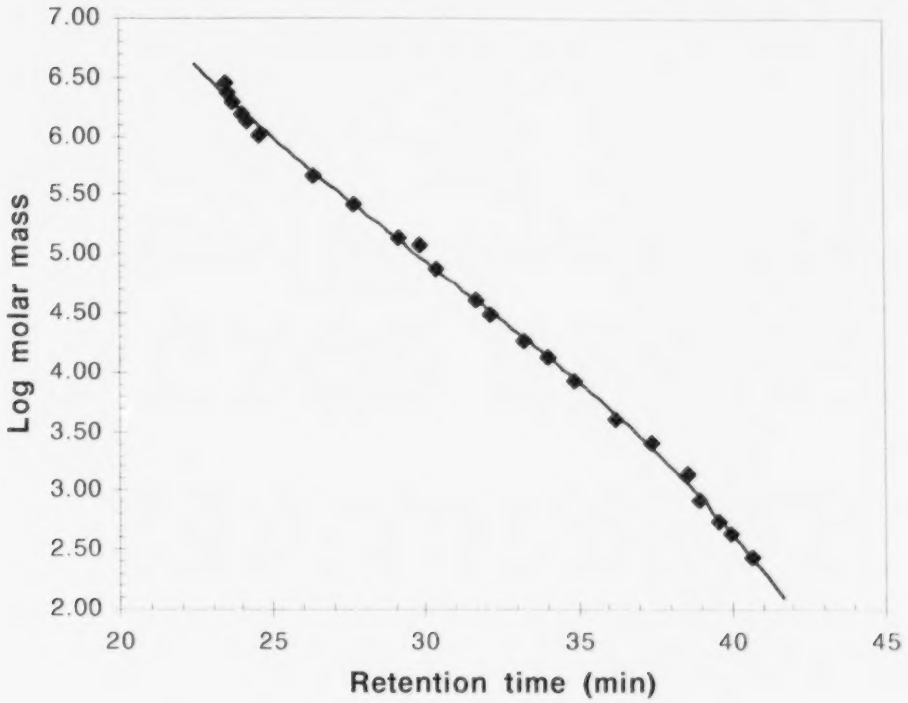

Figure 3.11: SEC calibration curve

3.5 Data collection and processing for TREF

The data generated by the TREF apparatus were recorded by an OPTO22 system and a 486 PC computer. The data collection system was recording the signal from the IR detector, the pressure transducer and the thermocouples. All these analog outputs were converted to digital signals by the OPTO22 system. The data stored on an ASCII file for each TREF run are described in Table 3.3

Table 3.3: Outputs from TREF in ASCII file

Column #	Data recorded	Units
1	Time of data collection	s
2	Set-point (not used as the temperature was controlled by the temperature chamber itself)	
3	Air temperature near the TREF column (not used)	°C
4	Temperature of the IR detector (not used)	°C
5	Temperature of the outlet line of the IR cell	°C
6	Temperature of the solvent at the outlet of the TREF column	°C
7	Air temperature near the TREF column (not used)	°C
8	Signal from IR detector	mV
9	Temperature of the IR cell	°C
10	Line pressure at the exit of the pump	bar/5

For analytical TREF, the data of interest are columns 6 and 8. The baseline of the IR signal is subtracted from column 8. Then, the data are normalized so that the sum of the IR signals is unity. This yields TREF profiles with all the same area.

$$IR_n = \frac{(\Delta T_i)(IR_i)}{\sum_i \Delta T_i IR_i} = \frac{IR_i}{\sum_i IR_i} \tag{3.1}$$

Equation 3.1 shows how the IR data are normalized. IR_n is the normalized IR signal; IR represent the IR signal, ΔT is the temperature step between two IR values and subscript i represents the individual data points. Once the data are normalized, the TREF profiles can be obtained by plotting the normalized IR signal versus the elution temperature (column 6).

For preparative TREF, the data processing was more laborious and involved several steps. The data of interest are in columns 1, 6 and 8. The first step of the data processing was to subtract the baseline from the IR signal. The next step was to isolate the data of the elution peak of each temperature interval, calculate the area and obtain the fraction of polymer eluted for each temperature interval. The peaks were isolated manually by looking at the values of the IR signals as a function of time and temperature. The weight fraction of each temperature interval was calculated by dividing the area of each peak by the sum of the area of all the peaks.

The data needed to produce the 3-D profiles of the cross fractionation are the temperature intervals, the weight fraction of each interval and the molar mass distribution of the TREF fractions. The MMD were obtained from ASCII files produced by the data acquisition system of the SEC apparatus. The 3-D profiles were constructed using the Axum software. The MMDs obtained from the SEC were normalized by areas. To produce the 3-D profile, the values of the MMDs were multiplied by the corresponding weight fraction of the temperature interval. This way, the areas of the MMD were normalized according to the weight fraction of the temperature interval. A routine was written within Axum to perform all the transformations to produce the 3-D profiles. More details are given in Appendix C.

3.6 Calibration curve for TREF

The primary elution curve (IR signal versus elution temperature) is adequate for comparing polyethylene samples and observing trends. However, it is also interesting to transform the raw data from TREF into a short-chain branching (SCB) distribution. From the SCB distributions, it is possible to calculate the molar or the mass concentrations of the comonomers in the LLDPE. To obtain quantitative information about SCB concentration from TREF, a calibration relating SCB concentration to elution temperature is required.

Many methods have been used to generate the TREF calibration curve (Bergström and Avela 1979, Wild et al. 1982, Nakano and Goto 1981, Usami et al. 1986, Kelusky et al. 1987, Karbashewski et al. 1992, and Pigeon and Rudin 1994). In all these methods, PTREF has been used to generate fractions for which the SCB concentration were measured. The SCB concentrations of the TREF fractions are usually obtained by FTIR or ^{13}C NMR. A calibration curve is then produced by plotting the elution temperature of the TREF fraction as a function of the SCB concentration, usually a linear relationship is used to fit the data. Calibrations have been produced using various type of polyethylene (HDPE, HP-LDPE, ethylene/butene, ethylene/octene LLDPE) and various solvents (TCB, o-DCB, o-xylene and α-chloronaphthalene).

A novel calibration for TREF has been introduced by Bonner et al. (1993). This method is based on the length of the crystallizable sequences between SCB, commonly referred to as the methylene sequence length (MSL). The relationship between the MSL and dissolution temperature closely

follows the relationship between melting temperature and chain length. Therefore, a derived form of the Flory melting equation (Equation 2.18) can be used to fit the experimental data points relating MSL to elution temperature. The data points are obtained by eluting sample with known MSL in TREF.

In linear polyethylene, the methyl groups at the end of the molecules behave like short-chain branches. If the molar masses of the linear molecules are low enough (molar mass < 10000), the crystallizable sequences between the methyl groups are sufficiently short to use TREF to produce a separation by molar mass. Therefore, data points for calibration can be obtained by eluting linear samples with known molar mass. The MSL is calculated from the molar mass using:

$$MSL = \frac{MM - 2}{14} \tag{3.2}$$

where MM is the molar mass of the polymer.

The samples used for the calibration were linear paraffin (C_{40} and C_{60}), three narrow MMD linear polyethylenes from the National Bureau of Standards and TREF fractions from a laboratory-produced HDPE (run #GC93048) having a broad molar mass distribution. The molar mass, MSL and the elution temperature of the various samples are shown in Table 3.4 and Table 3.5. The elution temperatures shown in Table 3.4 were measured at the half width of the elution peak. The TREF fractions of the HDPE were produced by performing PTREF on a 100 mg sample. The elution temperatures of these fractions were the average temperatures of the intervals. The molar masses from the TREF fractions of HDPE GC93048 were obtained by SEC.

Table 3.4: Standards for TREF calibration curve

Standard	Molar mass	MSL	Elution temperature (°C)
Tetracontane	562	40	29.0
Hexacontane	842	60	52.5
SRM 1482	13600	971	95.3
SRM 1483	32100	2286	97.8
SRM 1484	119600	8500	99.5

Table 3.5: Properties of TREF fractions from HDPE GC93048

Fraction	Temperature range (°C)	M_w	P_d	MSL	Elution temperature (°C)
F1	30-60	1101	1.13	79	45
F2	60-70	1794	1.14	128	65
F3	70-75	2368	1.12	169	72.5
F4	75-80	3035	1.13	217	77.5
F5	80-85	4086	1.14	292	82.5
F6	85-90	6014	1.15	429	87.5
F7	90-95	11296	1.29	807	92.5

Figure 3.12 shows MSL as function of the elution temperature. The line represents the calibration curve obtained by fitting Equation 2.18 to the data points. Values obtained for T_o^{ref} and c from the curve fitting are 373.47 K and 6.91×10^{-3}. It can be seen that the fitted curve is in excellent agreement with the experimental data points.

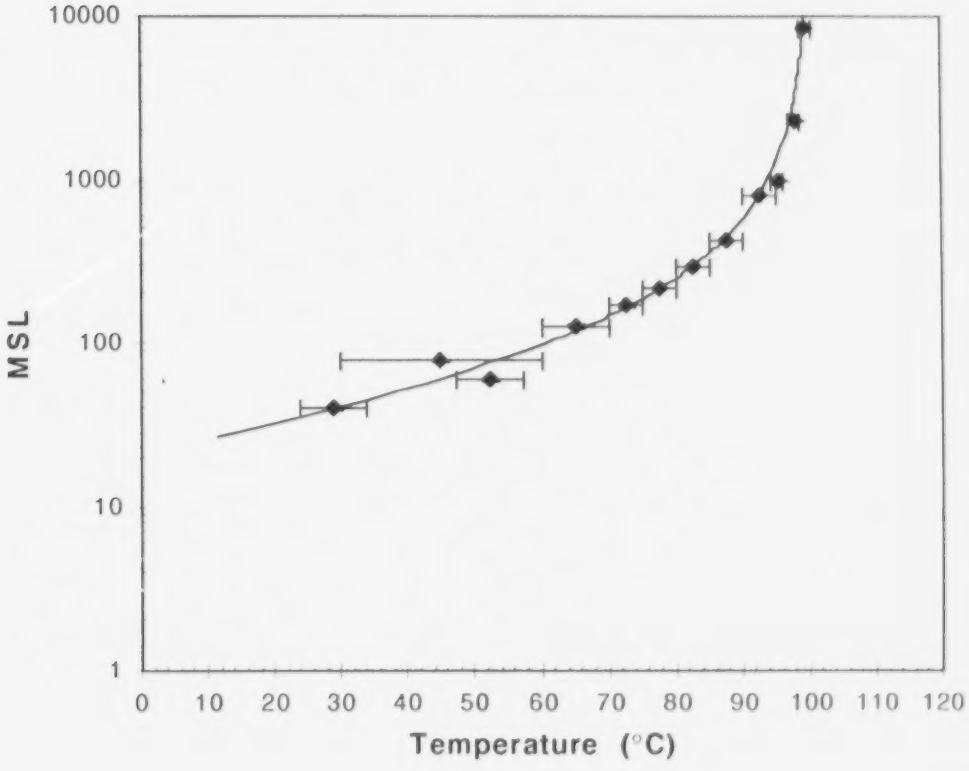

Figure 3.12: MSL versus elution temperature
standards (◆) equation (———)

From their experiments, Bonner et al. (1993) obtained 382.5 K for T_o^{tcb} and 6.36×10^{-3} for c. The differences in the parameters may be due to the use of a different solvent and from the definition of the elution temperature. For their calibration, Bonner et al. (1993) used the temperature at which the last trace of polymer had been seen to elute as the elution temperature. The problem with this way of evaluating the elution temperature is that it is more sensitive to the hydrodynamics of the column and to dissolution problems. Therefore it is more difficult to obtain reproducible measurements. The average temperature measured at the half width of the elution peak gives a better representation of the elution temperatures. The values of the elution temperatures are more reproducible.

One of the limitations of the method is the lack of suitable standards. It is difficult to find a series of linear polymers that will cover the whole range of elution temperature. The only available standards are paraffin and narrow molar mass polyethylenes from the National Bureau of Standards (SRM 1482, 1483 and 1484). These standards cover only the low and the high elution temperatures. It is very difficult to find standards for temperature ranging from 60 to 95°C. However, the use of TREF-SEC cross fractionation on a HDPE with broad MMD allows the generation of samples for these intermediate temperatures. This new method of generating "reference standard" is a great asset to the calibration curve developed by Bonner et al. (1993)

Since the main interest of ATREF is to measure branching concentration (or comonomer incorporation), it is more meaningful to translate the MSL data in terms of branching concentration (CH_3/1000C). This can be done easily by using the following relationship:

$$CH_3/1000C = \frac{2000}{MSL} \qquad (3.3)$$

The calibration curve generated using this relationship is shown in Figure 3.13 and it is also compared with data points available in the literature. From this figure it can be seen that the calibration curve generated from MSL is in agreement with the data points obtained from various authors. These data were generated from FTIR or ^{13}C NMR measurements on TREF fractions from ethylene/butene LLDPE produced in gas phase. The data follow the same trends but have an offset. These differences may be due to the use of different solvents and from the definition of the elution temperature. The size of the temperature interval in PTREF can also influence the results.

In the case of Usami et al. (1986) and Pigeon and Rudin (1994), large temperature intervals were used. The use of large temperature intervals reduces the accuracy of the results. The measurements of methyl group concentration give an average value for the temperature interval. The elution temperature corresponding to the methyl group concentration measured is the average value of the temperature interval. If large temperature intervals are used, the average temperature is not necessarily the temperature corresponding to the average methyl group concentration. For instance, if most of the polymer species were dissolved at the highest temperature of the interval, the elution temperature corresponding to the measured methyl group concentration of the interval should be higher than the average temperature of the interval.

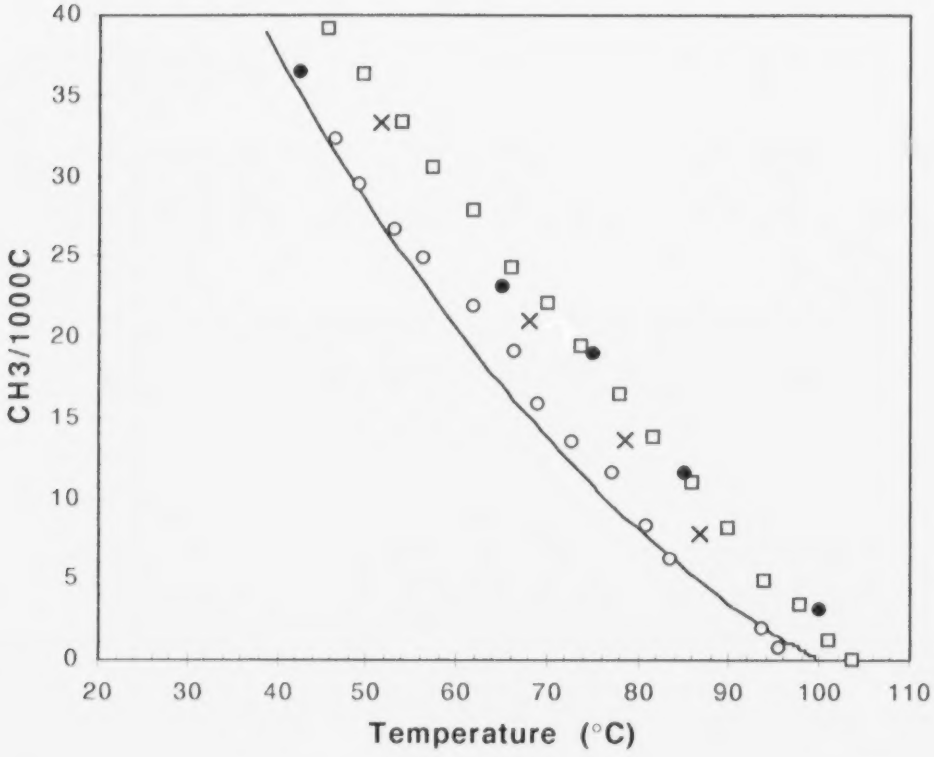

Figure 3.13: Comparison of calibration curve generated from the MSL-elution temperature relationship with data obtained from different authors using various solvents and analytical techniques:

(———) Calculated from MSL-elution temperature relationship
(O) Wild and Ryle 1982b (TCB, FTIR)
(×) Usami et al. 1986 (o-DCB, ^{13}C NMR)
(●) Pigeon and Rudin 1994 (TCB, ^{13}C NMR)
(□) Kelusky et al. 1987 (α-chloronaphtalene, ^{13}C NMR)

The method used in this work to generate the TREF calibration curve has many advantages over the conventional method. The calibration is based on a theoretical development and it produces a curve that follows the trends of the experimental data points over the range of the operating temperatures. The non-linearity in the CH_3-elution temperature relationship at high elution temperature is ignored by the linear approach of CH_3 versus elution temperature.

The MSL versus temperature relationship can explain the shapes of the TREF profiles. In a typical TREF profile of LLDPE, the peak at the low elution temperatures is always broad and the peak at high temperature is always narrow. The shape of the high temperature peak is explained by the insensitivity of TREF to MSL at high temperature. Materials with large difference in MSL elute practically at the same temperature. However, TREF is very sensitive to MSL at low temperature. Therefore, a branched polymer with a narrow SCB distribution can be eluted over a wide temperature range producing a broad peak.

Another advantage of the current calibration method is that the equipment needed to generate the calibration curve is the same as the one used for TREF-SEC cross fractionation. The calibration is achieved by performing a cross fractionation on a linear polyethylene with broad MMD and by eluting some standards using ATREF.

Besides all these advantages, this method for generating calibration for TREF has also some limitations. This calibration cannot be valid for all types of PE. As suggested by Karbashewski et al. (1993), TREF is sensitive to the effective rather than the average branching concentration. Therefore, this

calibration would be more accurate for random copolymer. To use this calibration curve, it must be assumed that the branches have a random distribution.

Another shortcoming of this calibration procedure is that the calibration curve is generated using a linear polyethylene sample. The methyl end groups were taken as short branches. The length of the side branches can affect the elution temperature (Wild 1990). Consequently, an error can be introduced in measurements made on ethylene/α-olefin LLDPE or other types of comonomer that have longer branches. However, the effect of the branch size has not been studied in detail (Wild, 1990).

The range of reliable application of the MSL equation has been discussed by Bonner et al. (1993). It is suggested that the MSL analysis might become invalid for MSL above 250. For values higher than 250 it is impossible to say whether or not the elution is controlled by short-chain branching because of chain folding. It is not known when chain folding occurs in TREF conditions (Bonner et al. 1993). Nevertheless, the results in Figure 3.12 indicate that the MSL temperature relationship gives a good representation of the experimental data. Figure 3.13 also shows that the relation for methyl group concentration versus temperature calculated from MSL is in agreement with experimental data obtained using FTIR and ^{13}C NMR.

Finally, it can be suggested that this calibration curve be used as a default when no other methods are available. This method yields a good estimation of the methyl group concentration. The best calibration curve is

obtained by performing ^{13}C NMR or FTIR on TREF fractions of the type of polymer to be studied.

4. Results and Discussion

The purpose of this project was to investigate the effect of H_2 and 1-butene concentrations on molar mass and chain branching distributions of laboratory produced ethylene/1-butene LLDPEs. The objective of the project was achieved by performing ATREF and TREF-SEC cross fractionations on the LLDPEs. The results of this study are presented in the five sections of this chapter. The effect of 1-butene concentration on MM and SCB distributions is presented first for the 1-butene series of experiments, followed by the effect of H_2 on the properties of LLDPEs. This is followed by a discussion of the validity of the results from the 1-butene and the H_2 series. Finally, preliminary results of analytical TREF of ethylene/vinyl acetate copolymers and ethylene/vinyltrimethoxysilane copolymers are presented in the last two sections. Details regarding the reaction conditions for production of the polymer are given in Appendix A, and conditions for the TREF experiments are given in Appendix B.

4.1 1-Butene series

The results from the 1-butene series come from the analysis of a series of ethylene/1-butene LLDPEs produced at various 1-butene concentrations in a gas phase semi-batch reactor over a commercial bisupported Ti catalyst. The cocatalyst was tri-n-hexylaluminum (TNHAL). The 1-butene concentration in the reactor ranged from 0 to 30 ml precharged (0 to 100 psi) and the sum of ethylene and 1-butene partial pressure was kept constant at 200 psi. The H_2 partial pressure was 100 psi for all experiments in this series. The length of the copolymerization was 2 hours and the temperature

was maintained to 70°C. More details about the operating conditions are given by Huang (1995).

4.1.1 ATREF of 1-butene series

Analytical TREF analyses were used to obtain branching distribution as a function of 1-butene concentration in the reactor. The ATREF analyses were performed using the conditions described in Chapter 3. A list of the TREF experiments and their corresponding operating conditions is given in Appendix A and B.

Figure 4.1 shows the ATREF profiles as a function of the amount of liquid 1-butene precharged in the reactor. The areas of the TREF profiles were normalized and the TREF profiles are off-set for clarity. The TREF profile for a polymer produced at the same conditions but without 1-butene present is displayed separately in Figure 4.2. It can be seen from the TREF profiles in Figure 4.1 that the amount of material that eluted at low temperature increased with increases in 1-butene concentration. In LLDPEs, the SCBs are produced by the incorporation of an α-olefin. An increase of 1-butene incorporation produces an increase of branching concentration, which explains the previous observation. The ATREF profiles clearly show that increasing 1-butene concentration increases the incorporation of 1-butene in the polyethylene. The mass ratio of comonomer to homopolymer in the LLDPEs changes from 1 to 13.3 while increasing the 1-butene concentration from 5 to 30 ml precharged. Homopolymer is the fraction of polymer which eluted at temperatures above 95°C.

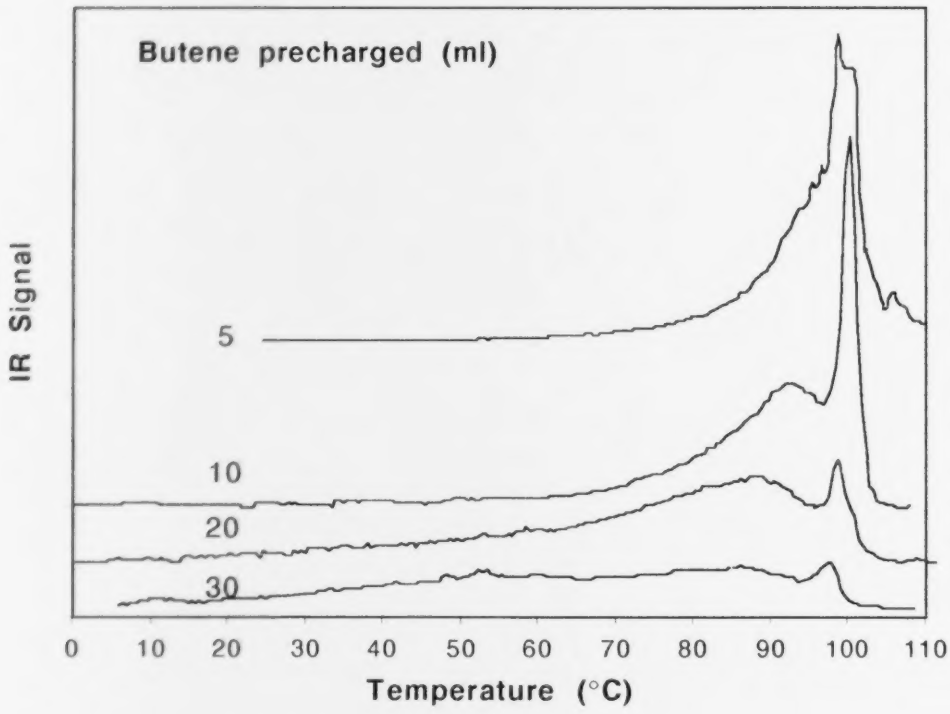

Figure 4.1: ATREF profiles of 1-butene series

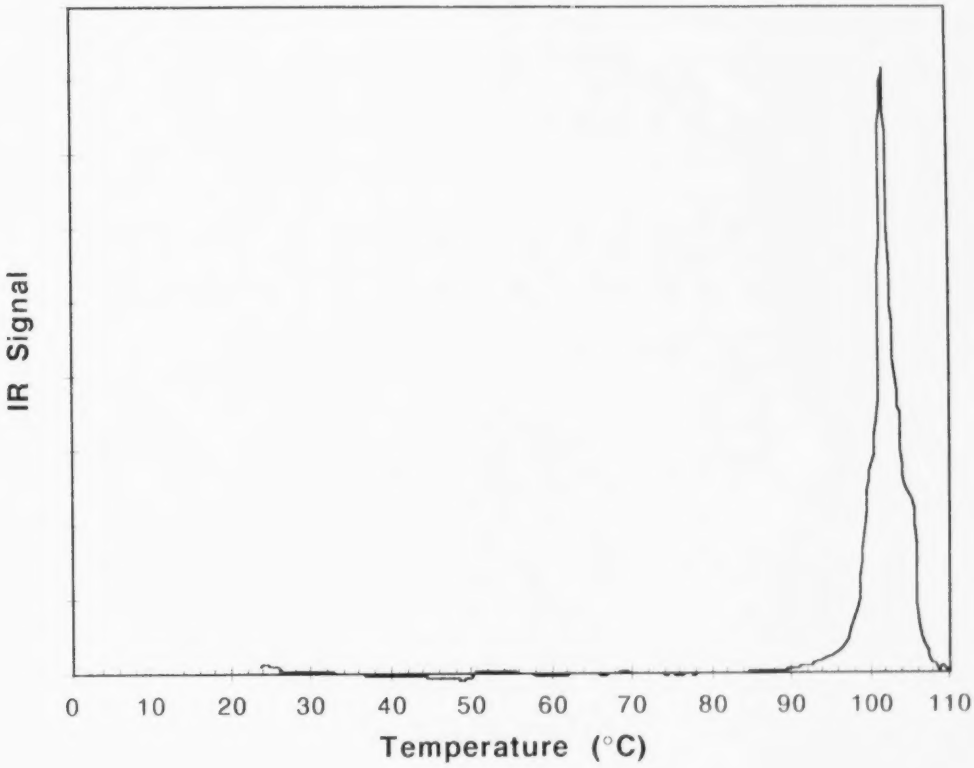

Figure 4.2: ATREF profile of PE homopolymer (0 ml 1-butene precharged)

The shapes of the TREF profiles are also of interest. Bimodal branching distributions can be observed in Figure 4.1 for the TREF profiles of the low 1-butene concentration samples (5 and 10 ml precharged). The bimodal distribution is a common characteristic of LLDPEs. The bimodal distribution is composed of a narrow peak at high temperature and a broad peak at lower temperature. The high temperature peak corresponds to homopolymer of ethylene and the low temperature peak corresponds to ethylene/1-butene copolymer. At higher 1-butene concentrations (20 to 30 ml precharged), the bimodal distribution became trimodal with two broad peaks for the ethylene/1-butene copolymer and a narrow peak at high temperature for the homopolymer of ethylene. The ATREF profile with an expanded ordinate for the 30 ml 1-butene run is shown in Figure 4.3 to more clearly show the multimodal character of the ATREF profiles obtained at high 1-butene concentration. Trimodal distributions have also been observed by Mirabella and Ford (1987) and Hosoda (1988).

The multimodality of the TREF profiles is usually explained by multiple active sites in supported catalysts. The TREF profiles of the 1-butene series suggest that two sites copolymerize ethylene and 1-butene with different rates, and a third site is responsible for the homopolymerization of ethylene.

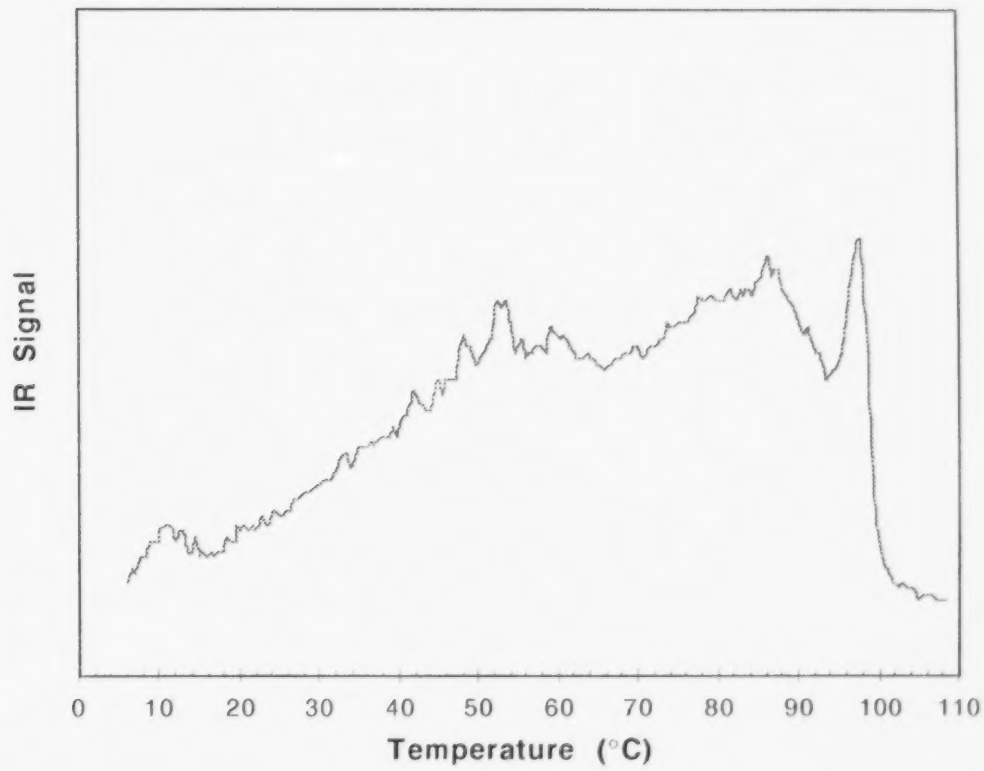

Figure 4.3: ATREF profile of ethylene/1-butene LLDPE (30 ml butene precharged)

The TREF profiles of the 1-butene series can be used to evaluate the reactivity ratios of the various sites of the supported catalysts. The reactivity ratios can be calculated from the average branching concentrations for each site and the comonomer concentrations in the reactor for a set of experiments (see Section 2.1.4). The average branching concentration of each site can be obtained from the deconvolution of the branching distributions obtained by TREF. Hosoda (1988) used Poisson distributions to deconvolute the trimodal branching distribution of a LLDPE and obtained the average CH_3/1000C for each peak.

The deconvolution of the branching distributions of the 1-butene series has been attempted. The attempt failed because of the lack of a suitable function to deconvolute the profiles and the impossibility to distinguish the two low temperature peaks in most samples.

The ATREF profiles can be transformed in branching concentration plots (amount of polymer as a function of degree of branching) by using a calibration curve such as the one shown in Figure 3.13. Figure 4.4 shows the branching distribution of the 30 ml 1-butene sample. The shape of the distribution is close to a reversed version of the ATREF profile shown in Figure 4.1

The TREF calibration curve was used to evaluate the average branching concentration and the amount of 1-butene incorporated in the polymer backbone. The values for the 1-butene series are shown in Table 4.1. The contributions of the methyl groups ending the polymer chains were neglected. The branching concentration increases from 2.3 to 22.4 with an increase in 1-butene precharged from 5 to 30 ml. The weight fractions of the

1-butene incorporated in the polymers are relatively small. The amount of 1-butene incorporated varies from 0.9 to 9.0 mass%.

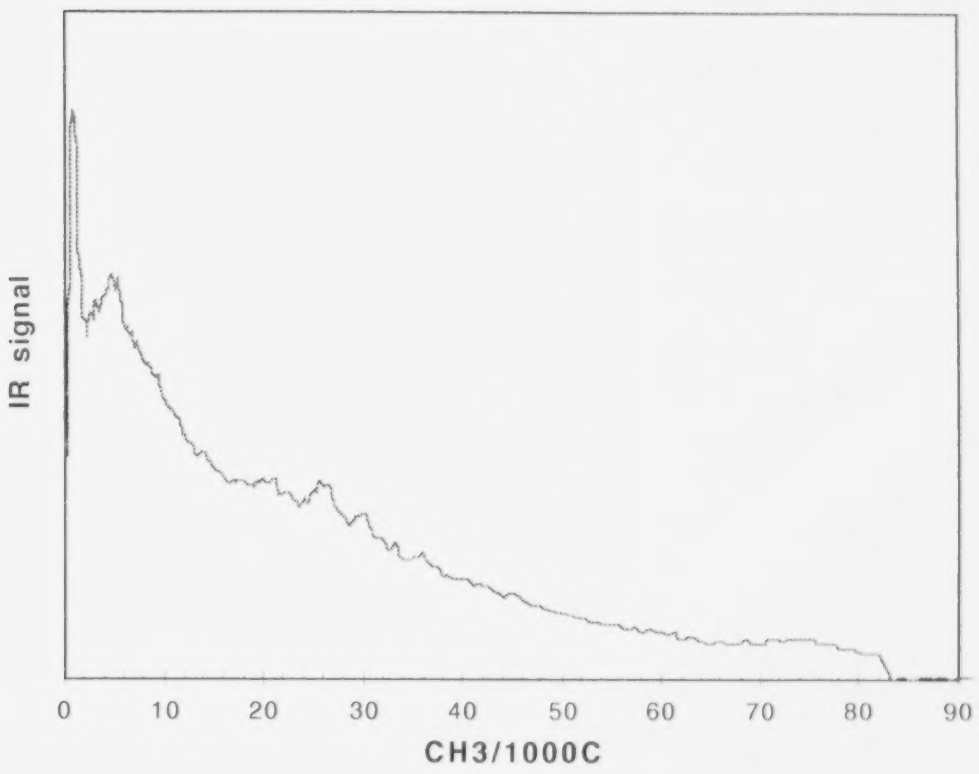

Figure 4.4: Branching distribution for the 30 ml 1-butene LLDPE

Table 4.1: Branching concentrations and 1-butene consumptions in the 1-butene series.

1-butene precharged (ml of liq.)	CH_3/1000C	1-butene content of LLDPE (mass%)	1-butene consumed (ml of liq.)	% of 1-butene consumed
5	2.3	0.9	0.9	18
10	6.0	2.4	2.8	28
20	15.1	6.0	6.9	35
30	22.4	9.0	7.4	25

The amounts of 1-butene consumed during the polymerization are listed in Table 4.1; they were calculated from the branching concentrations and the amount of polymer formed during each run (see Table A.2 in Appendix A for yield). The amount of 1-butene consumed was between 0.9 and 7.4 ml. These results indicate that 18 to 35% of the 1-butene initially injected was consumed during the runs.

The relation between the branching concentration and the amount of 1-butene precharged is shown in Figure 4.5. It can be seen that the branching concentration is a linear function of the 1-butene concentration. The regression line has a slope of 0.82 CH_3/1000C per ml of liquid 1-butene precharged.

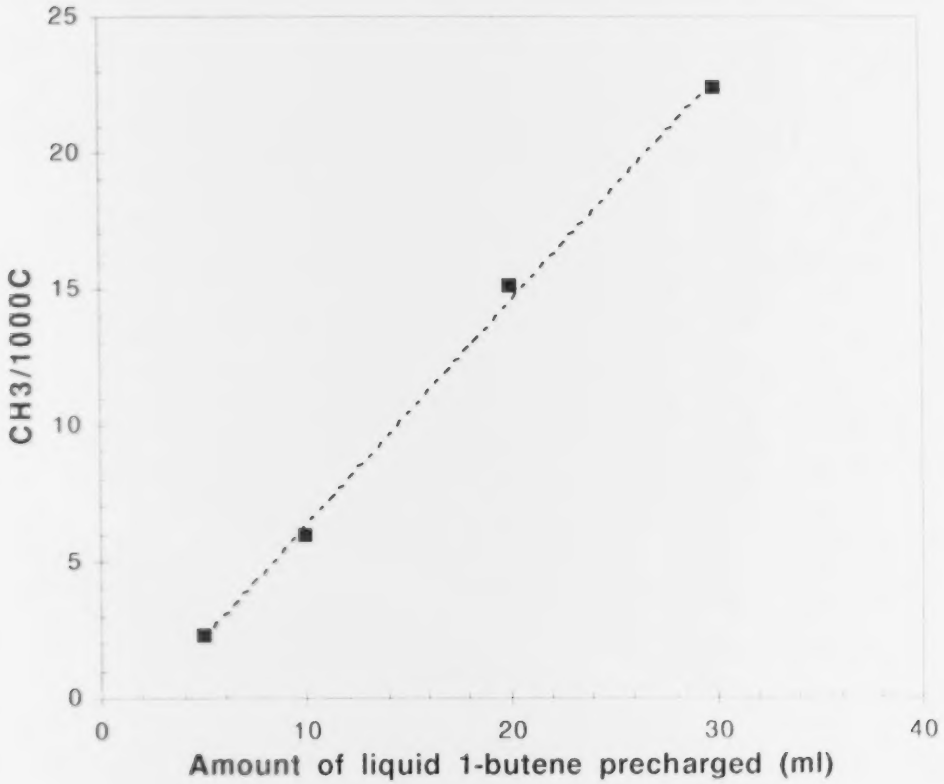

Figure 4.5: Branching concentration as a function of the amount of 1-butene precharged

4.1.2 TREF-SEC cross fractionation of the 1-butene series

TREF-SEC cross fractionations were done on the 1-butene series to obtain the MMDs as a function of the branching concentration. During the cross fractionation procedure, 8 or 9 TREF fractions were collected using the PTREF procedure described in Section 3.4.2.2. SEC analyses were performed on each fraction. The results can be presented as 3-dimensional plots showing combined branching and molar mass distributions of the LLDPEs. Figures 4.6 and 4.7 show such 3-D plots generated from the cross fractionation of the 5 and 20 ml 1-butene LLDPEs from the 1-butene series. The shapes of the TREF profiles can be seen in View 1 of both figures. The shapes of the profiles are similar to the ones obtained using ATREF. A trimodal distribution is observed for the sample made with 20 ml 1-butene recharged.

View 2 of Figures 4.6 and 4.7 shows the molar mass (MM) as function of elution temperature. It can be seen from both figures that an increase of 1-butene concentration in the reactor does not have a significant effect on the MM of the LLDPEs. The MMDs of the various TREF fractions remained at the same relative positions. However, the MMs of the TREF fractions are increasing as the elution temperature increases. This means that the MM increases with a decrease in branching concentration. This observation has been reported in many papers (Wild and Ryle 1982b, Mirabella and Ford 1987, Hosoda 1988, Karbashewski et al. 1992 and Barbatala et al. 1992).

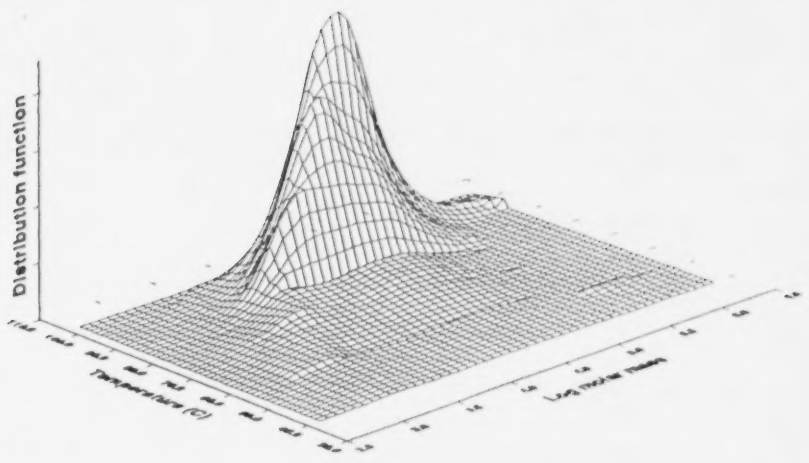

View 1

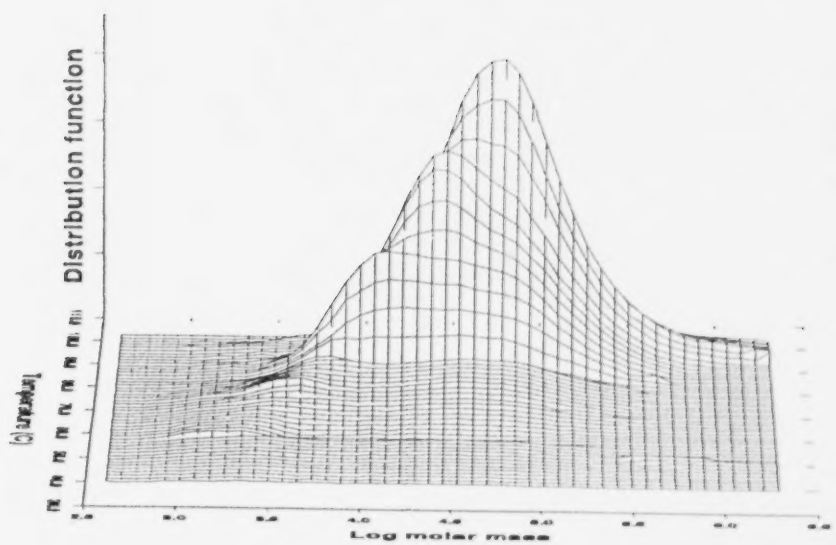

View 2

Figure 4.6: 3-D profiles for the 5 ml 1-butene experiment

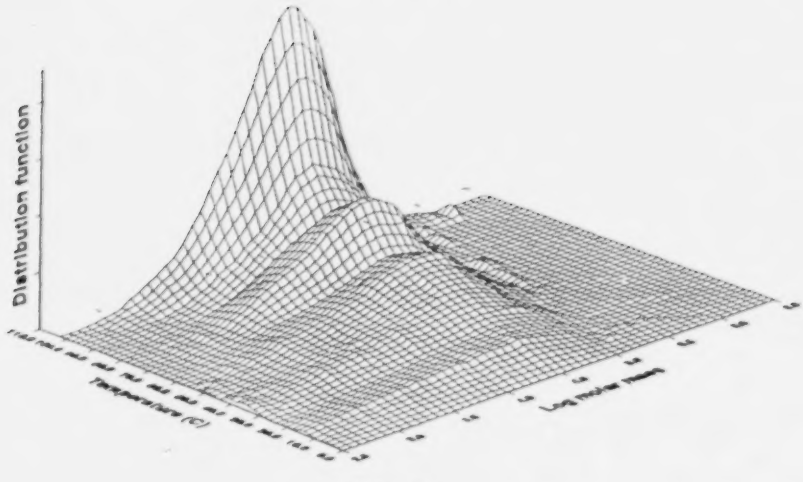

View 1

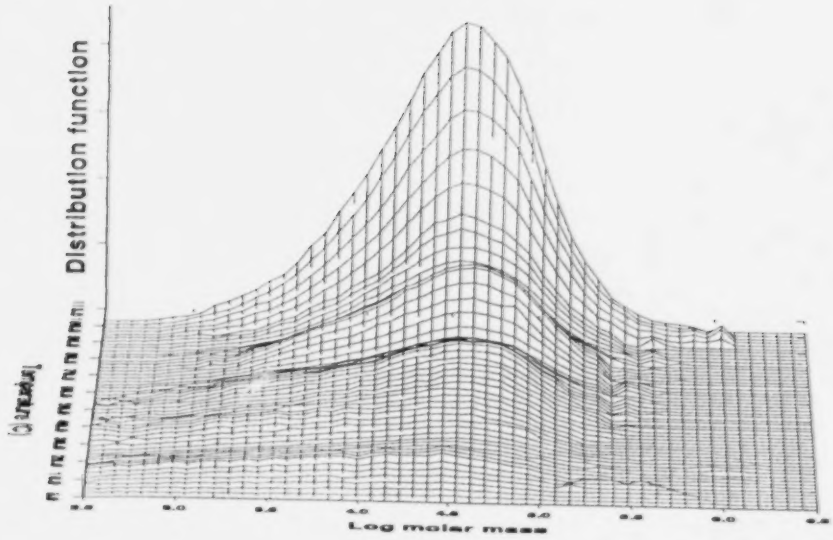

View 2

Figure 4.7: 3-D profiles for the 20 ml 1-butene experiment

The MMDs of a low temperature fraction (70-80°C) and a high temperature fraction (95-100°C) for the 5 and 20 ml 1-butene are displayed in Figures 4.8 and 4.9. The distributions for the two samples have some common features. In both cases the high temperature fraction exhibits a narrow MMD and the low temperature fraction exhibits a bimodal MMD.

By using the Peakfit software, the MMDs obtained from the cross fractionation were deconvoluted using Gaussian distributions. Samples of these deconvolutions are shown in Figures 4.10 to 4.13. The results show that two Gaussian curves were needed to fit the MMDs for the low temperature TREF fractions and only one Gaussian curve was usually needed to fit the MMDs of the high temperature fractions. In some cases, as in Figure 4.13, there was a high MM tail such that the entire MMD could not be completely described by a single Gaussian curve. These results are in agreement with the ATREF profiles which suggest that two types of catalytic sites copolymerize ethylene and 1-butene and one type of site produces the ethylene homopolymer. The MMDs of the low temperature fractions are broader or bimodal because the copolymer is produced by two types of active sites. The MMDs of the high temperature TREF fractions are narrow and unimodal because the homopolymer is produced by only one type of catalytic site.

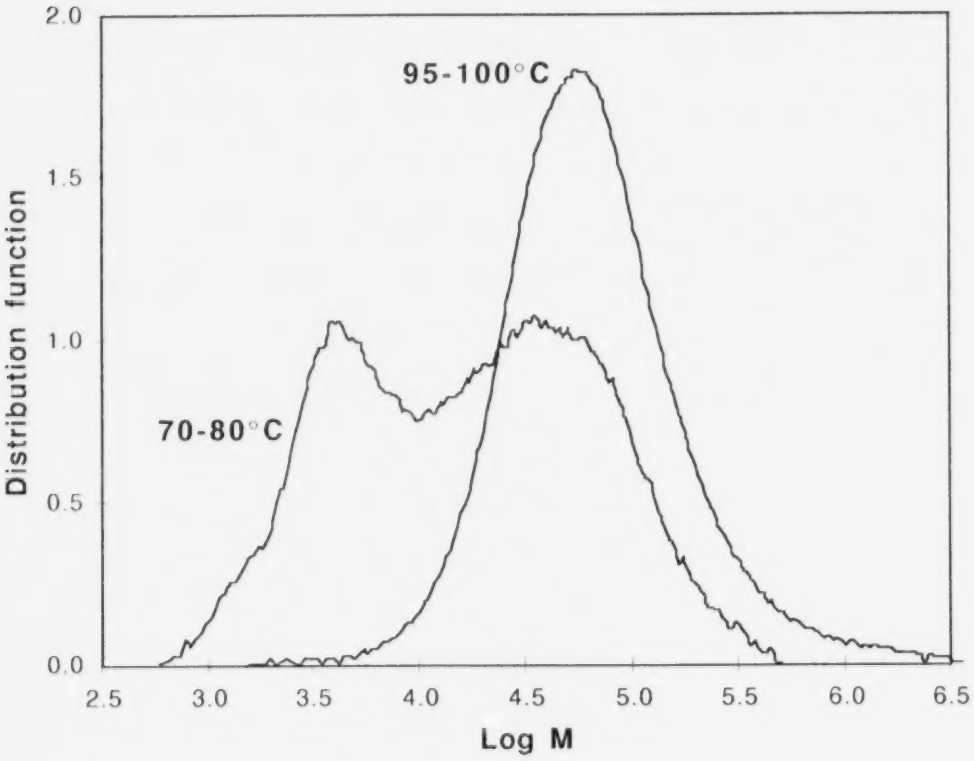

Figure 4.8: MMD of two TREF fractions of the 5 ml 1-butene LLDPE

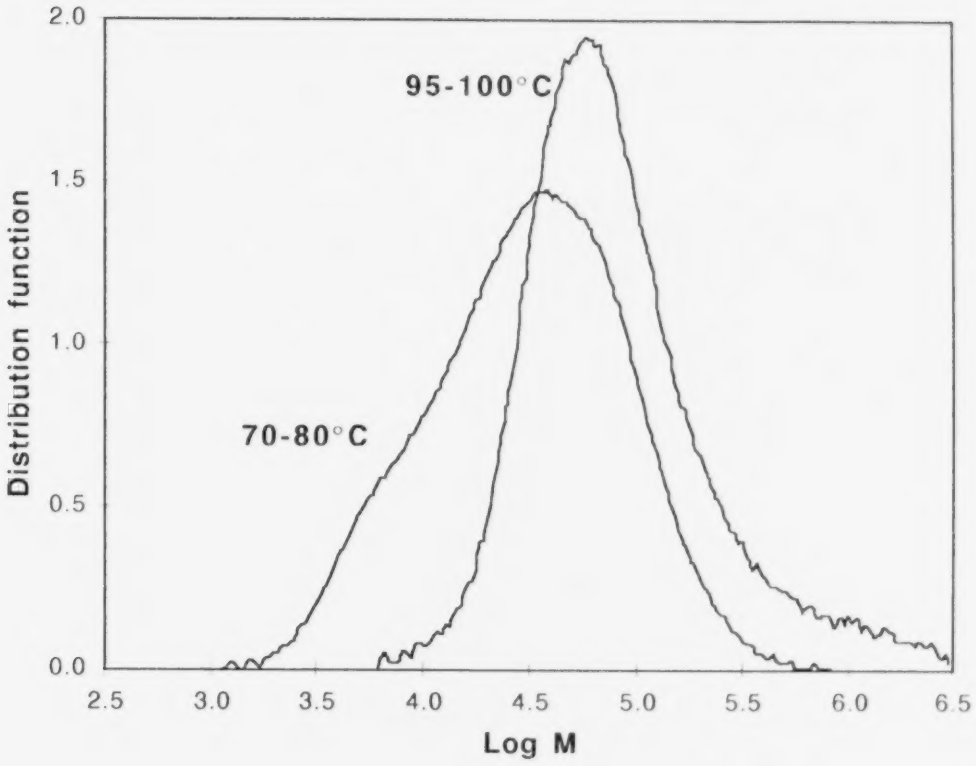

Figure 4.9:MMD of two TREF fractions of the 20 ml 1-butene LLDPE

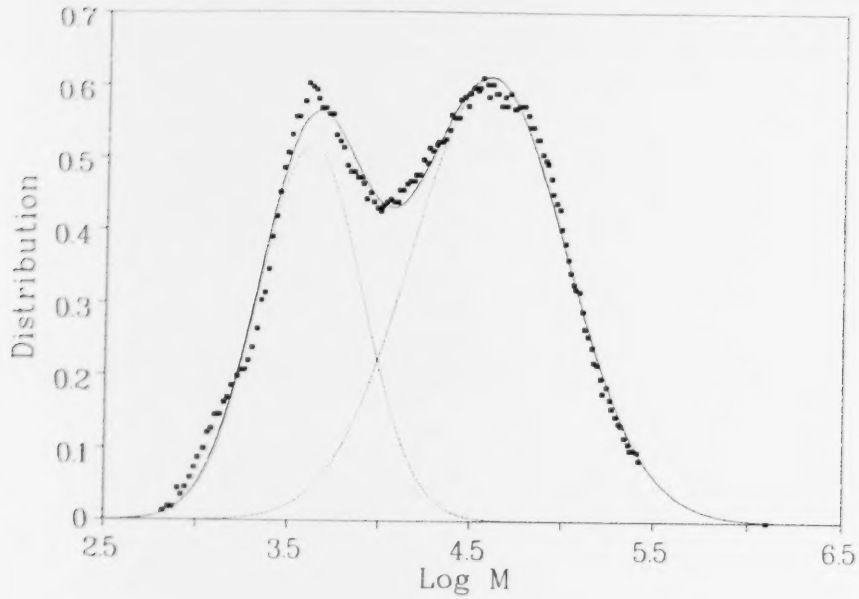

Figure 4.10: Fitted MMD of a low temperature fraction (70-80°C) of the 5 ml 1-butene LLDPE.

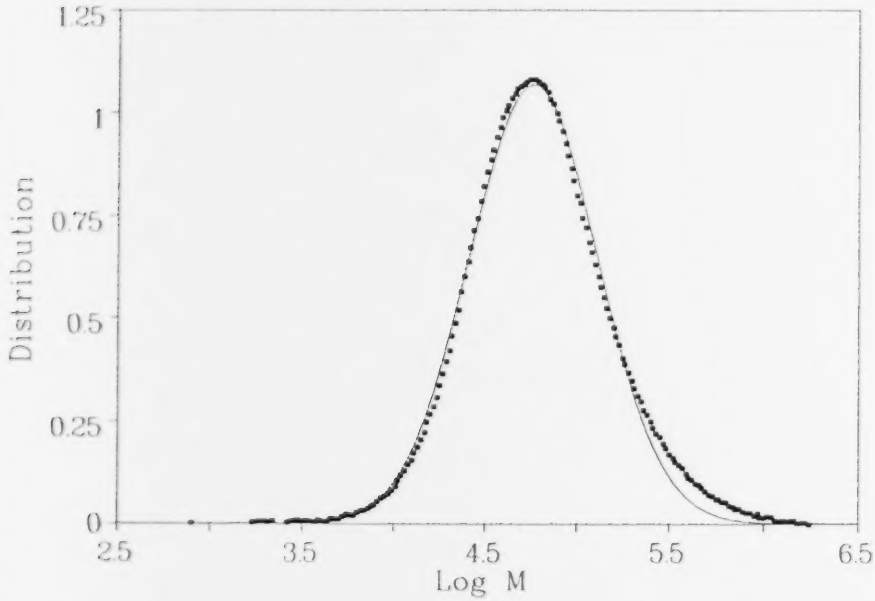

Figure 4.11: Fitted MMD of a high temperature fraction (95-100°C) of the 5 ml 1-butene LLDPE.

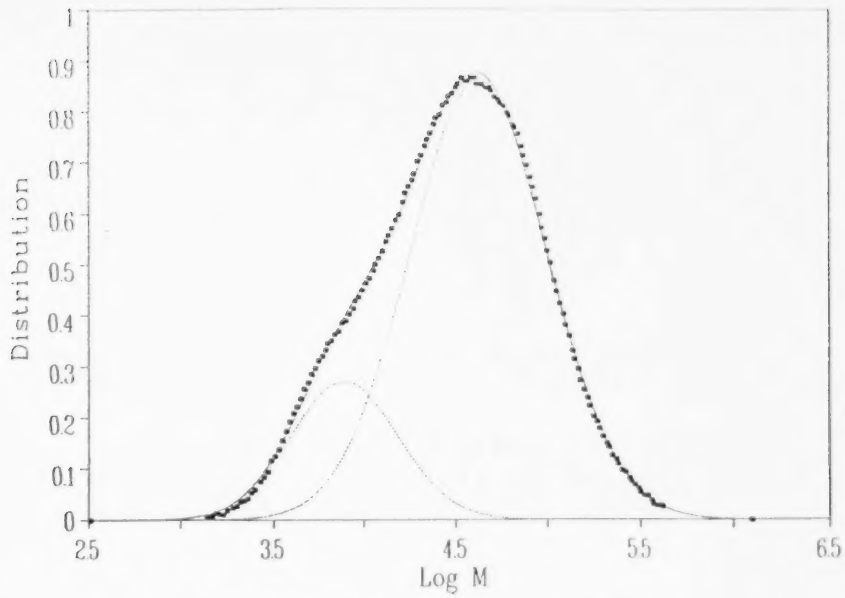

Figure 4.12: Fitted MMD of a low temperature fraction (70-80°C) of the 20 ml 1-butene LLDPE.

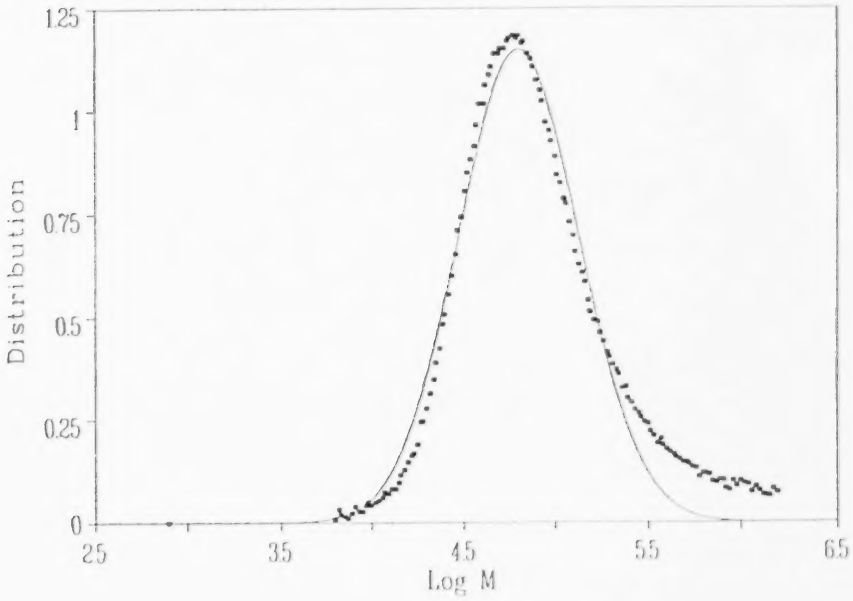

Figure 4.13: Fitted MMD of a high temperature fraction (95-100°C) of the 20 ml 1-butene LLDPE.

4.2 Hydrogen series

The samples for the H_2 series came from of a series of ethylene/1-butene LLDPEs produced at various H_2 concentrations in a gas phase semi-batch reactor over a commercial bisupported Ti catalyst. The cocatalyst was TNHAL. For all the runs in the H_2 series, 10 ml of liquid 1-butene was precharged (≈35 psi) to the reactor, and the ethylene partial pressure was 165 psi for all the polymerization runs. The H_2 partial pressure was varied from 0 to 300 psi in the various runs. The length of the copolymerization was 2 hours and the temperature was maintained to 70°C. For more details about the copolymerization runs see Appendix A and Huang (1995).

4.2.1 ATREF of hydrogen series

ATREF analyses were used to obtain the branching distribution as a function of the H_2 partial pressure. The ATREF analyses were performed using the conditions described in Chapter 3. The TREF profiles for the H_2 series are shown in Figure 4.14. The profiles are off-set for clarity. It can be seen in this figure that H_2 partial pressure does not have much effect on the branching distribution for H_2 pressures up to 200 psi. The copolymer-homopolymer ratios of the LLDPEs were between 0.6 and 1.3 for the samples with H_2 partial pressure less than or equal to 200 psi. The TREF profiles of these samples are bimodal with one broad peak at low temperature and a narrow peak at high elution temperatures.

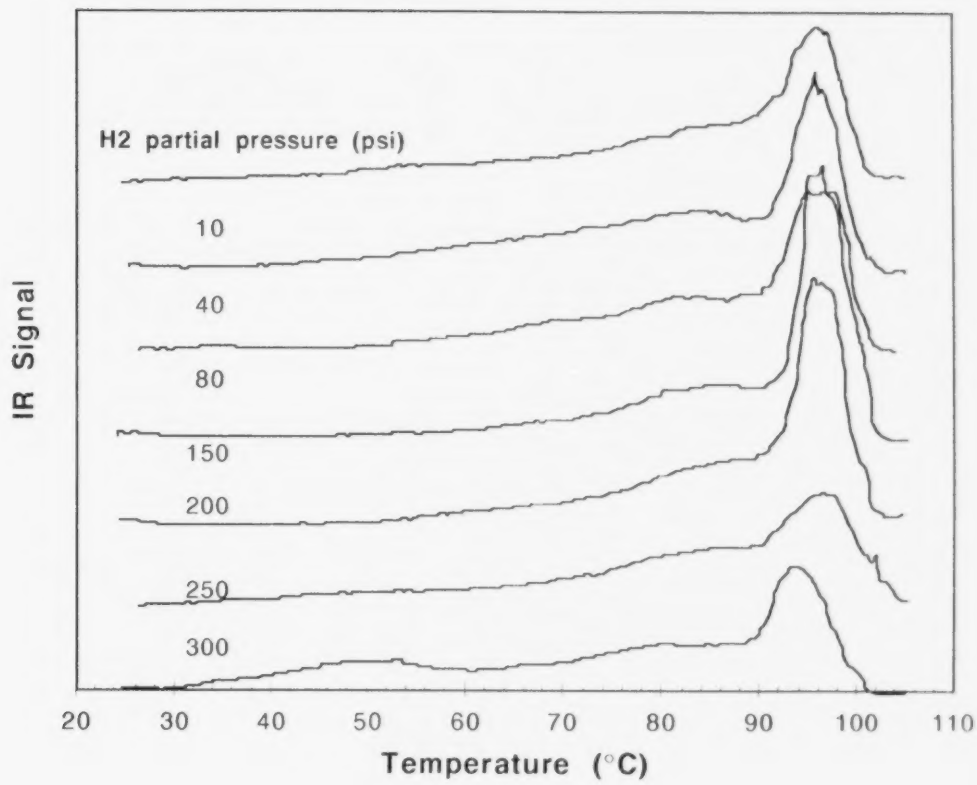

Figure 4.14: ATREF profiles of the H_2 series

For the samples with a H_2 partial pressure higher than 200 psi, the shape of the TREF profile changed. More material appears at low elution temperatures and at 300 psi, the profile is trimodal. There are two broad peaks at low temperature and a narrow peak at high temperature as observed in the 1-butene series. The TREF profiles of the 250 and 300 psi H_2 LLDPEs suggest that the increase in the H_2 partial pressure produced an increase of comonomer incorporation in the LLDPE. The copolymer-homopolymer ratios for the 250 and 300 psi samples were 1.6 and 2.0.

Figure 4.15 shows the effect of H_2 on the branching concentration of the LLDPE. The branching concentrations were obtained from the TREF profiles. The results indicate that H_2 does not have a significant effect on the comonomer incorporation. The points are very scattered. However, it can be seen that at high H_2 pressures (250 and 300 psi) there is a trend toward higher branching concentrations. The line in Figure 4.15 is a linear regression line for the 15 data points.

The results from the copolymerization runs show that the rate of copolymerization decreases with an increase of H_2 partial pressure. The increase of comonomer incorporation observed for the high H_2 partial pressures can be explained by H_2 decreasing the rate of polymerization over the sites responsible for the homopolymerization more than over the sites responsible for the copolymerization. Therefore, the relative amounts of ethylene/1-butene copolymer and ethylene homopolymer changed with changing H_2 pressure.

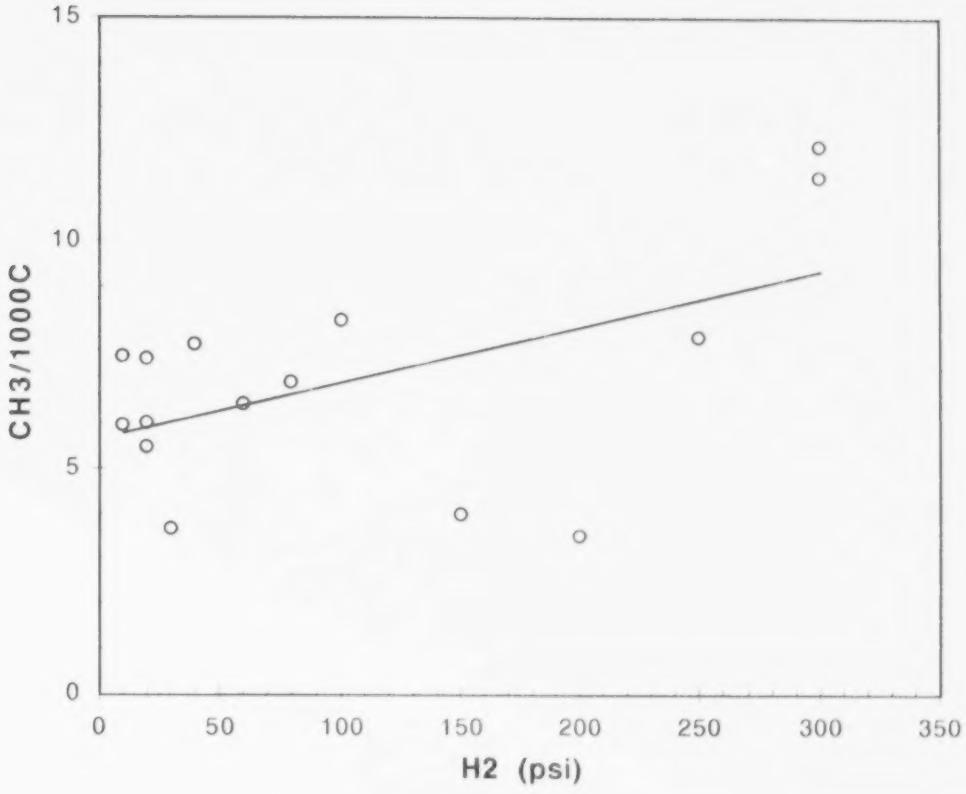

Figure 4.15: Effect of H_2 partial pressure on the average branching concentration of LLDPE

4.2.2 TREF-SEC cross fractionation of H_2 series

TREF-SEC cross fractionations were performed on the H_2 series samples to obtain the MMD as a function of the branching concentration. The effect of H_2 partial pressure on the MM of the PTREF fractions is shown in the 3-D profiles plotted in Figures 4.14 to 4.16. Three representative samples, made at low, medium and high H_2 pressure (40, 150 and 300 psi), were chosen to describe the effects of H_2 partial pressure on the MM and MMD.

View 1 of the series of figures shows the shape of the TREF and MMD profiles of the samples. It can be seen that the shapes of the profiles are in agreement with the ATREF profiles presented in Figure 4.14. The 3-D profiles show a bimodal branching distribution for the 40 and 150 psi H_2 samples and a trimodal distribution for the 300 psi H_2 sample. The trimodal distribution is less visible in the 3-D profile because of the lower resolution of PTREF.

View 2 of the same figures highlights the effects of H_2 partial pressure on the MM and MMD of the TREF fractions of the LLDPEs. H_2 does not affect the MM of the LLDPEs uniformly. In Figure 4.16, the MMD of all the TREF fractions are similar. However, as the H_2 partial pressure increases the MMDs of the low temperature fractions shift to the left of the high temperature MMDs (Figure 4.17 and Figure 4.18).

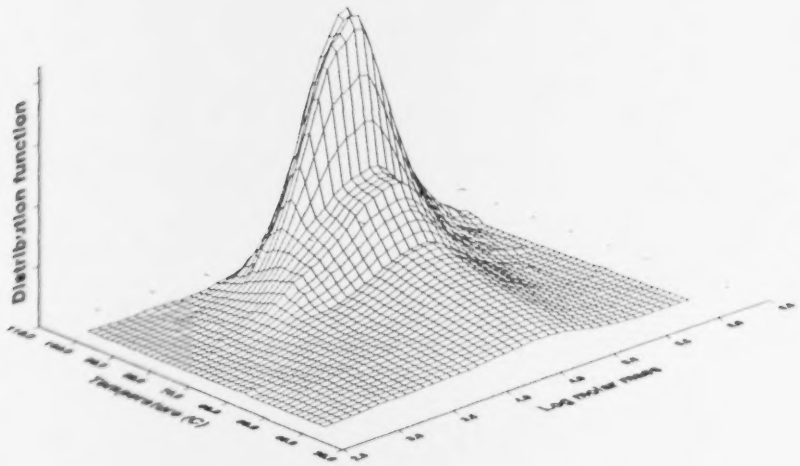

View 1

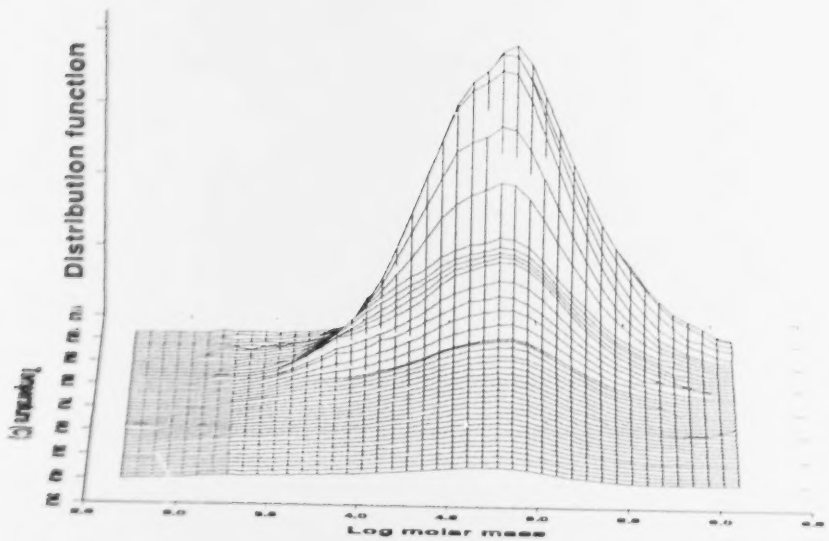

View 2

Figure 4.14: 3-D profiles of the 40 psi H_2 LLDPE

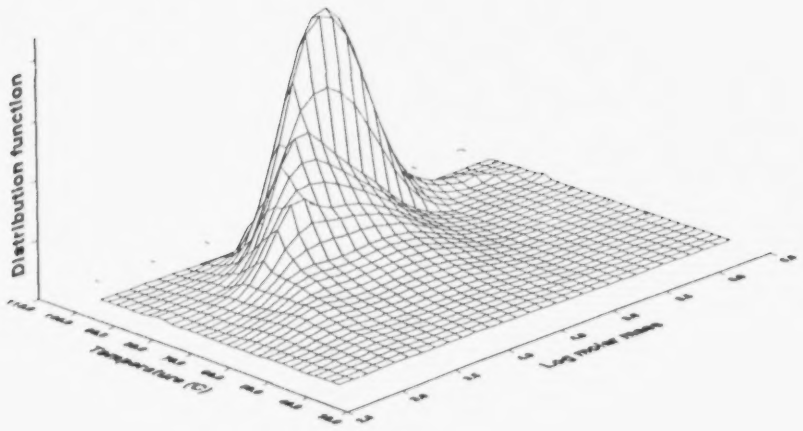

View 1

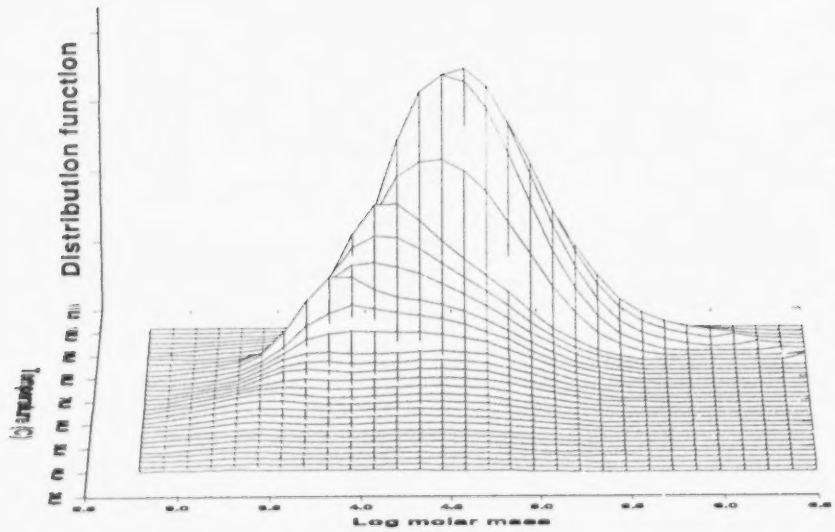

View 2

Figure 4.15: 3-D profiles of the 150 psi H_2 LLDPE

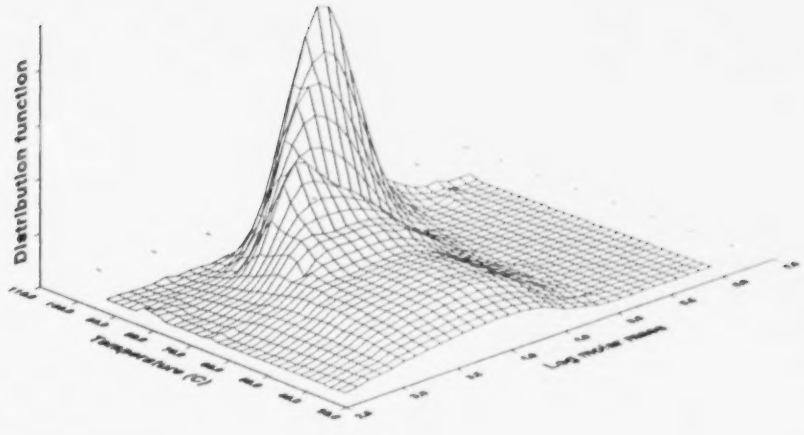

View 1

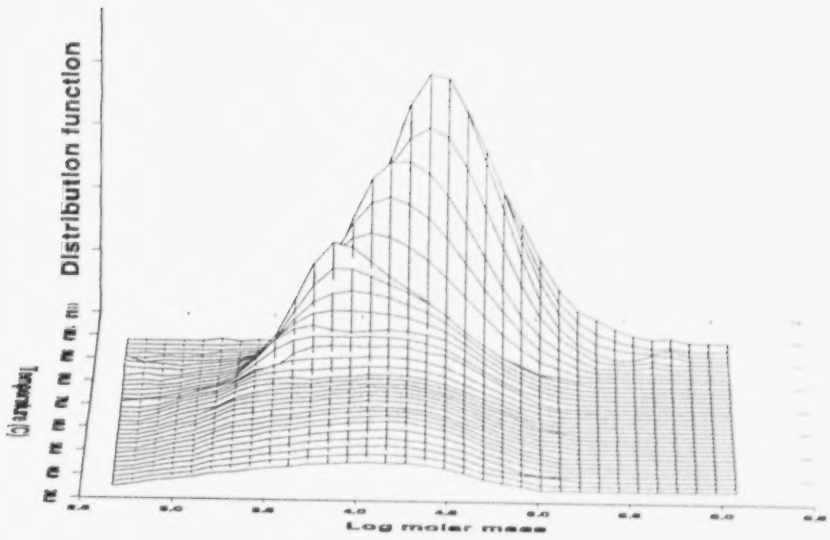

View 2

Figure 4.16: 3-D profiles of the 300 psi H_2 LLDPE

Figure 4.19 to Figure 4.21 show the MMD of a low temperature fraction (70-80°C) and a high temperature fraction (95-100°C) for the runs at 40, 150 and 300 psi H_2. These figures clearly show that hydrogen is a much more effective chain transfer agent for the copolymerization sites than for homopolymerization sites. The MMD of the low temperature TREF fractions (70-80°C) move toward lower MM as the H_2 partial pressure increases. However, the MMD of the high temperature fraction remained at the same position. The trend for low temperature fractions to have lower MM than the high temperature fractions is again observed for the H_2 series.

The shapes of the MMDs of the H_2 series are comparable to the 1-butene series. The low temperature fractions have bimodal MMDs and the high temperature fractions have narrow MMDs. As with the 1-butene series, two Gaussian functions are needed to fit the low temperature MMDs and only one is needed to fit the high temperature fractions (see Figure 4.22 and Figure 4.23). Therefore, the belief that two sites are responsible for the copolymerization of ethylene and 1-butene and only one site polymerizes ethylene is corroborated. The above mentioned effect of hydrogen chain transfer termination implies that the catalytic sites responsible for copolymerization are much more sensitive to hydrogen termination than the sites responsible for homopolymerization.

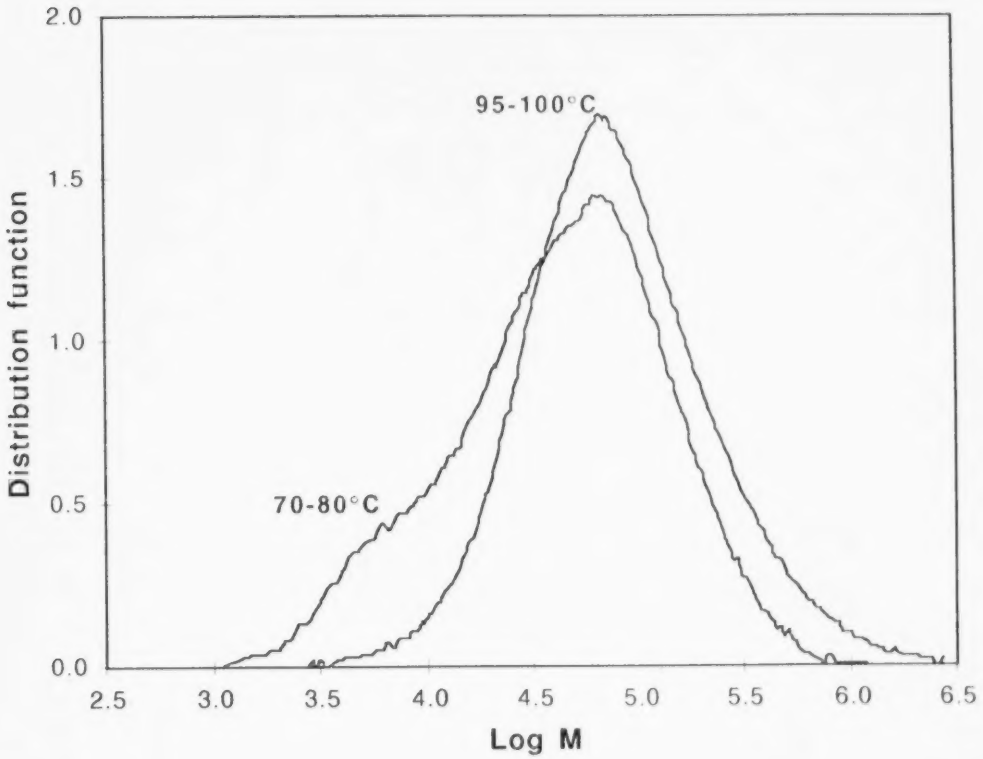

Figure 4.19: MMD of two TREF fractions of the 40 psi H_2 LLDPE

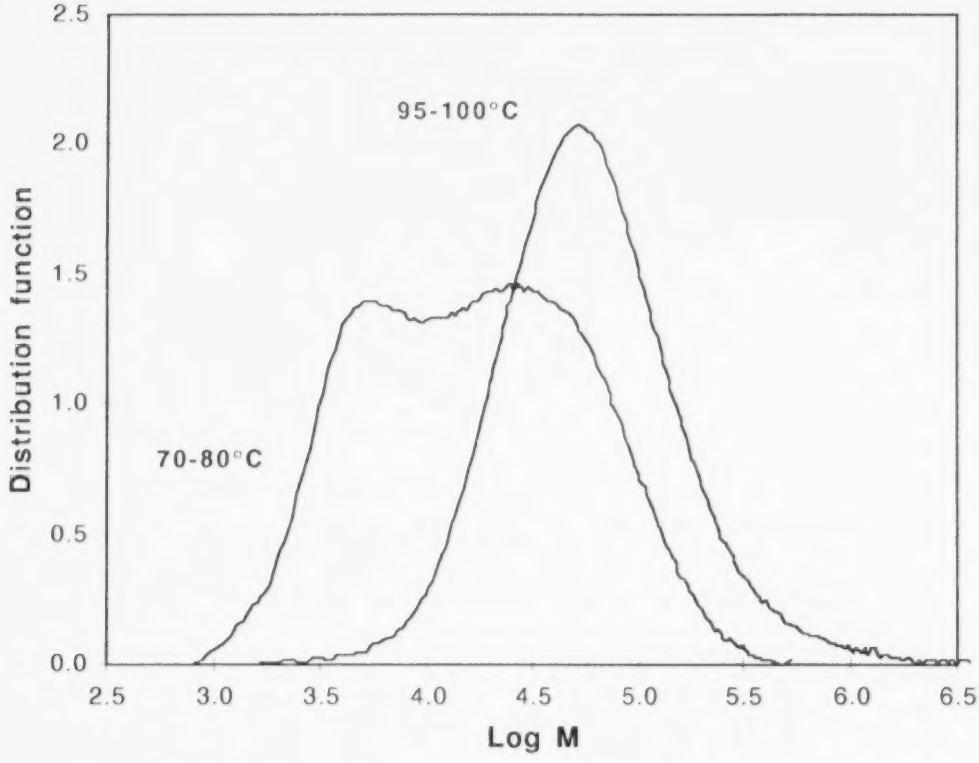

Figure 4.20: MMD of two TREF fractions the 150 psi H_2 LLDPE

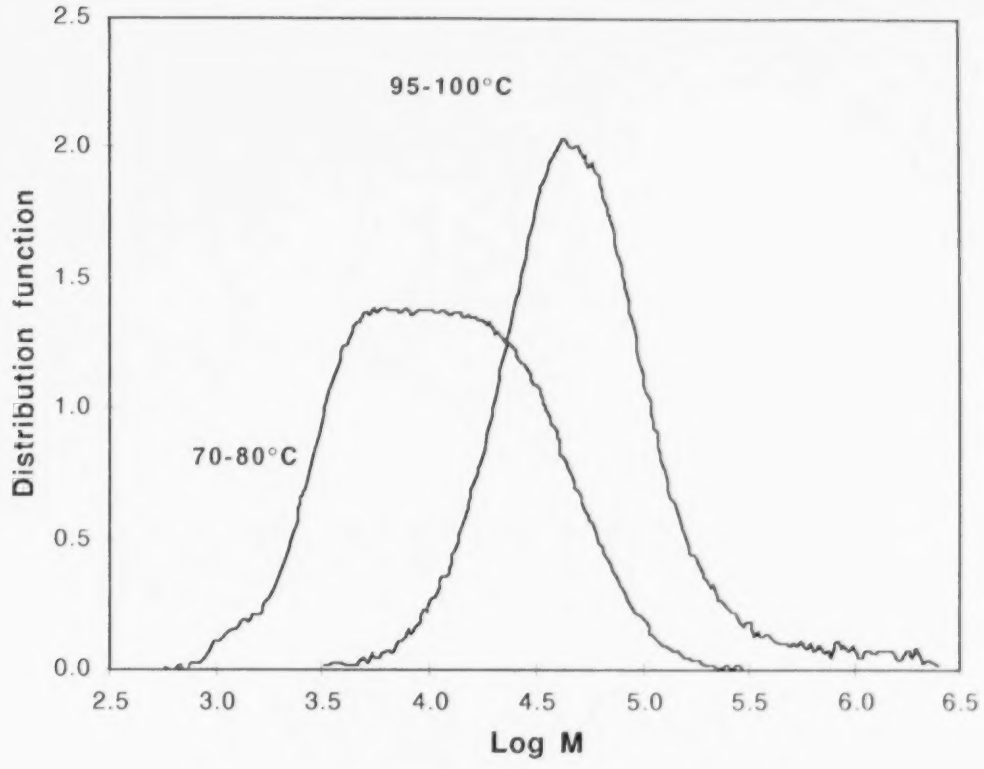

Figure 4.21: MMD of two TREF fractions of the 300 psi H_2 LLDPE

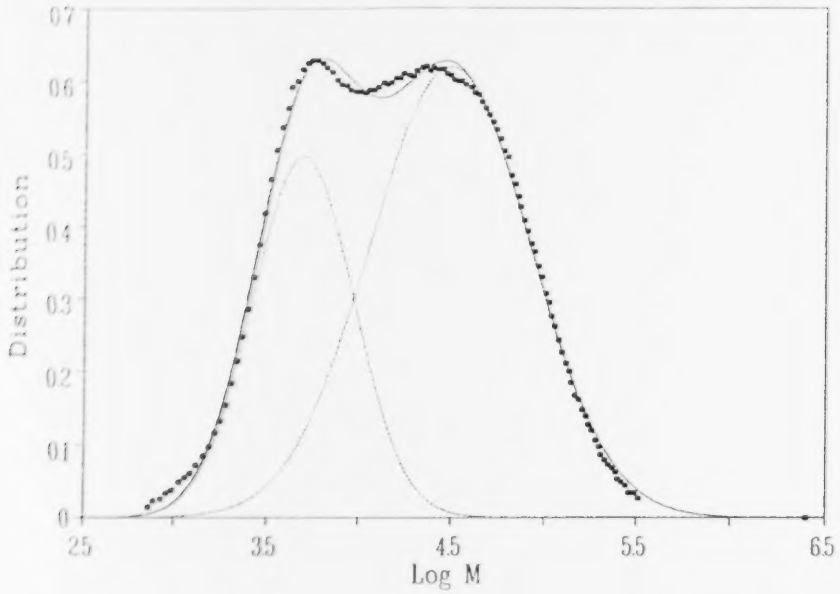

Figure 4.22: Fitted MMD of a low temperature fraction (70-80°C) of the 150 psi H_2 LLDPE

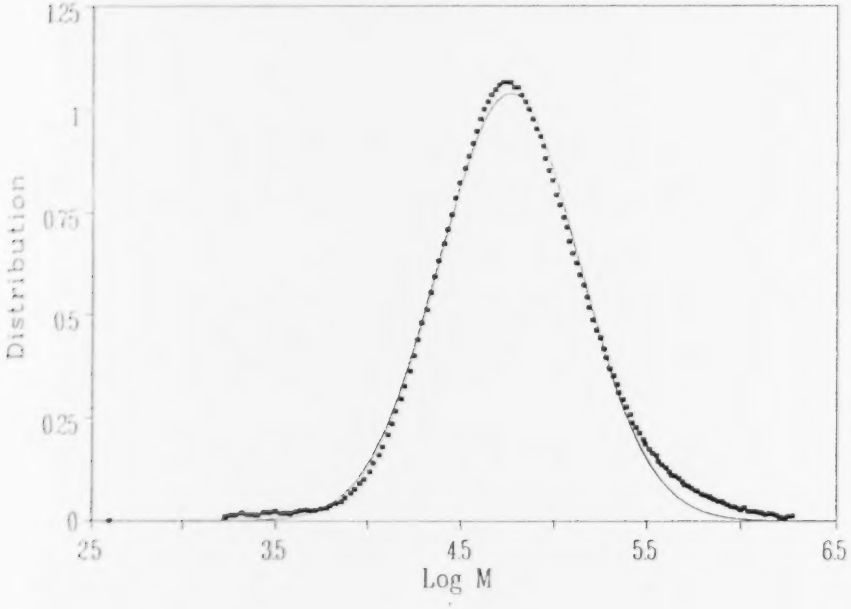

Figure 4.23: Fitted MMD of a high temperature fraction (95-100°C) of the 150 psi H_2 LLDPE

Figure 4.24 shows the effect of H_2 on M_w for high and low temperature PTREF fractions. The low temperature fraction consists of ethylene/1-butene copolymer and the high temperature fraction is essentially ethylene homopolymer. The M_w were normalized with respect to the M_w at 10 psi H_2

At low H_2 partial pressures (P_{H2} <50 psi), the effect of H_2 on M_w was very strong. There was a sharp decrease of M_w with an increase of H_2 partial pressure for both high and low temperature PTREF fractions. At 50 psi, M_w for both fractions had decreased to about 45% of their initial values at P_{H2} of 10 psi. At H_2 pressures higher than 50 psi, H_2 affects the MM of the TREF fractions differently. The molar mass of the high temperature fraction does not change significantly with increasing hydrogen pressure. It remains at about 40% of its initial value. However, the MM of the low temperature fraction continues to decrease linearly while increasing H_2 partial pressure. The M_w at 300 psi is about 15% of its initial value. These results show that H_2 is a better chain transfer agent for the copolymer than the homopolymer fraction of the LLDPEs.

The amounts of H_2 consumed during the polymerization experiments were calculated and the results are shown in Table 4.2. The H_2 consumptions were calculated from the molar masses and the amounts of polymer formed (see Table A.1 for yield). It was assumed that one H_2 molecule was consumed per polymer molecule formed. The initial amount of H_2 in the reactor was estimated by using the ideal-gas equation. No H_2 was fed to the reactor during the polymerization. The results in Table 4.2 show that the H_2 consumption is very low. The maximum percentage of H_2 consumed is 3.3% at 10 psi. Therefore, the sharp decrease of M_w at low H_2 pressures is not resulting from a lack of H_2 in the reactor.

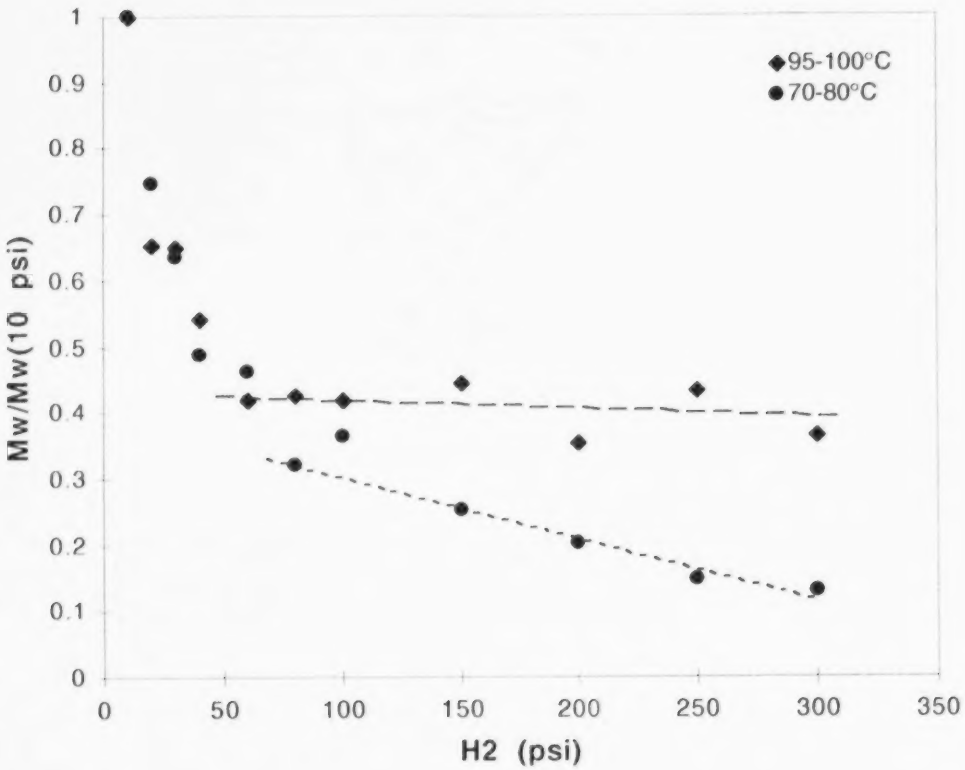

Figure 4.24: Effect of H_2 on M_w for different TREF fractions

Table 4.2: Percentages of H_2 consumed during the polymerization

H_2 (Psi)	% of H_2 consumed
10	3.3
20	2.8
30	1.3
40	1.2
60	1.4
80	1.0
100	1.0
150	1.3
200	0.9
250	0.6
300	2.8

4.3 Validity of the TREF-SEC results

When performing ATREF and PTREF on the LLDPEs, one concern is the validity of the results. For samples with high branching concentration, it is possible that some of the polymer did not crystallize. Therefore, these fractions would not be present in the TREF profiles. The total areas under the TREF profiles can be compared to verify if the amounts of polymer eluted remained relatively constant. The total area under the TREF profile is proportional to the total amount of polymer that has eluted from the TREF column.

The areas of all the ATREF and PTREF profiles obtained for the H_2 and 1-butene series were calculated and normalized with respect to the mass of polymer used in preparing the TREF samples. This way, all the areas can be compared on the same basis. Figure 4.25 shows a plot of the areas as a function of the average methyl group concentration of the samples. The values of CH_3/1000C for the PTREF runs were obtained from the ATREF profiles. It can be seen in Figure 4.23 that all the runs for the 1-butene series, except the one with CH_3/1000C of 22.4, have essentially the same area. The lower area for the most highly branched sample could be due to the loss of some non-crystallized very highly branched material. This loss would have occurred during the transfer of sample to the TREF column (see Section 3.4.1).

It is also interesting to observe that the areas of the 1-butene series are, on the average, about 10% higher than the areas of the H_2 series. The differences may have been caused by a small change in the setting of the IR detector wavelength. Between the time at which the 1-butene and H_2 series were analyzed, other characterizations were performed using a different

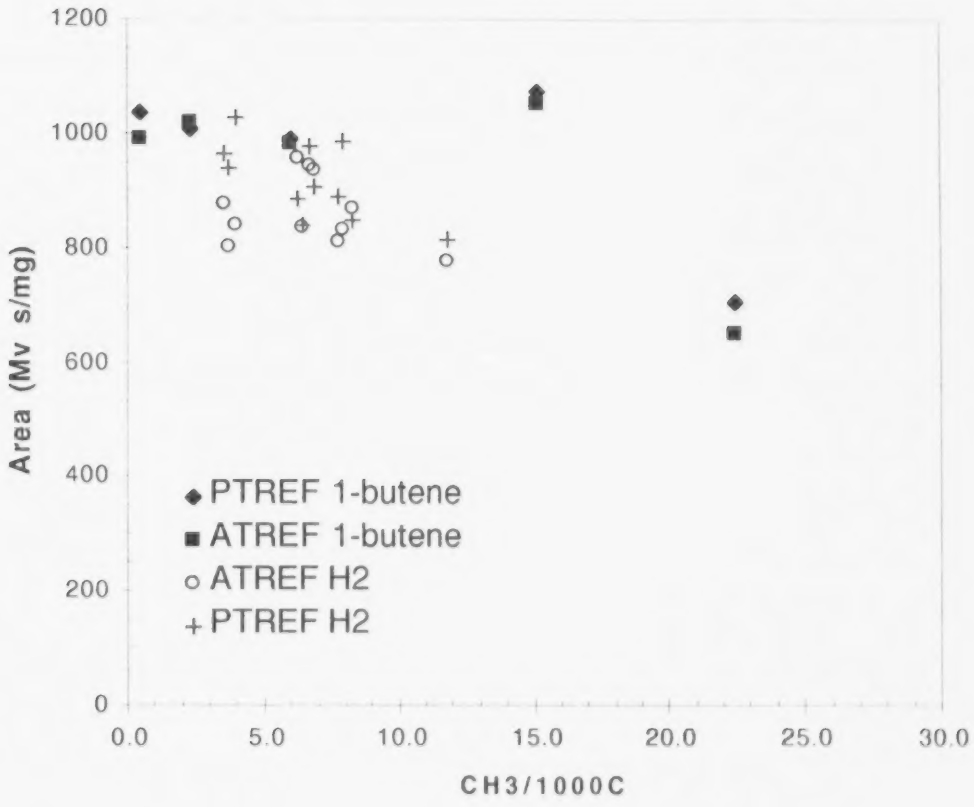

Figure 4.25: Areas of ATREF and PTREF runs versus the branching concentration of the corresponding LLDPEs

wavelength. A small difference in the wavelength setting might have occurred when the setting was returned to its original value of 3.38 μm. The resetting may not be exact because the setting is done with an analog dial.

Table 4.3 and Table 4.4 show the average values of the areas and their standard deviation based on 3 repeated analyses for the ATREF runs. It can be seen in these tables that the samples with low branching concentrations have higher standard deviations. The TREF profiles of these samples were less reproducible and there was also some dissolution problems at high temperatures. However, it is important to point out that when the areas were normalized to unity, the distributions were very reproducible even if the areas were different.

Table 4.3: Average area and standard deviation of the ATREF profiles for the 1-butene series

1-butene (ml)	Sample	CH_3/1000C	Average area (mV s/mg)	Std dev (mV s/mg)
0	GC94048	0.4	990	143
5	GC93049	2.3	1018	213
10	GC93051	6.0	984	60
20	GC93050	15.1	1052	13
30	GC93047	22.4	653	52

TREF-SEC cross fractionation involved the recovery of many fractions from the LLDPEs and the measurement of their MM using SEC. With all the steps involved in this procedure, some error can be introduced in the process. One way to verify the results from the TREF-SEC cross fractionation is to reconstruct the overall MMD of the LLDPEs and compare it with the MMD measured by SEC on the whole sample.

Table 4.4: Average Area and standard deviation of the ATREF profiles for the H_2 series

H2 (psi)	Sample	CH_3/1000C	Average area (mV s/mg)	Std dev (mV s/mg)
10	GC93028	7.5	863	236
	GC93032	6.0	999	140
20	GC93025	7.4	994	89
	GC93030	6.0	1026	217
	GC93036	5.5	855	122
30	GC93031	3.7	803	133
40	GC93027	7.7	813	152
60	GC93038	6.4	838	145
80	GC93039	6.9	935	89
100	GC93040	8.2	872	58
150	GC93045	4.0	842	56
200	GC93043	3.5	879	111
250	GC93046	7.9	833	125
300	GC93044	12.2	756	20
	GC93057	11.5	801	257

Figures 4.26 and 4.27 show the reconstructed MMDs of the 5 ml and 30 ml 1-butene LLDPEs. The MMDs were reconstructed by using the fitted curves from the MMDs of the individual TREF fractions. The MMDs were normalized using their corresponding weight fractions calculated from the cross fractionation. The distributions were normalized to have the same areas.

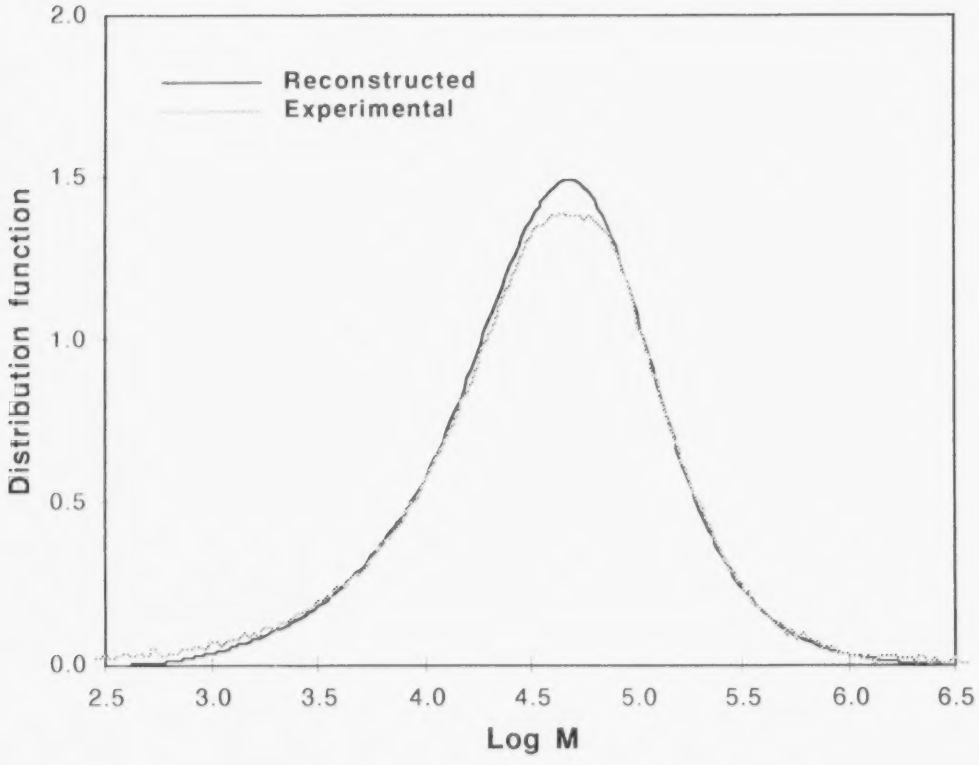

Figure 4.26: Reconstructed MMD of the 5 ml 1-butene LLDPE

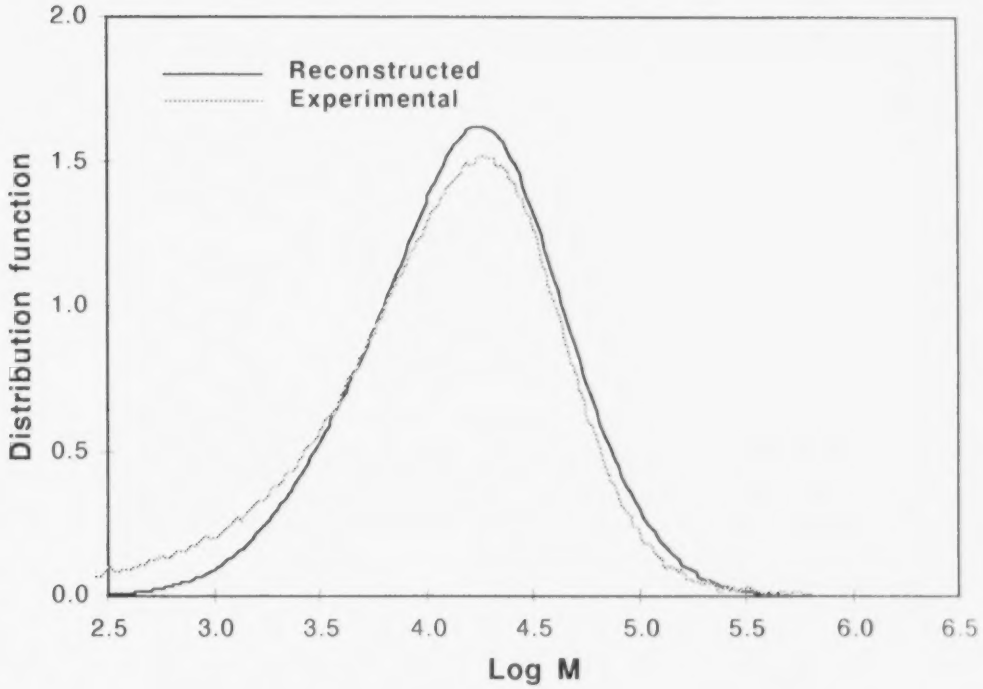

Figure 4.27: Reconstructed MMD of the 30 ml 1-butene LLDPE

For both samples, there is excellent agreement between the reconstructed MMD and the experimental distribution obtained from SEC. Similar results were obtained with other samples. The agreement between measured and reconstructed MMDs is excellent considering all the steps involved in the cross fractionation, in which some material could have been lost in addition to errors involved in fitting the MMDs. However, it can be seen in Figure 4.27 that for the sample with the high 1-butene content there is some low molar mass material missing in the reconstructed distribution. Branched materials with low molar mass were so easy to dissolve that they remained in solution. Therefore, all this material was washed away while the column was being filled. When we compare the total TREF areas in Table 4.3, it is seen that the total area under the TREF curve for the sample with the high branching concentration is about 35% smaller than all the other areas.

Separation by molar mass in TREF is a concern when performing TREF-SEC cross fractionation. As discussed in the previous chapter, if the molar mass of the polymer is lower than 10, 000, then separation by molar mass occurs in TREF. Separation by MM in TREF was investigated by performing a cross fractionation on a large sample (100 mg) of ethylene homopolymer with a broad molar mass distribution. The MMDs of the PTREF fractions eluted at temperatures lower than 95°C are shown in Figure 4.28. It can be seen that TREF produces a good separation by molar mass for the low MM material. The MMDs of the TREF fractions shown in this figure represent about 10 mass% of the whole LLDPE. The MMDs are very narrow with polydispersities of about 1.15 for all fractions except for the 90 to 95°C fraction which had a polydispersity of 1.29. These results were also used to generate some of the samples for the TREF calibration curve (see section 3.6).

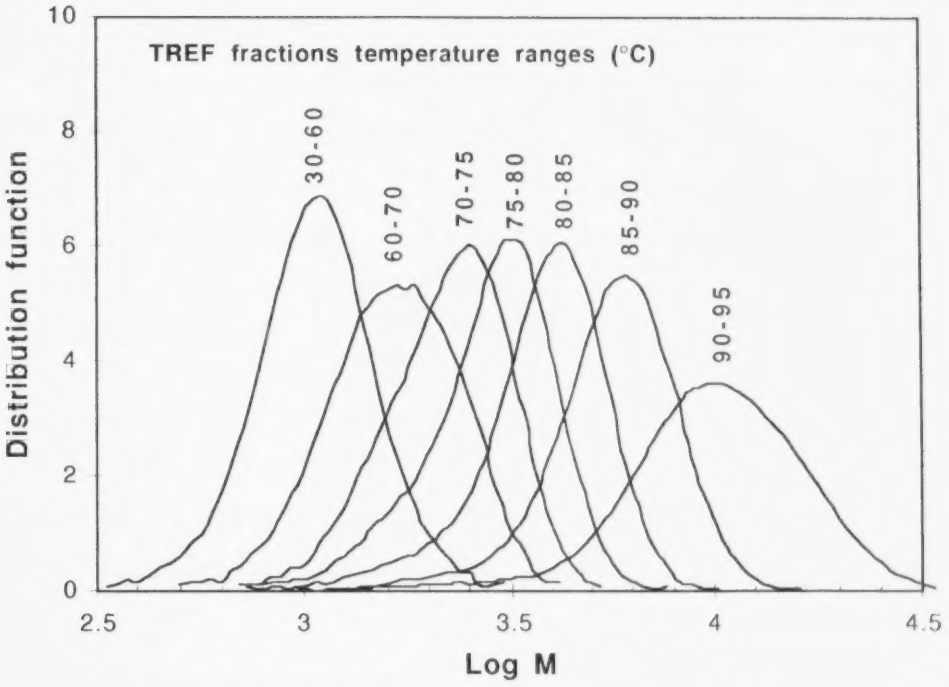

Figure 4.28: MMD of TREF fraction from a linear polyethylene (GC93048)

Separation by molar mass in TREF can modify the shape of the MMDs of the low temperature TREF fractions. Figure 4.8 is a good illustration of this problem. If the MMD of the low temperature fraction of this figure is compared with the one in Figure 4.9, it can be seen that the bimodal character of the distribution was exaggerated in Figure 4.8. This exaggeration occurred at a MM of about 3000, and it was caused by MM separation in TREF. It can be seen in Figure 4.28 that polymer with MM of about 3000 elutes in the 70-80°C interval. The effect of separation by MM in TREF is visible in the 5 ml 1-butene sample because the polymer that has eluted in that temperature interval represents only 7 mass% of the whole LLDPE. It was not visible for the 20 ml 1-butene sample because the same temperature interval represents 20 mass% of the whole LLDPE. The weight fraction of low MM polymer is usually very small compared to the weight fraction of the branched material. Therefore, this problem only appears for polymers with low branching concentration.

4.4 ATREF of ethylene/vinyl acetate copolymers

Ethylene/vinyl acetate (EVA) copolymers are semicrystalline materials that can also be characterized by TREF. Characterizations of EVA copolymers were reported by a few authors (Wild and Ryle 1982a, Kelusky et al. 1987 and Wild and Blatz 1992b). These copolymers are produced by free radical polymerization in high pressure processes.

A series of EVA copolymers obtained from AT Plastics were characterized by TREF in this project. The names and VA content of the sample investigated are given in Table 4.5. The VA content of the copolymers varied from 9% to 28% by mass. The TREF profiles of these samples are shown in Figure 4.29.

Table 4.5: Description of the EVA copolymers

Sample Name	VA content (mass%)
EVA-A	9
EVA-B	16
EVA-C	18
EVA-D	28

As expected, the TREF profiles of the EVA copolymers have shapes similar to the HP-LDPE. The TREF profiles of the EVA copolymers have a unimodal distribution which is a common feature of polymer produced by high pressure processes. It can also be observed that increasing the amount of VA in the copolymer increases the branching concentrations. Therefore, EVA copolymers with higher VA content elute at lower temperature.

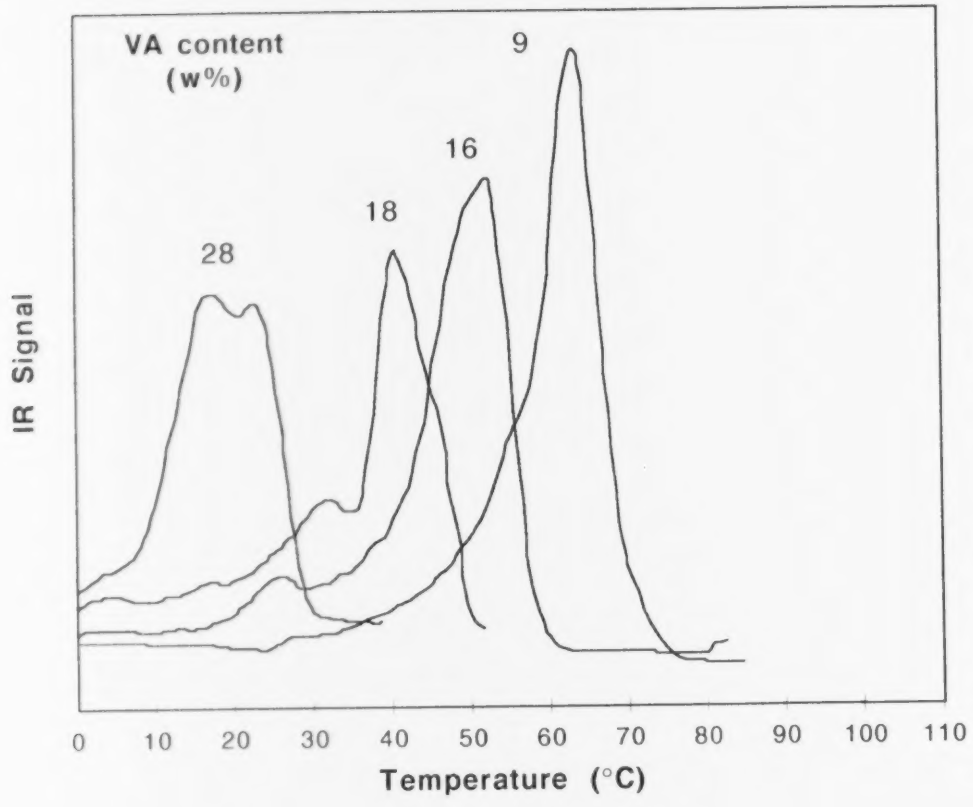

Figure 4.29: TREF profiles of EVA copolymers

It is also interesting to observe that TREF has a lower resolution for the high VA content. This is explained by the shape of the MSL-elution temperature relationship (see Chapter 3). As the MSL decreases, the slope of the MSL curve tends toward zero. Therefore, a small change in branching concentration will be spread out over a large temperature interval.

The average branching concentrations of the copolymers were computed and estimations of the EVA content were obtained. The results are shown in Table 4.6. The vinyl acetate content was estimated from the CH_3 content and the assumption that all the branches are due to acetate groups.

Table 4.6: Average branching concentration and estimated VA content of the EVA copolymers

Sample	CH_3/1000C	Estimated VA content (mass%)
EVA-A	22.8	12.8
EVA-B	39.2	20.7
EVA-C	50.7	25.7
EVA-D	63.8	30.9

The VA contents of the copolymers were evaluated using Equation 4.1, where $[CH_3]$ is the average branching concentration of the copolymer in CH_3 groups per backbone carbon. The numerator is the molar mass of VA multiplied by the branching concentration; the denominator represents the mass of the copolymer chain. Equation 4.1 is only valid for linear chains. Therefore, it is not necessarily valid for this type of copolymer produced in a high pressure process.

$$VA(mass\%) = \frac{0.086 \times [CH_3]}{14 + 0.059 \times [CH_3]} \times 100 \qquad (4.1)$$

Figure 4.30 shows the relationship between the real VA content and the values estimated using TREF and Equation 4.1. The two sets of data follow a linear relationship. The calculated values of VA content are consistently higher than the actual VA content. This is because the CH_3 concentration is not only due to vinyl acetate groups but also due to some regular side branching in the EVA molecules. The linear fit to the calculated versus the actual VA content shown in Figure 4.30 has an intercept of 5.68; this intercept value corresponds to a CH_3 concentration of 9.6 CH_3/1000C. This value is the same as the typical value of 10 CH_3/1000C obtained from TREF of HP-LDPE.

The distribution of the VA monomers in the LDPEs was obtained by performing ATREF on an EVA copolymer with the IR detector set to detect the absorbance of the carbonyl groups of the VA comonomers. The wavelength corresponding to the carbonyl groups is 5.71 μm. TREF profiles of EVA-B obtained by using two IR wavelengths are shown in Figure 4.31. The areas of the two profiles were normalized. The signal of the 5.71 μm TREF profile is very weak and noisy because the absorbance wavelength of the carbonyl group is on the shoulder of one of the solvent absorbance wavelength. It can be observed that the VA comonomers have a uniform distribution in the LDPE. Both profiles are similar in shape. Therefore, the VA comonomers were incorporated uniformly in the LDPE. Additional work with TREF, using solvents other than o-DCB, should be done to obtain more reliable TREF characterization of EVA.

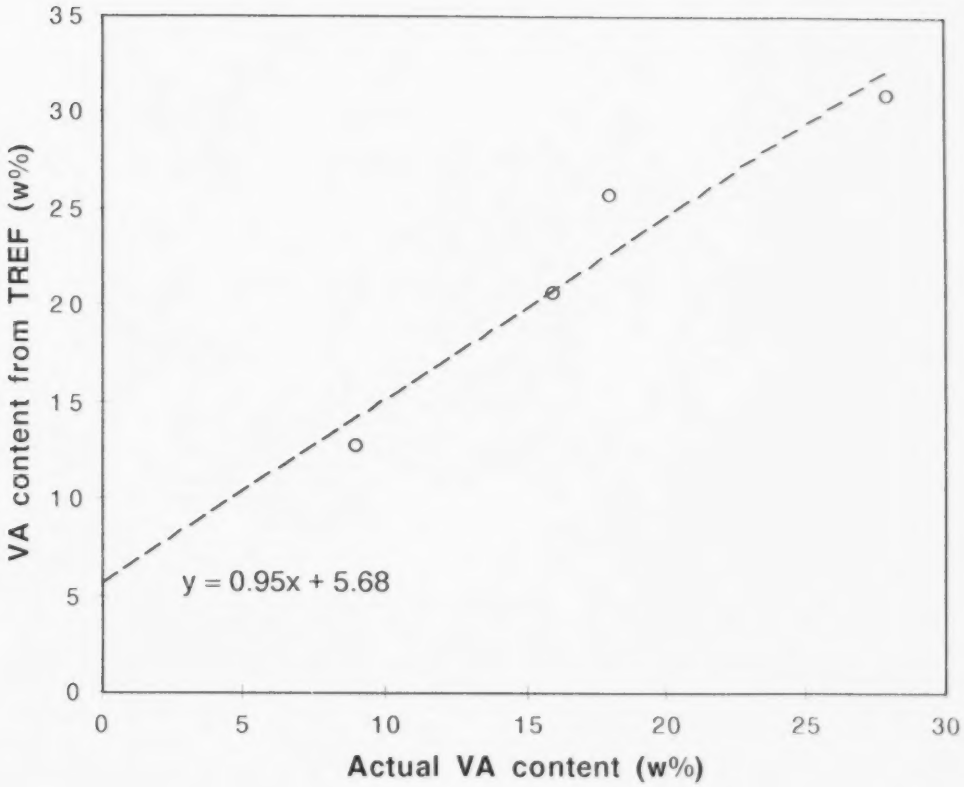

Figure 4.30: VA content estimated by TREF versus actual VA content of the EVA copolymers

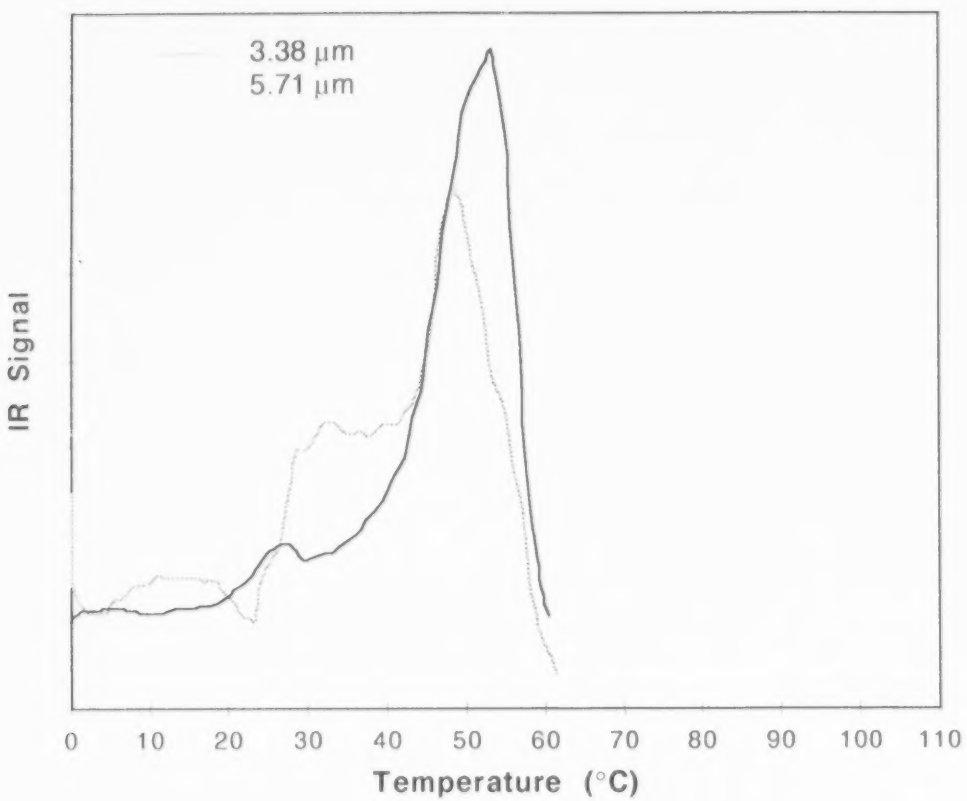

Figure 4.31: TREF profiles of EVA 1641 with two different IR wavelengths.

4.5 ATREF of ethylene/vinyltrimethoxysilane (VTMOS) copolymers

Ethylene/vinyltrimethoxysilane (VTMOS) copolymers are semicrystalline materials that can also be characterized by TREF. As with the EVA copolymers, these copolymers are produced by free radical polymerization in high pressure processes. The chemical formula of VTMOS is $H_2C=CHSi(OCH_3)_3$ and it has a MM of 148. Two ethylene/VTMOS copolymers were investigated: VTMOS-A and VTMOS-B. These copolymers contained 2.0 and 1.7 mass% VTMOS. The TREF profiles of these copolymers are shown in Figure 4.32.

The TREF profiles of the two ethylene/VTMOS copolymers are very similar since they have almost the same comonomer content. The shape of the TREF profiles is typical of a HP-LDPE with a unimodal distribution. Both profiles show a little shoulder on the right side of the distributions. It is also interesting to notice that the sample with the lower VTMOS content has a slightly higher branching concentration.

The IR absorbance of sample VTMOS-A in o-DCB was scanned to see if other wavelengths could be used for ATREF. Unfortunately, the scan did not reveal an other usable frequency. The problem is the solvent (o-DCB) has too many absorption peaks in the area of interest. It would be interesting to find another solvent which does not mask the IR absorption of VTMOS.

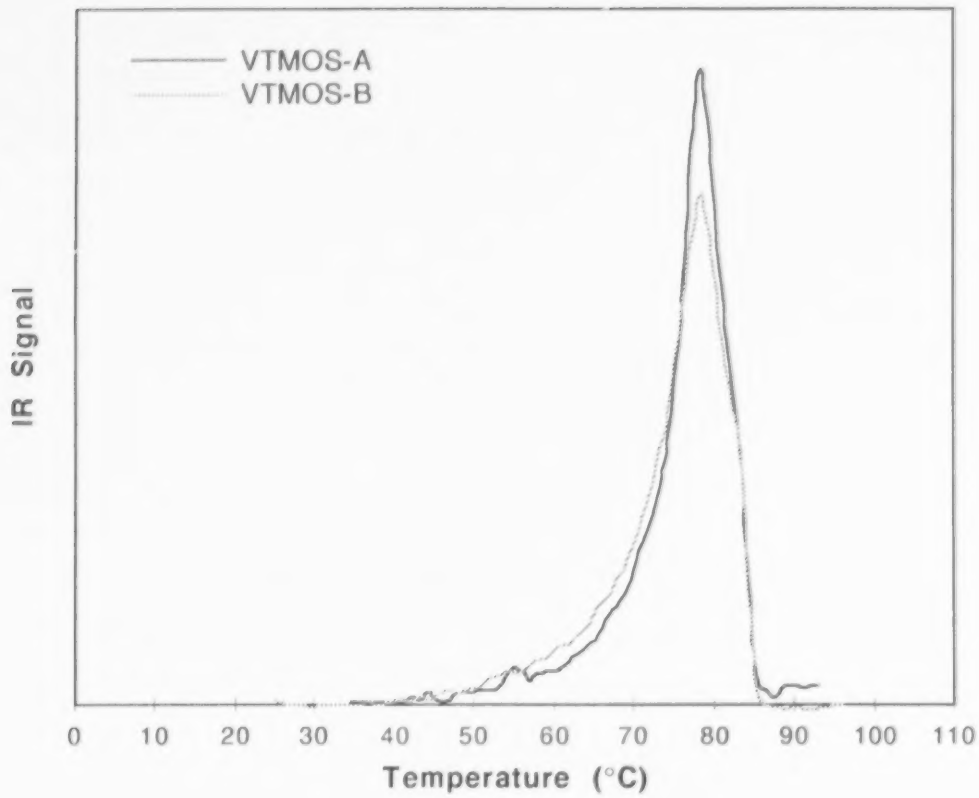

Figure 4.32: TREF profiles of ethylene/VTMOS copolymers

5. Conclusions and Recommendations

The effects of H_2 and 1-butene concentrations on the SCB and MM distributions of laboratory produced LLDPEs were investigated in this study. The LLDPEs produced in a gas phase semi-batch reactor over a commercial bisupported Ti catalyst were characterized using ATREF and TREF-SEC cross fractionation. To achieve this task, several modifications were made to the TREF apparatus which enhanced its reliability and operability. A method for PTREF was developed to generate fractions for analysis by SEC to obtain the MMDs as a function of TREF elution temperature. On the basis of the results from these experiments it is concluded that the modifications made to the equipment and the developed procedure produces reliable data. The reconstructed MMDs of the whole LLDPEs show that the results obtained from TREF-SEC cross fractionation are reliable.

The results from the ATREF analysis on the 1-butene series show that the comonomer incorporation in the ethylene/1-butene LLDPE is a strong function of 1-butene concentration in the reactor. The average branching concentration increased linearly with increasing 1-butene concentration. On the basis of the results from the ATREF analysis and the TREF-SEC cross fractionation, it is concluded that two catalytic sites copolymerize ethylene and 1-butene and one catalytic site produces a homopolymer of ethylene. The two sites responsible for the copolymerization explain the bimodal MMDs observed for the low temperature TREF fractions.

The ATREF analyses on the H_2 series show that H_2 pressures from 10 to 200 psi have a relatively small effect on 1-butene incorporation. At higher

H_2 pressures, the ratio of copolymer to homopolymer was increased. It is concluded that H_2 decreases the rate of polymerization over the sites responsible for homopolymerization more than over the sites responsible for copolymerization. The results from the TREF-SEC cross fractionation showed that H_2 is a more effective chain transfer agent for copolymer than homopolymer fractions of the LLDPEs.

The results from both the H_2 and 1-butene series support the postulate of multiple types of catalytic sites. The various sites involved in the polymerization behaved differently to changes in H_2 and 1-butene concentrations, producing multimodal SCB distributions and broad MM distributions. The information obtained from these results can be used for reactor modeling and for optimizing the reaction conditions to obtain products with desired specifications.

To complement the present investigation, it would be interesting to perform ATREF and TREF-SEC cross fractionation on a series of LLDPEs produced with different lengths of polymerization e.g. 0.1, 0.5, 1.0 and 1.5 h of polymerization in addition to the constant 2.0 h used to make the sample for the current work. This would generate SCB and MM distributions as a function of time.

Some improvements can be made to the current TREF apparatus. The automation of the sample collection in PTREF would reduce the work load of the operator considerably. The addition of a second IR detector would generate additional information about the structure of the polymers. The branching concentration would be obtained from the second IR detector. It would also be quite useful when analyzing other types of copolymers.

References

Albright, L.F. in "Processes for Major Addition-Type Plastics and Their Monomers", Robert E. Krieger Publishing Company, Malabar, Florida (1985).

Amundson, R.N., "Frontiers in Chemical Engineering Research: Needs and Opportunities", National Academic Press, Washington, D. C., p. 63 (1988).

Anderson, E.V., "Exports Provide Boost for Chemical Firm", C&EN. December 13, 1993, 47.

ASTM publication, "Absorbance of Polyethylene due to Methyl Groups at 1378 cm^{-1}", *The American Society of Testing and Materials (ASTM)*. Special Technical Publication, **D 2238-64** (1986).

Barbatala, A.,T. Bohossian and G. Delmas, "Fractionation and Characterization of Linear Low-Density Polyethylene at a Lower Critical Solution Temperature (LCST)", *Journal of Applied Polymer Science*, **46**, 411-420 (1992).

Bergstrom, C. and E. Avela, "Investigation of the Composite Molecular Structure of LDPE by Using Temperature Rising Elution Fractionation", *Journal of Applied Polymer Science*, **23**, 163-171 (1979).

Bonner, G.J., C.J. Frye and G. Capaccio, "A Novel Calibration for the Characterization of Polyethylene Copolymers by Temperature Rising Elution Fractionation", *Polymer*, **34** (16), 3532-3534 (1993).

Boor, J. Jr. "Ziegler-Natta Catalysts and Polymerizations", Academic Press, New York (1979).

Braun, D., W. Brendlein and G. Mott, "A Simple Method of Determining Copolymerization Reactivity Ratios by Means of a Computer", *European Polymer Journal*, **9**, 1007-1012 (1973).

Burdett, I.D., "A Continuing Success: The UNIPOL Process", *Chemtech*, October 1992, 616-623.

Caracotsios, M., "Theoretical Modeling of Amoco's Gas Phase Horizontal Stirred Bed Reactor for the Manufacturing of Polypropylene Resins", *Chemical Engineering Science*, **47** (9-11) 2591-2596 (1992).

Chakravarty, J., "Characterization of Polyolefins by Temperature Rising Elution Fractionation (TREF)", M.Sc. Thesis, University of Alberta, Edmonton, Canada (1993).

Cheremisinoff, N.P. in "Handbook of Polymer Science and Technology", Marcel Dekker Inc., New York , Vol. **I** 471-504 (1989).

Choi, K. Y. in "Handbook of Polymer Science and Technology", Marcel Dekker Inc., New York , Vol. I, 67-102 (1989).

Clement, J.W. and J.P. Thompson, "Cleaner Production: an Industrial Example", *J. Cleaner Prod*, **1** (1) 15-19 (1993).

Coeyan, M. and I. Young, "Healthy Demand Spurs US Plastics Growth", *Chemical Week*, June 1, 1994, 25-28.

Cossee, P., "Ziegler-Natta Catalyst 1. Mechanism of Polymerization of α-Olefins with Ziegler Natta Catalysts", *J. Catal*, **3**, 80- (1964).

de Carvalho, A.B.M., P.E. Gloor and A.E. Hamielec, "A Kinetic Mathematical Model for Heterogeneous Ziegler-Natta Copolymerization", *Polymer*, **30**, 280-296 (1989).

de Carvalho, A.B.M., P.E. Gloor and A.E. Hamielec, "A Kinetic Model for Heterogeneous Ziegler-Natta Copolymerization. Part 2: Stereochemical Sequences Length Distribution", *Polymer*, **31**, 1294- (1990).

de Kok, A.C. and A.C. Oomens, "Calibration in High Temperature Gel Permeation Chromatography of Linear Polyethylenes", Journal of Liquid Chromatography, **5** (5), 807-817 (1982).

Defoor, F., G. Groeninckx, H. Reynaers, P. Schouterden and B. Van Der Heijden, "Thermal and Morphological Characterization of Binary Blends of Fractions of 1-Octene LLDPE", *Journal of Applied Polymer Science*, **47**, 1839-1848 (1993).

"Encyclopedia of Polymer Science and Engineering", Wiley, New York, 431-455 (1986).

Desreux, V. and M.C. Spiegels, "Fractionation and Extraction of Polyethylene", *Bulletin of Society of Chemistry, Belgium*, **59**, 476-489 (1950).

Galvan, R. and M. Tirell, "Molecular Weight Distribution Prediction for Heterogeneous Ziegler-Natta Polymerization using a Two-Site Model", *Chemical Engineering Science*, **41** (9), 2385-2393 (1986).

Gilet, L., M.-F. Grenier-Loustalot and J. Bounoure, "Quantitative Analysis of Mixtures of Ethylene- and Propylene-Based Polymers by Temperature-Rising Elution Fractionation and ^{13}C Nuclear Magnetic Resonance", *Polymer*, **33** (21), 4605-4610 (1992).

Glockner, G., "Temperature Rising Elution Fractionation: A Review", *Journal of Applied Polymer Science, Applied Polymer Symposium*, **45**, 1-24 (1990).

Hazlitt, L.G., "Determination of Short-Chain Branching Distribution of Ethylene Copolymer by Automated Analytical Temperature Rising Elution Fractionation (Auto-ATREF)", *Journal of Applied Polymer Science, Applied Polymer Symposium*, **45**, 25-37 (1990).

Hosada, S., "Structural Distribution in Linear Low-Density Polyethylenes", *Polymer Journal*, **20** (5), 383-397 (1988).

Huang, J.C., M.Sc. Thesis (to be submitted), University of Alberta, Edmonton, Canada (1995).

Karbashewski, E. and A. Rudin, "A Note on the Effect of Comonomer Sequence Distribution on TREF Branching Distributions", *Polymer Engineering and Science*, **33** (20), 1370-1371 (1993).

Karbashewski, E., L. Kale, A. Rudin, W.J. Tchir, D.G. Cook and J.O. Pronovost, "Characterization of Linear Low Density Polyethylene by Temperature Rising Elution Fractionation and by Differential Scanning Calorimetry", *Journal of Applied Polymer Science*, **44**, 425-434 (1992).

Karoglanian, S.A. and I.R. Harrison, "A Comparative Study of ULDPE Utilizing DSC and TREF", *Thermochim. Acta*, **212**, 143-149 (1992).

Karol, F.J. in "Organometallic Polymers", Academic Press, New York, 135-143 (1978).

Kelusky, E.C., C.T. Elston and R.E. Murray, "Characterizing Polyethylene-Based Blends With Temperature Rising Elution Fractionation (TREF) Techniques", *Polymer Engineering and Science*, **27** (20), 1562-1571 (1987).

Kissin, Y.V. "Isospecific Polymerization of Olefins with Heterogeneous Ziegler-Natta Catalysts", Springer-Verlag, New York (1985).

Kissin, Y.V. in "Handbook of Polymer Science and Technology", Marcel Dekker Inc., New York, Vol. **I**, 103-131 (1989).

Layman, P., "Europe Looks to 'New Perspectives' in Polymers", *C&EN*, October 31, 1994, 10-11.

McAuley, K.B., J.F. MacGregor and A.E. Hamielec, "A Kinetic Model for Industrial Gas-Phase Ethylene Copolymerization", *AIChE Journal*, **36**(6), 837-850 (1990).

Mills, P.J. and J.N. Hay, "The Lamella Size Distribution in Non-Isothermally Crystallized Low Density Polyethylene", *Polymer*, **25**, 1277-1280 (1984).

Mirabella, F.M., "Impact Polypropylene Copolymers: Fractionation and Structural Characterization", *Polymer*, **34** (8), 1729-35 (1993).

Mirabella, F.M., Jr., and E.A. Ford. "Characterization of Linear Low-Density Polyethylene: Cross-Fractionation According to Copolymer Composition and Molecular Weight", *Journal of Polymer Science, Part B: Polymer Physics*, **25**, 777-790 (1987).

Nakano, S. and Y. Goto, "Development of Automatic Cross Fractionation: Combination of Crystallizability Fractionation and Molecular Weight Fractionation", *Journal of Applied Polymer Science*, **26**, 4217-4231 (1981).

Neves, C.J., E. Monteiro and A.C. Habert, "Characterization of Fractionated LLDPE by DSC, FTIR, and SEC", *Journal of Applied Polymer Science*, **50**, 817-824 (1993).

Pigeon, M.G. and A. Rudin, "Branching Measurement by Analytical TREF: A Fully Quantitative Technique", *Journal of Applied Polymer Science*, 51, 303-311 (1994).

Pigeon, M.G. and A. Rudin, "Comparison of Analytical and Preparative TREF Analysis: A Mathematical Approach to Correcting Analytical TREF Data", *Journal of Applied Polymer Science*, **47**, 685-696 (1993).

Provder, T, "Detection and Data Analysis in Size Exclusion Chromatography", ACS Symposium Series 352, American Chemical Society, Washington, DC (1987).

Rodriguez, F., "Principles of Polymer Systems", Hemisphere Publishing Corporation, New York (1989).

Rotman, D., M. Roberts and G. Morris, "Catalysts" *Chemical Week*, October 5, 1994, 25-29.

Schumacher, J.W. in "Chemical Economics Handbook", SRI International, 580.1300 (1994).

Schumacher, J.W. in "Chemical Economics Handbook", SRI International, 580.1320 (1993).

Seymour, R. B. in "History of Polyolefins", D. Reidel Publishing Company, Boston (1986).

Shiramaya, K., T. Okada and S.I. Kita, "Distribution of Short-Chain Branching in Low-Density Polyethylene", Journal of Polymer Science, Part A **3**, 907-916 (1965).

Sinclair, K.B. and R.B. Wilson, "Metallocene Catalysts: A Revolution in Olefin Polymerization", *Chemistry and Industry*, **21**, (1994)

Skoog, D.A. and J.J. Leary, "Principles of Instrumental Analysis", Saunders College Publishing, New York (1992).

Staub, R.B. in "Polyethylene 1933-83", Golden Jubilee Conference 8-10 June 1983, Plastic and Rubber Institute, London (1983).

Tait, J.T. in "History of Polyolefins", D. Reidel Publishing Company, Boston, 213-242 (1986)

Usami, T. in "Handbook of Polymer Science and Technology", Marcel Dekker Inc., New York , Vol. **II**, 435-483 (1989).

Usami, T., Y. Gotoh and S. Takamaya, "Generation Mechanism of Short-Chain Branching Distribution in Linear Low-Density Polyethylenes", *Macromolecules*, **19** (11), 2722-2726 (1986).

Usami, T., Y. Gotoh, H. Umemoto and S. Takamaya, "Characterization of Impact-Resistant Poly(Propylene-Ethylene) Copolymers by 13C Nuclear Magnetic Resonance Spectroscopy, Temperature-Rising Elution Fractionation-Size Exclusion Chromatography, and Transmission Electron Microscopy", *Journal of Applied Polymer Science: Applied Polymer Symposium*, **52**, 145-158 (1993).

Waters Dynamic Solutions, "Gel Permeation Chromatography Option Operator's Manual", Dynamic Solutions, Division of Millipore, Ventura, California (1989).

Wild, L. "Temperature Rising Elution Fractionation", *Advances in Polymer Science*, **98**, 1-47 (1990).

Wild, L. and C. Blatz, "Development of High Performance TREF for Polyolefin Analysis", *Proceeding of the American Chemical Society, Division of Polymeric Materials Science and Engineering*, **67**, 153-154 (1992).

Wild, L. and T.R. Ryle. "Crystallizability Distribution of Polymers: A New Analytical Technique", *Polymer Preprints, American Chemical Society*, **18**, 182-188 (1977).

Wild, L., "Composition Distributions in Polyolefins: A Job for TREF", *Trends in Polymer Science*, **1** (2), 50-55 (1993).

Wild, L., "Recent developments in TREF". *TREF Workshop, Pennsylvania State University, College Station*, PA., USA. Nov. 30-Dec. 1 (1989).

Wild, L., T.R. Ryle and D.C. Knobeloch, "Branching Distribution in LLDPEs", *Polymer Preprints of American Chemical Society*, **23**(2), 133-134 (1982b).

Wild, L., T.R. Ryle, D.C. Knobeloch and I.R. Peat, "Determination of Branching Distribution in Polyethylene and Ethylene Copolymers", *Journal of Polymer Science*, **20**, 441-455 (1982a).

Xie, T., K.B. McAuley, J.C.C. Hsu and D.W. Bacon, "Gas Phase Ethylene Polymerization: Production Processes, Polymer Properties, and Reactor Modeling", *Ind. Eng. Res.*, **33**, 449-479 (1994).

Zhou, X.-Q., Hay, J.N., "Fractionation and Structural Properties of Linear Low Density Polyethylene", *European Polymer Journal*, **29** (2-3), 291-300 (1993).

Appendix A : Descriptions of Polymers Characterized by TREF

Tables A.1 to A.3 of Appendix A contain details about the production conditions and properties of the polymer samples characterized by ATREF and PTREF. The ATREF and PTREF operating conditions for each run are given in Tables A.4 to A.6.

Table A.1 contains the polymerization conditions for the samples in the H_2 series. The file names which contain the raw TREF data for each sample are also given. The samples are listed according to H_2 pressure used during the polymerizations. All the TREF file names begin with an E followed by the date of the TREF elution and a letter to identify runs performed on the same day. For all the runs the amount of liquid 1-butene precharged was 10 ml and the sum of the partial pressure of ethylene and 1-butene was kept constant at 200 psi for all runs. The H_2 partial pressure varied from 0 to 300 psi. The length of the copolymerization period was 2 h and the reactor temperature was 70°C for all runs. The copolymerizations were performed in a gas phase semi-batch reactor using a commercial bisupported Ti catalyst. The cocatalyst was TNHAL. More details about the operating conditions are given by Huang (1995).

Table A.1: Description of polymers and reaction conditions for the H_2 series.

Run	H2 (psi)	Yield (g)	Mn	Mw	Pd	ATREF Files	PTREF Files
GC93023	0	67.48	106100	611700	5.77	E930828A E940508A E940615B E940616A	E941125A
GC93024	0	76.87	112800	571000	5.06	E940808C	
GC93028	10	26.68				E940919B E940920B E940925A	E940919A E940920A
GC93032	10	45.00	56000	227800	4.07	E940804C E940805A E940808A	E940826A E940829A
GC93025	20	49.68	36600	148100	4.05	E940907B E940908B E940921B	E940908A E940909B
GC93030	20	36.70	42500	167700	3.95	E940727A E940727B E940727C	E940817A

Table A.1 (contd.)

Run	H2 (psi)	Yield (g)	Mn	Mw	Pd	ATREF Files	PTREF Files
GC93036	20	41.73				E940809B E940810A E940811B	E940921A E940926A
GC93031	30	37.00	39900	159400	3.99	E940815A E940815B E940816A	E940830A E940831A
GC93027	40	30.25	26100	112200	4.30	E940508B E940526A E940530A E940725A E940726A E940825B	E940819A E940822A
GC93038	60	50.92	24900	103100	4.14	E940506A E940603A E940603B E940615A E940705A E940818A E940819B	E940620A E940621A

Table A.1 (contd.)

Run	H2 (psi)	Yield (g)	Mn	Mw	Pd	ATREF Files	PTREF Files
						E940823A	
GC93039	80	38.22	20800	83800	4.03	E940823B E940824A E940825A	E940901A E940907A
GC93040	100	40.57	17400	67100	3.86	E940616B E940617A E940617B E940706A E940707A E940901B E940906A E940906B	E940622A E940628A
GC93045	150	48.54	10400	30000	5.77	E940628D E940629A E941007A E941007B E941011A	E940705B E940707B
GC93043	200	32.30	7800	55700	7.14	E940621D E940623A	E940708A E940808B

Table A.1 (contd.)

Run	H2 (psi)	Yield (g)	Mn	Mw	Pd	ATREF Files	PTREF Files
						E940623B E941011B E941012A E941012B	
GC93046	250	20.92	6000	43600	7.27	E940630A E940728A E940728B E940728C E941013B E941014A E941014B	E940809A E940810B
GC93044	300	3.88	3700	67700	18.30	E940915B E940916A E940923A	E940914A E940915A
GC93057	300	75.04	6100	25300	4.15	E940729A E940804A E940804B	E940811A E940816B

Table A.2 contains the polymerization conditions for the samples of the 1-butene series. The operating conditions were similar to the operating conditions of the H_2 series previously described. The H_2 partial pressure was kept constant to 100 psi for all the runs. The amount of liquid 1-butene precharged was changed from 0 to 30 ml and the sum of ethylene and 1-butene partial pressure was kept at 200 psi.

Table A.2: Description of polymers and reaction conditions for the 1-butene series.

Run	1-butene (ml)	Yield (g)	Mn	Mw	Pd	ATREF Files	PTREF Files
GC93048	0	69.68	26500	116600	4.40	E941115A E941128A E941128B	E941116A E941122A
GC93049	5	55.12	16000	96800	6.05	E941109A E941129A	E941115B E941117A
GC93051	10	36.30	13100	86900	6.63	E941129B E941130A E941130B	E941121A E941124A
GC93050	20	68.46	10700	71000	6.63	E941116B E941130C	E941118A E941123A
GC93047	30	49.25	10600	52600	4.96	E941110A E941122B E941124B	E941109B E941114A

Table A.3 contains the description of the EVA copolymers characterized by ATREF. The VA contents and the files corresponding to the TREF runs are listed in this table.

Table A.3: Description of the EVA copolymers .

Sample	VA content (mass%)	Files
EVA-A	9	E941103B E941102A E941024B
EVA-B	16	E941102B E941102C E941103A E941108A E941108B
EVA-C	18	E941101C E941031A E941101A
EVA-D	28	E941101C E941031A E941101A

Table A.4 contains the description of the ethylene/VTMOS copolymers characterized by ATREF. The VTMOS content and the files corresponding to the TREF runs are listed in this table.

Table A.4: Description of the VTMOS copolymers.

Sample	VTMOS content (mass%)	Files
VTMOS-A	2.0	E950117A E950117B E950117C
VTMOS-B	1.7	E950118A E950118B E950118C

Appendix B : Description of ATREF and PTREF Analyses

Appendix B contains all the details of the ATREF and PTREF analyses performed in this project.

Table B.1 is a list of all the ATREF runs and their operating conditions. The experimental runs are listed chronologically and the letter E stands for elution. Off-column crystallization was used for all the samples and the cooling rate was 1.5°C/h during crystallization. Unless mentioned otherwise, the TREF columns were packed with 100 mesh glass beads and 5 mg of polymer was used for the analysis. The IR detector was set to 3.38 μm for all the runs unless mentioned otherwise in the comments.

Table B.1: Operating conditions for the ATREF runs

File	Sample	Crystallization solvent	Heating rate (°C/min)	Solvent flow rate (ml/min)	Elution Solvent	TREF Area (mV s/mg)	Comments
E930828A	GC93023	o-xylene	2	1.0	o-DCB	0	Used Celite for packing; Trouble with IR detector, no signal
E940131	SRM 1482	o-xylene	2	1.0	o-DCB	357	Good run
E940202A	Tetracontane	o-xylene	2	1.0	o-DCB	860	Good run
E940202B	SRM 1482	o-xylene	2	1.0	o-DCB	567	Good run
E940209A	Tetracontane	o-xylene	0.5	1.0	o-DCB	281	Good run
E940428A	Hexacontane	o-xylene	2	1.0	o-DCB	764	Lost some polymer while filling the column
E940503A	SRM 1483	o-xylene	2	1.0	o-DCB	665	Good run
E940503B	SRM 1483	o-xylene	2	1.0	o-DCB	492	Good run
E940505A	SRM 1484	o-xylene	2	1.0	o-DCB	542	Filtration without membrane
E940505B	SRM 1484	o-xylene	2	1.0	o-DCB	479	Good run
E940506A	GC93038	o-xylene	2	1.0	o-DCB	973	Good run
E940508A	GC93023	o-xylene	2	1.0	o-DCB	1200	Good run
E940508B	GC93027	o-xylene	2	1.0	o-DCB	0	IR cell leaked
E940526A	GC93027	o-xylene	2	1.0	o-DCB	0	Good run

Table B.1 (contd.)

File	Sample	Crystallization solvent	Heating rate (°C/min)	Solvent flow rate (ml/min)	Elution Solvent	TREF Area (mV s/mg)	Comments
E940530A	GC93027	o-xylene	2	1.0	o-DCB	0	Noise in the profile
E940530B	Tetracontane	o-xylene	2	1.0	o-DCB	2047	Good run
E940530C	Tetracontane	o-xylene	2	1.0	o-DCB	775	Good run
E940601B	Hexacontane	o-xylene	2	1.0	o-DCB	1066	Good run
E940602A	Hexacontane	o-xylene	2	1.0	o-DCB	1692	Good run
E940603A	GC93038	o-xylene	2	1.0	o-DCB	577	Good run
E940603B	GC93038	o-xylene	2	1.0	o-DCB	666	Good run
E940615A	GC93038	o-xylene	2	1.0	o-DCB	830	Good run
E940615B	GC93023	o-xylene	2	1.0	o-DCB	841	Tailing at high temperature
E940616A	GC93023	o-xylene	2	1.0	o-DCB	816	Good run
E940616B	GC93040	o-xylene	2	1.0	o-DCB	897	Good run
E940617A	GC93040	o-xylene	2	1.0	o-DCB	900	Good run
E940617B	GC93040	o-xylene	2	1.0	o-DCB	941	Good run
E940621D	GC93043	o-xylene	2	1.0	o-DCB	850	Good run
E940623A	GC93043	o-xylene	2	1.0	o-DCB	849	Good run
E940623B	GC93043	o-xylene	2	1.0	o-DCB	761	Good run
E940628D	GC93045	o-xylene	2	1.0	TCB	819	Good run

Table B.1 (contd.)

File	Sample	Crystallization solvent	Heating rate (°C/min)	Solvent flow rate (ml/min)	Elution Solvent	TREF Area (mV s/mg)	Comments
E940630A	GC93046	o-xylene	2	1.0	TCB	710	Good run
E940705A	GC93038	o-xylene	2	1.0	TCB	929	Good run
E940706A	GC93040	o-xylene	1	0.5	TCB	927	Good run
E940707A	GC93040	o-xylene	1	0.5	TCB	765	Good run (see ❶)
E940725A	GC93027	o-xylene	1	0.5	TCB	857	Good run (see ❶)
E940726A	GC93027	o-xylene	1	0.5	TCB	937	Good run (see ❶)
E940727A	GC93030	o-xylene	1	0.5	TCB	1270	Good run (see ❶)
E940727B	GC93030	o-xylene	1	0.5	TCB	856	Good run (see ❶)
E940727C	GC93030	o-xylene	1	0.5	TCB	953	Good run (see ❶)
E940728A	GC93046	o-xylene	1	0.5	TCB	748	Good run (see ❶)
E940728B	GC93046	o-xylene	1	0.5	TCB	833	Good run (see ❶)
E940728C	GC93046	o-xylene	1	0.5	TCB	774	Good run (see ❶)
E940729A	GC93057	o-xylene	1	0.5	TCB	804	Good run (see ❶)
E940804A	GC93057	o-xylene	1	0.5	TCB	819	Good run (see ❶)
E940804B	GC93057	o-xylene	1	0.5	TCB	781	Good run
E940804C	GC93032	o-xylene	1	0.5	TCB	941	Good run
E940805A	GC93032	o-xylene	1	0.5	TCB	1159	Tailing

Table B.1 (contd.)

File	Sample	Crystallization solvent	Heating rate (°C/min)	Solvent flow rate (ml/min)	Elution Solvent	TREF Area (mV s/mg)	Comments
E940808C	GC93024	o-xylene	1	0.5	TCB	845	Tailing
E940809B	GC93036	o-xylene	1	0.5	TCB	992	Good run
E940810A	GC93036	o-xylene	1	0.5	TCB	757	Good run
E940811B	GC93036	o-xylene	1	0.5	TCB	815	Good run
E940815A	GC93031	o-xylene	1	0.5	TCB	843	Good run
E940815B	GC93031	o-xylene	1	0.5	TCB	911	Good run
E940816A	GC93031	o-xylene	1	0.5	TCB	655	Good run
E940818A	GC93038	o-xylene	1	0.5	TCB	885	Noise in the profile produced by TFE lubricant sprayed near the IR detector
E940819B	GC93038	o-xylene	1	0.5	TCB	975	Good run
E940823A	GC93038	o-xylene	1	0.5	TCB	871	Good run
E940823B	GC93039	o-xylene	1	0.5	TCB	0	Good run
E940824A	GC93039	o-xylene	1	0.5	TCB	998	Good run
E940825A	GC93039	o-xylene	1	0.5	TCB	872	Good run
E940825B	GC93027	o-xylene	1	0.5	TCB	643	Good run
E940901B	GC93040	o-xylene	1	0.5	TCB	864	Good run
E940906A	GC93040	o-xylene	1	0.5	TCB	852	Tailing

Table B.1 (contd.)

File	Sample	Crystallization solvent	Heating rate (°C/min)	Solvent flow rate (ml/min)	Elution Solvent	TREF Area (mV s/mg)	Comments
E940907B	GC93025	o-xylene	1	0.5	TCB	1097	Good run
E940908B	GC93025	o-xylene	1	0.5	TCB	950	Good run
E940915B	GC93044	o-xylene	1	0.5	TCB	530	Good run
E940916A	GC93044	o-xylene	1	0.5	TCB	703	Good run
E940919B	GC93028	o-xylene	1	0.5	TCB	696	Good run
E940920B	GC93028	o-xylene	1	0.5	TCB	1029	Good run
E940921B	GC93025	o-xylene	1	0.5	TCB	936	Good run
E940923A	GC93044	o-xylene	1	0.5	TCB	1035	Good run
E940925A	GC93028	o-xylene	1	0.5	TCB		Good run
E941007A	GC93045	o-xylene	1	0.5	TCB	868	Good run
E941007B	GC93045	o-xylene	1	0.5	TCB	926	Good run
E941011A	GC93045	o-xylene	1	0.5	TCB	805	Good run
E941011B	GC93043	o-xylene	1	0.5	TCB	799	Good run
E941012A	GC93043	o-xylene	1	0.5	TCB	947	Good run
E941012B	GC93043	o-xylene	1	0.5	TCB	1066	Good run
E941013B	GC93046	o-xylene	1	0.5	TCB	910	Good run
E941014A	GC93046	o-xylene	1	0.5	TCB	1075	Good run

Table B.1 (contd.)

File	Sample	Crystallization solvent	Heating rate (°C/min)	Solvent flow rate (ml/min)	Elution Solvent	TREF Area (mV s/mg)	Comments
E941024A	EVA2842M	o-xylene	1	0.5	TCB	0	No signal, all the polymer remained in solution
E941024B	EVA1020	TCB	1	0.5	TCB	860	Good run
E941029A	EVA2842M	o-DCB	1	0.5	o-DCB	784	Good run
E941030A	EVA2842M	o-DCB	1	0.5	o-DCB	789	Good run
E941031A	EVA1880M	o-DCB	1	0.5	o-DCB	80	Nothing on the TREF profile
E941101A	EVA1880M	o-DCB	1	0.5	o-DCB	914	Good run
E941102A	EVA1020	o-DCB	1	0.5	o-DCB	843	Good run
E941102B	EVA1641	0-DCB	1	0.5	o-DCB	846	Good run
E941102C	EVA1641	o-DCB	1	0.5	o-DCB	1069	Good run
E941103A	EVA1641	o-DCB	1	0.5	o-DCB	774	Good run
E941108A	EVA1641	o-xylene	1	0.5	o-DCB	530	IR set at 5.71 μm; wrong flow rate at the beginning (1.4 ml/min); weak signal
E941108B	EVA1641	o-xylene	1	0.5	o-DCB	324	IR set at 5.71 μm; good run
E941109A	GC93049	o-DCB	1	0.5	o-DCB	868	Good run

Table B.1 (contd.)

File	Sample	Crystallization solvent	Heating rate (°C/min)	Solvent flow rate (ml/min)	Elution Solvent	TREF Area (mV s/mg)	Comments
E941115A	GC93048	o-DCB	1	0.5	o-DCB	889	Good run
E941116B	GC93050	o-DCB	1	0.5	o-DCB	1043	Good run
E941122B	GC93047	o-DCB	1	0.5	o-DCB	617	Good run
E941124B	GC93047	o-DCB	1	0.5	o-DCB	690	Good run
E941128A	GC93048	o-DCB	1	0.5	o-DCB	0	Good run
E941128B	GC93048	o-DCB	1	0.5	o-DCB	1091	Good run
E941128C	GC93049	o-DCB	0	0.5	o-DCB		Good run
E941129A	GC93049	o-DCB	1	0.5	o-DCB	1169	Good run
E941129B	GC93051	o-DCB	1	0.5	o-DCB	0	Good run
E941130A	GC93051	o-DCB	1	0.5	o-DCB	1027	Good run
E941130B	GC93051	o-DCB	1	0.5	o-DCB	942	Good run
E941130C	GC93050	o-DCB	1	0.5	o-DCB	1062	Good run
E950117A	VTMOS 910	o-DCB	1	0.5	o-DCB	621	Good run
E950117B	VTMOS 910	o-DCB	1	0.5	o-DCB	751	Good run
E950117C	VTMOS 910	o-DCB	1	0.5	o-DCB	423	Good run
E950118A	VTMOS 930	o-DCB	1	0.5	o-DCB	514	Good run
E950118B	VTMOS 930	o-DCB	1	0.5	o-DCB	439	Good run

Table B.1 (contd.)

File	Sample	Crystallization solvent	Heating rate (°C/min)	Solvent flow rate (ml/min)	Elution Solvent	TREF Area (mV s/mg)	Comments
E950217A	SRM 1482	o-DCB	1	0.5	o-DCB	854	Good run
E950217B	SRM 1482	o-DCB	1	1.0	o-DCB	912	Good run
E950217C	SRM 1483	o-DCB	1	1.0	o-DCB		Good run
E950217D	SRM 1484	o-DCB	1	1.0	o-DCB	1068	Good run
E950224A	SRM 1483	o-DCB	1	1.0	o-DCB	928	Good run
E950224B	SRM 1484	o-DCB	1	1.0	o-DCB	818	Good run

Note:

❶ An extra peak appeared at about 60°C. This extra peak was caused by an sudden increase of temperature in the temperature chamber. This problem was caused by an improper temperature control that occurred when the refrigeration unit of the temperature chamber stopped. To avoid this problem, the setting of the controller must were changed. The proportional band was set to 3.0 and the integrator was set to 0. The default parameters were 3.0 and 100 respectively.

a) o-DCB = ortho-dichlorobenzene

b) TCB = 1, 2, 4 trichlorobenzene

Table B.2 is a list of the PTREF runs and their operating conditions. The runs are listed chronologically and the letter E stands for elution. Off-column crystallization was used for all the samples and the cooling rate was 1.5°C/h. Unless mentioned otherwise, the TREF columns were packed with 100 mesh glass beads and 20 mg of polymer was used for the analysis. The IR detector was set to 3.38 μm. A stepwise procedure was used for all the runs (see Chapter 3). The proportional band of the controller of the temperature chamber was set to 5.0 and the integrator was set to 300 for optimum temperature control.

Table B.2: Operating conditions of the PTREF runs

Files	Samples	Crystallization solvent	Elution solvent	Area (mV s/mg)	Comments
E940503C	GC93023	o-xylene	o-DCB		Pressure problem, column plugged.
E940510A	GC93023	o-xylene	o-DCB		Pressure problem, column plugged.
E940525A	GC93023	o-xylene	o-DCB		IR cell cracked and leaked
E940531A	GC93023	o-xylene	o-DCB		Concentration too low for analysis by SEC
E940606A	GC93023	o-xylene	o-DCB		IR cell leaked
E940620A	GC93038	o-xylene	o-DCB	910	Good run
E940621A	GC93038	o-xylene	o-DCB	766	Good run
E940622A	GC93040	o-xylene	TCB	848	Good run
E940628A	GC93040	o-xylene	TCB	666	Good run
E940705B	GC93045	o-xylene	TCB	1052	Good run
E940707B	GC93045	o-xylene	TCB	1002	Good run
E940708A	GC93043	o-xylene	TCB	958	Good run
E940808B	GC93043	o-xylene	TCB	973	Good run

Table B.2 (contd.)

Files	Samples	Crystallization solvent	Elution solvent	Area (mV s/mg)	Comments
E940809A	GC93046	o-xylene	TCB	1001	Good run
E940810B	GC93046	o-xylene	TCB	972	Good run
E940811A	GC93057	o-xylene	TCB	800	Good run
E940816B	GC93057	o-xylene	TCB	834	Good run
E940817A	GC93030	o-xylene	o-DCB	769	Good run
E940819A	GC93027	o-xylene	TCB	913	Good run
E940822A	GC93027	o-xylene	TCB	871	Good run
E940826A	GC93032	o-xylene	TCB	920	Good run
E940829A	GC93032	o-xylene	TCB	975	Good run
E940830A	GC93031	o-xylene	TCB	926	Good run
E940831A	GC93031	o-xylene	TCB	954	Good run
E940901A	GC93039	o-xylene	TCB	920	Good run
E940907A	GC93039	o-xylene	TCB	895	Good run
E940908A	GC93025	o-xylene	TCB	764	Good run
E940909B	GC93025	o-xylene	TCB	887	Good run
E940914A	GC93044	o-xylene	TCB	830	Good run

Table B.2 (contd.)

Files	Samples	Crystallization solvent	Elution solvent	Area (mV s/mg)	Comments
E940915A	GC93044	o-xylene	TCB	794	Good run
E940919A	GC93028	o-xylene	TCB	1045	Good run
E940920A	GC93028	o-xylene	TCB		Fractionation aborted; trouble with the temperature chamber controller.
E940921A	GC93036	o-xylene	TCB	979	Good run
E940926A	GC93036	o-xylene	TCB	1036	Good run
E941109B	GC93047	o-DCB	o-DCB	656	Good run
E941114A	GC93047	o-DCB	o-DCB	760	Good run
E941115B	GC93049	o-DCB	o-DCB	1061	Good run
E941116A	GC93048	o-DCB	o-DCB	982	Good run
E941117A	GC93049	o-DCB	o-DCB	952	Good run
E941118A	GC93050	o-DCB	o-DCB	441	Good run
E941121A	GC93051	o-DCB	o-DCB		Good run
E941122A	GC93048	o-DCB	o-DCB	1094	Good run
E941123A	GC93050	o-DCB	o-DCB	1075	Good run
E941124A	GC93051	o-DCB	o-DCB	990	Good run

Table B.2 (contd.)

Files	Samples	Crystallization solvent	Elution solvent	Area (mV s/mg)	Comments
E941125A	GC93023	o-xylene	o-DCB		IR cell leaked at high temperature; tailing

Table B.3 is a list of all the PTREF runs and the elution temperature ranges over which each fraction was collected.

Table B.3: Temperature intervals of the TREF fractions from PTREF runs

Files	Temperature intervals of the TREF fractions (°C)									
	F1	F2	F3	F4	F5	F6	F7	F8	F9	F10
E940503C										
E940510A										
E940525A										
E940531A										
E940606A										
E940620A	40-60	60-71	71-81	81-86	86-91	91-96	96-101			
E940621A	38-58	58-68	68-78	78-82	82-87	87-92	92-97	97-102		
E940622A	30-50	50-60	60-70	70-80	80-85	85-90	90-95	95-100		
E940628A	30-50	50-60	60-70	70-80	80-85	85-90	90-95	95-100		
E940705B	30-50	50-60	60-70	70-80	80-85	85-90	90-95	95-100		
E940707B	30-50	50-60	60-70	70-80	80-85	85-90	90-95	95-100		

Table B.3 (contd.)

Files	Temperature intervals of the TREF fractions (°C)									
	F1	F2	F3	F4	F5	F6	F7	F8	F9	F10
E940708A	30-50	50-60	60-70	70-80	80-85	85-90	90-95	95-100		
E940810B	30-50	50-60	60-70	70-80	80-85	85-90	90-95	95-100		
E940811A	30-50	50-60	60-70	70-80	80-85	85-90	90-95	95-100		
E940816B	30-50	50-60	60-70	70-80	80-85	85-90	90-95	95-100	100-105	
E940817A	30-50	50-60	60-70	70-80	80-85	85-90	90-95	95-100	100-105	
E940819A	30-50	50-60	60-70	70-80	80-85	85-90	90-95	95-100	100-105	
E940822A	30-50	50-60	60-70	70-80	80-85	85-90	90-95	95-100	100-105	
E940826A	30-50	50-60	60-70	70-80	80-85	85-90	90-95	95-100	100-105	
E940829A	30-50	50-60	60-70	70-80	80-85	85-90	90-95	95-100	100-105	
E940830A	30-50	50-60	60-70	70-80	80-85	85-90	90-95	95-100	100-105	
E940831A	30-50	50-60	60-70	70-80	80-85	85-90	90-95	95-100	100-105	
E940901A	30-50	50-60	60-70	70-80	80-85	85-90	90-95	95-100	100-105	
E940907A	30-50	50-60	60-70	70-80	80-85	85-90	90-95	95-100	100-105	
E940908A	30-50	50-60	60-70	70-80	80-85	85-90	90-95	95-100	100-105	
E940909B	30-50	50-60	60-70	70-80	80-85	85-90	90-95	95-100	100-105	
E940914A	30-50	50-60	60-70	70-80	80-85	85-90	90-95	95-100	100-105	

Table B.3 (contd.)

Files	Temperature intervals of the TREF fractions (°C)									
	F1	F2	F3	F4	F5	F6	F7	F8	F9	F10
E940915A	30-50	50-60	60-70	70-80	80-85	85-90	90-95	95-100	100-105	
E940919A	30-50	50-60	60-70	70-80	80-85	85-90	90-95	95-100	100-105	
E940920A										
E940921A	30-50	50-60	60-70	70-80	80-85	85-90	90-95	95-100	100-105	
E940926A	30-50	50-60	60-70	70-80	80-85	85-90	90-95	95-100	100-105	
E941109B	30-50	50-60	60-70	70-80	80-85	85-90	90-95	95-100		
E941114A	0-20	20-30	30-40	40-50	50-60	60-70	70-80	80-90	90-95	95-100
E941115B	30-50	50-60	60-70	70-80	80-85	85-90	90-95	95-100	100-105	
E941116A	30-80	80-90	90-95	95-100	100-105	105-110	110-115			
E941117A	30-60	60-70	70-80	80-85	85-90	90-95	95-100	100-105		
E941118A	0-30	30-40	40-50	50-60	60-70	70-80	80-90	90-95	95-100	100-105
E941121A	30-60	60-70	70-80	80-85	85-90	90-95	95-100	100-105		
E941122A	30-80	80-90	90-95	95-100	100-105	105-110				
E941123A	0-50	50-60	60-70	70-80	80-90	90-95	95-100	100-105		
E941124A	30-60	60-70	70-80	80-85	85-90	90-95	95-100	100-105		
E941125A	30-60	60-70	70-80	80-85	85-90	90-95	95-100	100-105	105-110	

Appendix C : Data processing for ATREF and PTREF

ATREF

The sequence of actions listed below was performed to process the data from ATREF to generate the TREF profile, to obtain the average branching concentration and to produce a distribution of branching concentration.

- Columns 6 and 8 from the TREF files were imported.

- The baseline of the IR signal was subtracted from the IR values; the value of the baseline was obtained by examining the values of the IR signal at low and high temperature.

- The values of the IR signal were normalized so that their sum was unity by using Equation 3.1

$$IR_n = \frac{(\Delta T_i)(IR_i)}{\sum_i \Delta T_i IR_i} = \frac{IR_i}{\sum_i IR_i} \qquad (3.1)$$

- The branching concentrations were evaluated for each temperature by using Equation C.1. This relationship between elution temperature and CH_3/1000C was obtained by fitting a polynomial function to the data points generated from the MSL versus elution temperature relationship.

$$CH_3/1000C = -2.05672\times10^{-9}\,T^5 + 7.97200\times10^{-7}\,T^4 - 1.30741\times10^{-4}\,T^3 + 1.66526\times10^{-2}\,T^2 - 1.87420\,T + 92.47 \quad \text{(C.1)}$$

- The average branching concentration of each sample was evaluated by using Equation C.2.

$$[CH_3]_{avg} = \sum_i IR_{ni}[CH_3]_i \quad \text{(C.2)}$$

where $[CH_3]_{avg}$ is the average branching concentration; IR_n is the weight fraction of material that has a branching concentration of $[CH_3]$

- To generate the plot of the branching distribution of a sample, the values of the IR signal were transformed to conserve the same relative areas by using equation C.3 (see Appendix of Bonner et al 1993).

$$IR_c = IR_n \frac{\Delta T}{\Delta C} \quad \text{(C.3)}$$

where IR_c is the IR value used in the branching distribution plot; $\frac{\Delta T}{\Delta C}$ is the slope of the calibration curve of elution temperature versus branching concentration.

PTREF

The sequence of actions listed below was performed to process the data from PTREF to obtain the weight fraction of each temperature interval.

- Columns 1, 6 and 8 of the data file were needed for the data processing.
- The baseline of the IR signal was subtracted from the IR values; the value of the baseline was obtained by examining the values of the IR signal.
- The PTREF elution peaks were isolated by scanning the data. The data corresponding to the increase of temperature and the constant temperature step were discarded. Only 38 data points were kept for each elution peak. The 38 data points correspond to 3 min. of elution (the real interval of time between each reading was 4.72 s instead of 4 s).
- The weight fraction of each temperature interval was obtained by summing the IR signals of each peak and by dividing each of them by the total of all the peaks.

The software Axum was used to generate the 3-D profiles. A routine was written to generate the file used to produced the 3-D profiles. This routine imported the MMD from the SEC files, normalized them with the weight fraction of the corresponding temperature interval. Then, the MMDs and their elution temperatures were placed sequentially in a new file in three columns: Log MM, distribution function and elution temperature. The 3-D profiles were generated by using that file.

The Axum routine used to perform this task is called GPCdata.hst. This routine is included in the next two pages. To use this routine, a data sheet containing the names of the MMDs files, the weight fraction of each interval and the elution temperature was needed. These data must be placed in 3 columns. The columns must have the following names: "Names" for the MMDs files, "F" for the weight fractions and T for the elution temperatures. The elution temperatures were the averages of each temperature interval. The data sheet generated by this routine is named Profile. It was saved under another name after the data processing was completed.

GPCDATA.HST

```
// load and transform data from GPC
string sourceDS=currentdsname();
// find how many files to load
LONG Number_of_files=length(Names);

//loop trough all file names

LONG i;
for (i=1; i<=Number_of_files; i++)
{currentDS *SourceDS;
//load each file in the Names column
STRING file_name = Names[i]+".prn";
string data_sheet= Names[i] ;
Float temp=T[i];
Float Fac=F[i];

//If problem while importing the data, try a higher value for StartRow

Import FileName = *file_name, FileType = ASCII, DataSheet = *data_sheet, StartCol = 3,
EndCol = 6, NameRow = 0, StartRow = 55, EndRow = END, Delimiters = { ,\t};
DeleteCol {2 4};
Convert {1} using log;

clearcol {3};
\3=CUMSUM(\2);
\2=\2/(MAX(\3))*Fac;

DeleteCol {\3};
FillNumCol {3} using addseq with args = {-1, temp, 0, 0};
SaveDS *data_sheet ,datasheet=*data_sheet ;

//This creates a datasheet used for the 3D profiles
//After execution of the program, save this datasheet under a different name
```

```
createDS {profile};

CurrentDS *data_sheet;
CopyBlock from DataSheet = *data_sheet, Columns = {1..3}, Rows = {1..end} to DataSheet =
profile, StartColumn = 1, StartRow = end;
currentDS *SourceDS;
}
```

Appendix D : List of Material Needed for TREF

For the sample preparation, the following materials are needed:

Pierce Hypo Vial, clear

Volume (ml)	Chromatographic Specialties catalog number
15	P12911
30	P12944

Tegrabon Silicon Septa

90/10 mil (silicon/Teflon), 20 mm diameter

Chromatographic Specialties catalog number: C669120

Aluminium seal

20 mm, gold

Chromatographic Specialties catalog number: P13183

Disposable stirrers

Teflon , 3x12 mm, 100 pkg.

Fisher catalog number: 14-511-60A

To perform TREF analyses the following materials are needed:

Glass beads untreated

80/100 mesh

Chromatographic Specialties catalog number: C23076

Frits

Diameter	Pore size (µm)	Swagelock catalog number
1/2"	7	*-696-631
3/8"	5	*-696-112
3/8"	10	*-696-120

The frits can be ordered from Edmonton Valve & Fitting. About one month is required for delivery.

Appendix E : Description of the IR cell

The details of the IR cell heater designed for the TREF apparatus are shown in Figures E.1 and E.2. The catalog number of the various components and replacement parts are also given.

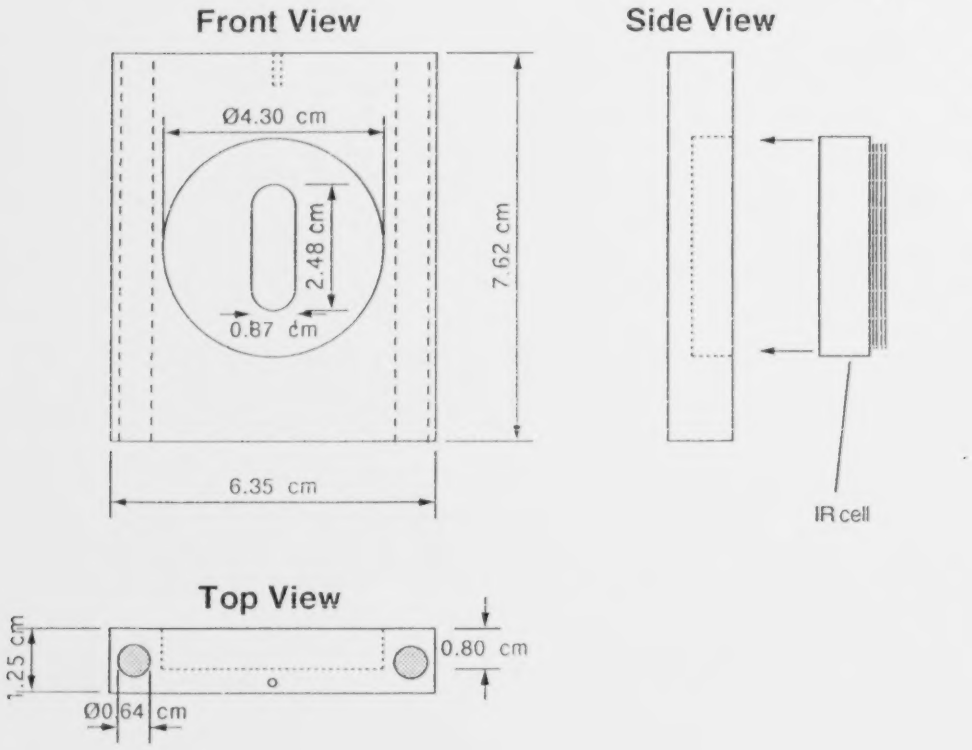

Figure E.1: Diagram of the IR cell heater

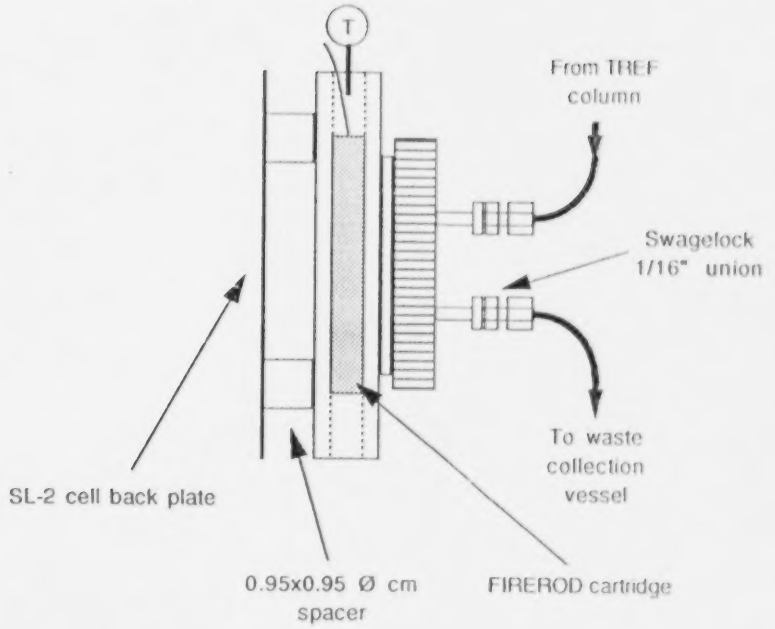

Figure E.2: Diagram of the IR cell and heater arrangement

The main body of the cell heater was constructed from an aluminium plate. The other parts needed were the FIREROD cartridge and a SL-2 cell demountable cell kit, and two 1/16" Swagelock union. The part numbers are given below.

SL-2 demountable cell kit

Catalog number: 0006-4153

International Crystal Laboratories

FIREROD cartridge

1/4"Ø x 2", 120V 125W

TRU-TEMP Electric Ltd.

Figure E.3 show a diagram of the SL-2 cell with all its components. The cell must be assembled as shown in this figure. The replacement parts and their catalog number are also listed in the next page. All these items were ordered from International Crystal Laboratories. Delivery of parts took about one month.

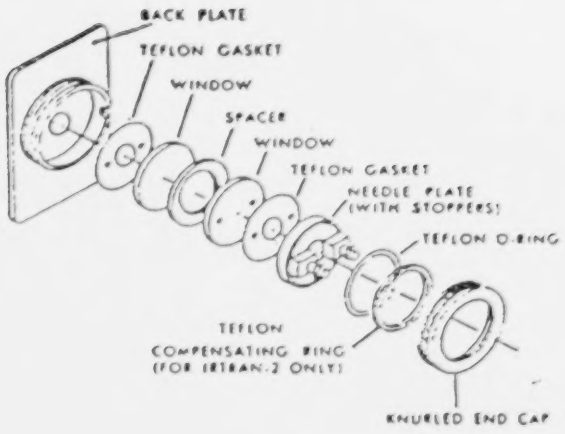

Figure E.3: Demountable SL-2 cell with all its components

CaF_2 discs

32x3 mm CaF_2 disc, polished and drilled

Catalog number: 002D-336

32x3 mm CaF_2 disc, polished

Catalog number: 002D-259

O-ring

32 mm Teflon O-ring

Catalog number: 0001-4293

Spacer

32 x 0.5 mm Teflon spacer

Catalog number: 0001-2111

Gasket

32 mm Teflon gasket

Catalog number: 0001-1466